The Effect of Lane Departure Warning Systems on Cross-Centerline Crashes

David Alexander Holmes

Thesis submitted to the faculty of the Virginia Polytechnic Institute and State University in partial fulfillment of the requirement for the degree of

Master of Science
In
Mechanical Engineering

Hampton C. Gabler, Chair
Warren N. Hardy
Steve C. Southward

April 16, 2018
Blacksburg, Virginia Tech

Keywords: vehicle safety, active safety, opposite direction crashes, lane keeping

The Effect of Lane Departure Warning Systems on Cross-Centerline Crashes

David Alexander Holmes

ABSTRACT

Cross-centerline crashes occur rarely in the United States but are especially severe. This type of crash is characterized by one vehicle departing over a centerline and encountering a vehicle traveling in the opposite direction. In recent years, automakers have started developing and implementing lane departure warning (LDW) on newer vehicles. This system provides the potential to reduce or significantly impact the frequency of cross-centerline crashes. The objective of this thesis was to estimate the potential crash and injury benefits of a LDW system if installed on every vehicle in the US fleet.

This research includes the following 1) a characterization of cross-centerline crashes in the United States today with current and future prevention methods, 2) a reconstruction methodology used for all crashes including rollovers and heavy vehicles, and 3) a simulation model and approach method used to estimate potential benefits of LDW systems on cross-centerline crashes.

Cross over to left crashes account for only 4% of non-junction non-interchange crashes but account for 44% of serious injury crashes of the same type. As part of this research, 42 cross-centerline crashes were reconstructed and simulated as if they had a LDW system installed. Accounting for driver capability to react to a LDW alert, crash reduction benefits ranged from 22 – 30%.Using injury risk curves, the probability of experiencing a MAIS2+ injury in a cross-centerline crash was reduced by 29% when using a LDW system.

The Effect of Lane Departure Warning Systems on Cross-Centerline Crashes

David Alexander Holmes

GENERAL AUDIENCE ABSTRACT

Cross over to left crashes occur rarely but are typically very severe. Cross over to left crashes include wrong side of road crashes, cross over to left due to loss of control, and cross over to left over centerline crashes, also known as cross-centerline crashes. Cross-centerline crashes are typically very severe due to the high closing speeds of both vehicles. Lane departure warning (LDW) is a safety system developed by auto manufacturers designed to help drivers stay in their travel lane. Upon leaving your lane without using a turn signal, a LDW system will provide an alert to warn you to stay in your lane. While LDW systems have been found to be effective for preventing road departure crashes, there have been few studies on their effectiveness for preventing cross-centerline crashes.

The research objective of this thesis was to estimate the number of crashes in the United States that would be avoided if every vehicle was equipped with a LDW system. It was also of interest to determine the number of front-row occupants who would not experience a greater than moderate level of injury (MAIS2+) with a LDW system installed.

To form the dataset, 42 crashes were initially selected, reconstructed, and simulated as if the encroaching vehicle had a LDW system installed. The speed profile of the vehicle was constructed using crash simulation software and an approach model in order to predict the vehicle speed prior to the crash. Driver capability to react to a LDW warning was also accounted for resulting in a range of benefits. With a LDW system installed, 22- 30% of cross-centerline crashes would be avoided. The probability of experiencing a MAIS2+ injury was also reduced by 29% when a LDW system was installed.

ACKNOWLEDGEMENTS

This research was funded by Toyota Motor Corporation and Toyota Engineering & Manufacturing North America, Inc.

I would like to start my thanking my advisor, Dr. Gabler, for guiding me throughout graduate school. I started as an intern and your willingness and help for me before and during graduate school has been invaluable. I can sincerely say that my current aims and future career path would never have been possible without your grace and aid. I would like to also thank Dr. Hardy and Dr. Southward for agreeing to be on my committee and provide feedback.

I would also like to acknowledge Rini Sherony, Chuck Gulash, Takashi Hasegawa, and Katsuhiko Iwazaki from Toyota for providing me invaluable feedback and suggestions on my simulations and possible improvements.

Thank you to everybody in the lab who has been with me during my time here. Special thanks to John Scanlon who I worked with closely while I was an intern. You were always available whenever I had questions and were an invaluable help when I started my own project. I would also like to specially thank Whitney Tatem for always bringing a ray of sunshine into the lab.

Thank you to my sisters, Emily and Katherine, who were with me during my years as a graduate student. Also thank you to my mom and dad who always supported my endeavors. I would like to especially thank my grandfather, Joachim Neckere, and my grandmother for their never ending support for me.

Table of Contents

1 Introduction 1
1.1 Background 1
1.2 Opposite Direction Crash Scenarios 2
1.3 Factors Influencing Cross-Centerline Crashes 3
1.3.1 Influence of road geometry 3
1.3.2 Driver behavior 5
1.4 Infrastructure Prevention Methods 7
1.4.1 Widen road 7
1.4.2 Implementation of 2+1 Roadway design 7
1.4.3 Centerline rumble strips 9
1.4.4 Summary of Infrastructure based solutions 14
1.5 Active Safety Systems 14
1.5.1 Lane Departure warning and prevention systems 15
1.5.2 Head-on crash avoidance systems 17
1.6 Research Objective 19
1.7 Structure 19
2 Data Sources 20
2.1 Introduction 20
2.2 NMVCCS 20
2.3 NASS/CDS 21
2.4 Injury Severity 22
2.5 EDR Records 23
3 Reconstructing Cross-Centerline Crashes 25
3.1 Introduction 25
3.2 Trajectory Reconstructions 25
3.3 Speed Reconstruction 33
3.4 Heavy Vehicle Crashes 35
3.4.1 Motivation 35
3.4.2 Reconstruction methodology 35
3.4.3 Validation 37
3.4.4 Results 39
3.4.5 Limitations 45
3.5 Rollovers 46
3.5.1 Motivation 46
3.5.2 Reconstruction methodology 46
3.5.3 Validation 48
3.5.4 Results 49
3.5.5 Limitations 53
3.6 Final Crash Reconstruction Dataset 54
4 Using Event Data Recorders to Model Driver Actions Prior to Impact 56
4.1 Introduction 56
4.2 Objective 57
4.3 Approach 57
4.4 Data Source 58
4.5 Determining Pre-Crash Driver Behavior 59

4.6 Development of the Approach Model 61
4.7 Model Validation 62
4.8 Results 62
4.8.1 Evasive maneuvers prior to a cross-centerline crash 62
4.8.2 Effect of speed limit and pre-impact braking 67
4.8.3 Braking Level model 68
4.8.4 Approach model 71
4.9 Conclusion 74
5 Crash Benefits of LDW Systems Applied to Cross-Centerline Crashes 75
5.1 Introduction 75
5.2 Objective 76
5.3 Methodology 76
5.3.1 Data source 77
5.3.2 Crash reconstructions 78
5.3.3 LDW Simulation 81
5.4 Results 85
5.4.1 Passenger Vehicle LDW Dataset Composition 85
5.4.2 Passenger Vehicle LDW Benefits 90
5.4.3 Heavy Vehicle and Rollover Crashes dataset composition 92
5.4.4 Heavy Vehicle And Rollover LDW Crash Benefits 96
5.5 Discussion 97
5.6 Limitations 98
6 Injury Benefits of LDW Systems 100
6.1 Introduction 100
6.2 Methodology 100
6.2.1 Injury Risk Modeling 100
6.2.2 Determining Frontal Injury Risk 101
6.2.3 Determining Injury Benefits 103
6.3 Results 104
7 Summary of Findings 107
7.1 Goal 107
7.2 Cross-centerline crashes in the United States 107
7.3 Development of reconstruction methodology for cross-centerline crashes 107
7.4 Estimation of crash and injury benefits of an LDW system 108
7.5 Publication Plan 109
7.6 Future Work 109
References 111
Appendix 118
A.1 Cross-Centerline Measurements Reconstruction Protocol 118
A.2 PC-Crash Reconstruction Protocol 124
A.3 Heavy Vehicle Specification Sheet Example 131
A.4 Special Vehicle PC-Crash Rollover Reconstruction Protocol 132

List of Figures

Figure 1. From left to right opposite direction crash configurations. A) Cross over to left over centerline B) cross median crashes C) Cross over to left due to control loss D) Wrong side of the road E) cross over to right then cross over to left 2
Figure 2. Example of a 2+1 roadway design. The most common divider between the lanes is either a painted line or a barrier. 8
Figure 3-Road diagram for installation of a centerline rumble strip. 10
Figure 4. A) The vehicle begins to cross over the lane line and a warning is given to the driver. B) Either the driver takes steering action or the LDP system automatically initiates steering. 15
Figure 5. Sample HCAAS crash scenario. Originally the vehicle 1 (blue) impacts the vehicle 2 (green) head-on. With a HCAAS installed and operational on vehicle 1, the system activates steering and provides a warning to the driver as the vehicle is drifting over the centerline. The driver reacts to the warning and steers to avoid the crash. 18
Figure 6. Scene diagram from NMVCCS case #2005012695762. Vehicle 1 travels north, crosses the centerline, and impacts Vehicle 2 head-on. 26
Figure 7. Depiction of the path to point. The black line represents a straight path while the green line represents a curved path. In this scenario, the green path is the most likely vehicle path. 28
Figure 8. NMVCCS Case Number: 2006005289522. Example of where the heading of the vehicle as drawn on the scene diagram does not match the recorded vehicle trajectory. 29
Figure 9. NMVCCS scene diagram from case #2005012695762 after annotation with measurements. Red points are the front center of vehicle 1. Blue points are the front center of Vehicle 2. The green points mark the start and end points of the lane lines. 31
Figure 10. Process to fit a circle between two vehicle position points. X and Y represent the vehicle position at both points and θ represents the heading of the vehicle. In this scenario, r is the radius of the circle and is unknown. 32
Figure 11. NMVCCS case number 2005011269043. (A) Original NMVCCS scene diagram. (B) Vehicle trajectory reconstruction in MATLAB. (C) Vehicle animation with accurate vehicle dimensions. 33
Figure 12. Phases of a cross-centerline crash. This section describes the process of reconstructing the impact speed for all cases. 33
Figure 13. Generic truck_2axle model in PC-Crash. This model was commonly used with custom specifications for heavy vehicle crash reconstruction. 37
Figure 14. In this limited dataset, passenger vehicles travel faster and experience much high delta-Vs than heavy vehicles. 40
Figure 15. Injury distribution in heavy vehicle crashes 43
Figure 16. Comparison of the EDR speed and the final PC-Crash simulation impact speeds. The black line depicts a Y=X fit. If the PC-Crash simulated impact speeds were exactly equal to the EDR reported speeds, every point would be on that line. 44
Figure 17. Illustration of the rollover reconstruction methodology process 47
Figure 18. Scatter plot comparing EDR speed to PC-Crash speed in rollover crashes. 52
Figure 20. Diagram of a cross-centerline crash depicting the 4 distinct phases of a cross-centerline crash: (1) approach phase, (2) encroachment, (3) evasive action, and (4) impact. 56
Figure 21. NASS/CDS case number 168005837. Scene diagram of cross-centerline crash. Vehicle 1(traveling north) crosses over the centerline and impacts V2. Data from the EDR in vehicle 2 is shown on the right side. Vehicle 2 applies the brakes (brake status shown in red) at

t=-2 seconds resulting in a decrease in speed. The extrapolated impact speed is shown as a point at t=-0.5 seconds 60
Figure 22. Analysis of driver speed behavior prior to impact. 63
Figure 23. Illustration of the pre-crash motions of each vehicle separated by encroaching and non-encroaching. 64
Figure 24. Driver actions prior to impact. Data drawn from the 19 cases that had both braking and steering data. 65
Figure 25. Analysis of steering direction in cross-centerline crashes. Conducted on 13 vehicles that initiated an evasive steering maneuver. Labels illustrate the representative number of vehicles. 66
Figure 26. Distribution of different approach speeds at different speed limits. There is a positive correlation between approach speed and speed limit. 67
Figure 27. Distribution of deceleration prior to impact. 68
Figure 28. Logistic regression plot indicating braking models performance 71
Figure 29. Plot of actual approach speed versus the predicted approach speed. There is good correlation between the model results and the actual results. 73
Figure 30. General methodology to estimating crash benefits of LDW systems. 77
Figure 31. Vehicle speed profile used in simulations 80
Figure 32. LDW lateral acceleration ramp function. 84
Figure 33. Diagram of LDW system activation criteria and speed profile of the vehicle throughout the simulation. 84
Figure 34. Comparison of lane departure angle in the cross-centerline dataset and road departure angle from NCHRP 17-43. 87
Figure 35. Distribution of approach speed compared to impact speed for both vehicles 88
Figure 36. Critical reasons for the cross-centerline crash 89
Figure 37. Visual description of LDW estimated crash benefits. 90
Figure 38. Difference in crash configuration when driver initiates evasive steering. (A) Without LDW system. (B) With LDW system 91
Figure 39. Body type distribution of vehicles reconstructed using special reconstruction methodology. 93
Figure 40. Injury comparison between rollover, heavy vehicle, and passenger vehicle crashes. . 95
Figure 41. Critical reasons behind crash for rollover and heavy vehicle crashes. Raw number of cases is shown in the parentheses. 96
Figure 42. Time to collision at the point of first lane departure. Many drivers had a chance to react prior to the crash. 98
Figure 43. Frontal injury risk curve for a female belted occupant from 13 to 64 years old. 102
Figure 44. Occupant injuries in cross-centerline crashes displayed using the KABCOU scale. 104
Figure 45-The black line depicts a straight line transition between the points and the green line depicts a curved transition. As can be seen the green line most closely approximates the likely vehicle path. 123

List of Tables

Table 1. Nationwide statistics on cross-over-to-left crashes. Presented using data from Kusano et al (2013) [1]. 1
Table 2. Road geometry factors associated with severity of cross-centerline crashes 4
Table 3. Daily Traffic Average and Comparison of Crash Rate. Data from Potts et al. (2003) [17]. 8
Table 4. Compilation of effectiveness numbers for centerline rumble strips for different collision types. Presented originally in Torbic et al. (2009) [23]. 11
Table 5. Summary of crash reduction effectiveness by solution 14
Table 6. All measurements collected along with the source of the measurement. 29
Table 7. NMVCCS heavy vehicle reconstruction results 39
Table 8. Summary of database contents 41
Table 9. Composition of excluded cases for validation 42
Table 10. NMVCCS cross-centerline rollover crashes reconstruction results. Vehicles are designated as either the rollover vehicle (vehicle that experienced rollover) or non-rollover vehicle. 49
Table 11. NASS/CDS Rollover reconstruction cases with a comparison between EDR data and PC-Crash simulations 51
Table 12. Breakdown of final NMVCCS Case set 55
Table 13. Deceleration thresholds for braking levels 61
Table 14. Summary of NASS/CDS EDR Data Source 62
Table 15. Coefficients and p-values for heavy braking model 69
Table 16. Coefficients and p-values for Light Braking Model 70
Table 17. Coefficients of approach speed model 72
Table 18. Coefficients of the final approach speed model 73
Table 19. Maximum deceleration values for different road conditions 80
Table 20. Detailed count of exclusion reasons for passenger vehicle crashes 85
Table 21. Data composition. Distribution of road alignment, number of lanes, speed limits, day/night, and weather conditions 86
Table 22. Exclusion reasons for heavy vehicle and rollover cases 92
Table 23. Comparison of impact speed and delta-V across the datasets used in this study. 94

1 Introduction

1.1 Background

Opposite direction crashes occur when two vehicles traveling in opposite directions impact each other. These crashes are commonly described as head-on crashes but can also be sideswipe crashes. Opposite direction crashes can be especially severe due to the high closing speeds of the vehicles involved in the crash. Cross over to left crashes are one scenario fitting the definition of an opposite direction crash. In a cross over to left crash, a vehicle crosses over the centerline and impacts another vehicle traveling in the opposite direction.

Using data from GES 2010, NASS-CDS 2006-2010, and FARS 2010, Kusano et al. (2013) found that despite only accounting for 5% of non-junction vehicle-to-vehicle crashes, cross-over-to-left crashes accounted for 44% of serious injury and 49% of fatal crashes nationwide [1]. Table 1 below shows the frequency of these crashes nationwide using this data [1]. Cross-over to left crashes resulted in 2,711 fatalities in 2010 and over 30,000 crashes where one occupant sustained a serious injury (defined as AIS 3 or greater) [1].

Table 1. Nationwide statistics on cross-over-to-left crashes. Presented using data from Kusano et al (2013) [1].

Data Source	Severity	Years	Frequency
NASS-GES	All Severities	2010	57,164
NASS-CDS	Serious Injury	2006 – 2010	31,512
FARS	Fatal Crashes	2010	2,711

Similar results have been reported at the state level. Using data from the Maine Department of Transportation, Garder et al. (2006) found that head-on crashes were overrepresented with regards to fatalities. On non-interstate rural roads in Maine, head on crashes accounted for nearly half of all traffic fatalities statewide despite accounting for less than 5% of all crashes [2].

In terms of crash cost, Zaloshnja et al. (2006) found that one of the most costly crashes was where multiple vehicles crashed head-on on a non-intersection road with a speed limit greater than 50 mph. Combining all non-intersection head-on crash scenarios, the total cost amounted to more than 21.5 billion dollars (in $2001) in the United States from 1999 – 2001 [3].

1.2 Opposite Direction Crash Scenarios

Opposite direction crashes can be categorized into five scenarios: cross over to left over centerline, cross over to left over centerline due to loss of control, cross-median crashes, wrong side of road crashes, and cross over to right leading to overcorrection and subsequent cross over to left crashes [1]. Figure 1 provides sample diagrams illustrating each of these crash scenarios.

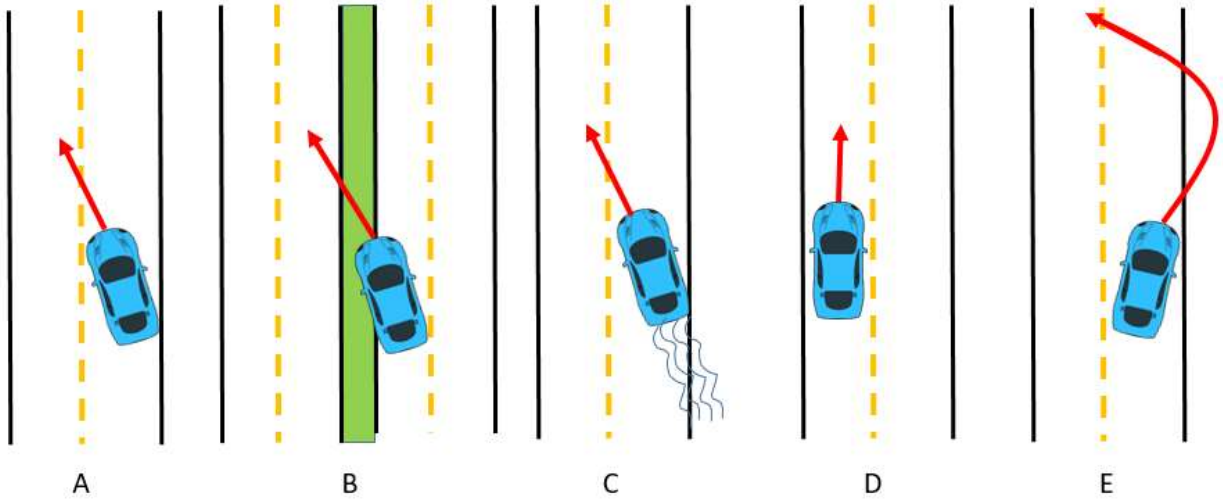

Figure 1. From left to right opposite direction crash configurations. A) Cross over to left over centerline B) cross median crashes C) Cross over to left due to control loss D) Wrong side of the road E) cross over to right then cross over to left

Of particular interest are the first two scenarios hereafter referred to as cross-over-to-left crashes. These crashes are significantly overrepresented among all serious injury and fatal crashes [1, 2].

1.3 Factors Influencing Cross-Centerline Crashes

1.3.1 INFLUENCE OF ROAD GEOMETRY

Cross-centerline head-on crashes are rare but typically result in severe injuries and a high crash cost. To determine the causes of these crashes, numerous studies have analyzed the locations where they occur to determine if there were correlations between road geometry and cross-centerline crash frequency and severity [4-8]. Kusano et al. (2013) found that the majority of these crashes in the US occurred on rural two lane undivided roads [1].

Zhang et al. (2005) and Deng et al. (2006) analyzed the effect of road characteristics on frequency and severity of head-on crashes respectively using data from two lane rural roads in Connecticut from 1996 -2001 [5, 8]. Zhang et al. (2005) found the factors that correlated with crash frequency were the maximum magnitude of a horizontal curve, the summation of absolute change rate of horizontal curvature, the summation of absolute change rate of vertical curvature, and the speed limit. Interestingly, speed limit was not found to be correlated to head-on crash frequency.

Deng et al. (2006) found the factors correlated to severity were road conditions, density of access points, pavement width, and day/night [5]. Pavement width was found to be the most significant factor with an increase in pavement width strongly correlated to a decrease in severity. This finding is supported by other studies [4, 6, 8]. Kusano et al. (2013) found a correlation between speed limits and severity [1]. All of these factors and explanations (assigned by this author) are shown in Table 2.

Table 2. Road geometry factors associated with severity of cross-centerline crashes

Factor	Potential Explanation
Road Conditions	Wet, icy, or snowy roads give a higher likelihood of vehicle losing traction and crossing the centerline
Density of access points	High density of access points means vehicles have to navigate through each access point and deal with cross traffic and merging scenarios.
Pavement width	Higher pavement width provides more lateral space between vehicles allowing more time for both drivers to react prior to a collision
Day/Night	During night, visibility conditions are affected increasing the driver reaction time to an oncoming vehicle
Speed Limit	Higher speed limits typically indicate both vehicles are traveling faster resulting in a higher delta-V at impact.

The presence and sharpness of curves has been found by numerous studies to be an especially important roadway characteristic on opposite direction head-on crash frequency. Kusano (2013) found that the most common pre-crash maneuver for an encroaching vehicle was going straight or negotiating a curve with this occurring in 88% to 94% of all cross over to left crashes on rural two-lane roads [1]. Zhang [8], Hosseinpour [6], and Al-Senan [4] all found that road curvature was a significant characteristic in predicting head on crash sites. The most common characteristic found was the degree of horizontal curvature but Zhang et al. (2005) also found that the change rate of horizontal curvature and the sum of the absolute change rate of horizontal curvature played a role in predicting head-on crash frequency [8]. Al-Senan found that

the number of reverse curves with zero tangents, also referred to as S-curves, played a factor in determining whether a head-on crash would occur [4].

Road curvature may influence the frequency of head-on crashes because drivers negotiating a curve tend to depart to the outside of the curve and strike a vehicle traveling in the opposite direction. Kusano et al. (2013) provided evidence to support this theory stating that drivers more often depart to the outside of the curve than the inside of the curve in cross-over-to-left crashes [1].

Summarizing the findings from these papers, the most likely site for a head-on cross-over-to-left crash were undivided narrow two lane rural roads with a high speed limit (> 40 mph) and a curve to the right. The American Association of State Highway and Transportation Officials (AASHTO) developed a Strategy Highway Safety Plan(SHSP) between 1997 and 2004 to reduce highway fatalities. As part of their plan to reduce head-on crashes, ASHTO targeted two lane rural roads as a primary area of concern [9].

1.3.2 DRIVER BEHAVIOR

A popular belief is that head on crashes are caused by overtaking or passing maneuvers. Numerous studies have shown however that overtaking is not a significant cause of these head-on crashes. Two studies performed by the Federal Highway Administrations Highway Safety Information System concluded that crashes occurring during overtaking maneuvers were not a significant problem [10, 11]. The AASHTO SHSP supported this theory after discovering that only 4.2% of head-on crashes occurred during overtaking maneuvers [9]. Later studies, such as the ones performed by Kusano et al. (2013) and Garder et al. (2006), both found similar results concluding that overtaking was not a significant factor in head-on crashes [1, 2].

The AASHTO SHSP additionally looked at construction zones to investigate if different and unusual traffic patterns caused by construction influenced head-on crashes. The authors discovered that different traffic patterns were not an influence. Only 1.9% of non-interchange non-junction head-on crashes occurred in construction zones [9].

However, driver impairment was a factor in many of these crashes. Kusano found that alcohol was involved in 13.8% of serious injury opposite direction crashes and 17.1% of fatal crashes [1]. Garder similarly found that alcohol or drugs was a factor in 8.3% of all head-on opposite direction crashes and 11.1% of fatal crashes [2]

The major cause of these crashes that several studies have agreed on is a driver making an unintentional maneuver such as inadvertent lane departure. This could occur because the driver is distracted, asleep, or traveling too fast for road conditions [1, 2]. Garder found that illegal/unsafe speed played a role in 32% of crashes while driver inattention/distraction was a factor in 28%. In many cases the role of speed in causing a crash can be defined by the road conditions. Often people travel too fast on wet roads, lose control of their vehicle and cross over the centerline.

From infrastructure-based crash prevention methods, there may be little to be done about speeding. Speed limits can be reduced on roads that exhibit a high number of the geometric features discussed above that appear to influence the frequency of head-on crashes. However, several studies have shown poor obedience with posted speed limits and more importantly, that lowering the speed limit will not influence the average vehicle speed [12, 13].

1.4 Infrastructure Prevention Methods

Road departure crashes can be prevented through countermeasures, e.g. roadside barriers [14, 15], but cross-centerline crashes may require other countermeasures described in the discussion which follows.

1.4.1 WIDEN ROAD

One option for reducing the crash rate on these rural two lane roads is to increase the road width. As discussed in the above section, several papers have shown the influence of road and shoulder width on the crash rate of rural two lane roads [4, 6, 7]. However, expanding the width of a road is often expensive ($1-3 million/mile) and can take anywhere from 5 – 10 years [9].

Zegeer et al. (1980) proposed a method of evaluating the cost-effectiveness of expanding a road and suggested that individual states look at locations with a high crash risk and evaluate using his formula shown in Equation 1 [7].

$$B_{pw} = (C_a)(R)(N)(PWF) \quad (1)$$

where B_{pw} is the present worth benefits expected from a highway improvement, C_a is the average cost of each crash for each crash affected by the improvement, R is the annual percentage reduction in crashes due to widening, N is the annual number of crashes influenced by improvements, and PWF is the present-worth factor to convert benefits to present-day values [7]. This formula provided a quantitative way of assessing the potential benefits expected from a road widening project. In his study of run off road and opposite direction crashes, Zegeer found that wide lanes (11 – 12 ft lane width) had an crash rate of between 10-39% lower than narrow lanes (9 ft lane width) [7].

1.4.2 IMPLEMENTATION OF 2+1 ROADWAY DESIGN

One solution, implemented in some locations in Europe, is the 2+1 roadway design. Figure 2 illustrates how this design creates a passing lane for select sections of an expressway. The demarcation between the lanes of opposite direction traffic is either a lane marking or a cable barrier. Over 1000 km (600 miles) of roadways using this design have been installed across Europe as a way of reducing crashes on high volume two lane roads [16, 17].

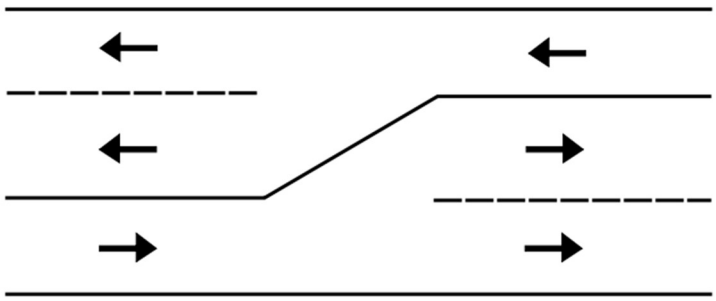

Figure 2. Example of a 2+1 roadway design. The most common divider between the lanes is either a painted line or a barrier.

Several studies have performed an analysis of the crash performance before and after the implementation of 2+1 lane roads [16, 17]. Potts et al. (2003) performed a meta-analysis of the use and effectiveness of 2+1 roads in Germany, Finland, and Sweden [17]. The two factors of interest were the average daily traffic and a comparison of the crash rate before and after the introduction of 2+1 roads. As can be seen in Table 3, results varied from a 22% reduction in crash rate up to a 55% reduction [17]. Sweden was the only country in the study that implemented a cable barrier between the two directions of travel. This barrier may have led to the higher reduction in crash rate compared to the other countries that only used painted lines as a divider.

Table 3. Daily Traffic Average and Comparison of Crash Rate. Data from Potts et al. (2003) [17].

Country	Average Daily Traffic(vehicles)	Change in Crash Rate
Germany	15,000-25,000	-36%
Finland	14,000 with peaks of 20 – 25k on weekends	-22 to -46%
Sweden	4,000 – 20,000	-55%

An evaluation of 2+1 road design conversions in Sweden by Carlsson et al. (2009) also found a high reduction in crash rate after implementation. Carlsson found a reduction of 76% in the number of fatalities on the roads that were converted to 2+1 design [16]. Supporting the above theory about the use of a physical barrier versus painted lines, he found that that the fatal-serious injury rate per million axle-pair km (FSI-rate) for 2+1 painted roads was 80% higher than 2+1 roads with cable barriers [16].

To fully evaluate implementing a 2+1 roadway design as a crash reduction method, Carlsson also evaluated the associated factors and possible drawbacks of a 2+1 design. There have been concerns that the use of a cable barrier separating lanes of opposing direction traffic might cause an increase in motorist severe injury rate [16]. Several studies have shown motorcycle collisions with barriers to be more severe than traditional car impacts with a barrier [18, 19]. Some motorcyclist activist groups have referred to cable barriers as "cheese cutters" [18]. Carlsson et al. (2009) conducted a study monitoring the fatal and serious injury rate per million axle-pair kilometers (FSI-rate) over a network of 1,170 km of 2+1 roads in Sweden in order to compare the FSI-rate for 2+1 roads to the nationwide rate. He concluded that there was no evidence to suggest an increased fatality risk for motorcyclists on 2+1 roads with cable barriers [16]. In the US, Daniello (2011) also found no evidence that cable barriers offer a greater injury risk than guardrails for motorcycles [18, 20-22].

Several reports have suggested that 2+1 road designs might be suitable in the United States on high traffic rural roads [16, 17]. However, to date no studies have been performed on the use or implementation of 2+1 roads in the United States.

1.4.3 CENTERLINE RUMBLE STRIPS

Centerline rumble strips are another solution for reducing head-on crashes that has been implemented in the United States. Similar to shoulder rumble strips, centerline rumble strips produce a vibration that alerts the driver if they drift out of their lane and into opposite direction traffic. Centerline rumble strips have a number of parameters including offset from centerline, continuous versus intermittent, and width and spacing between the individual rumble markings. Figure 3 below depicts a typical installation of a centerline rumble strip.

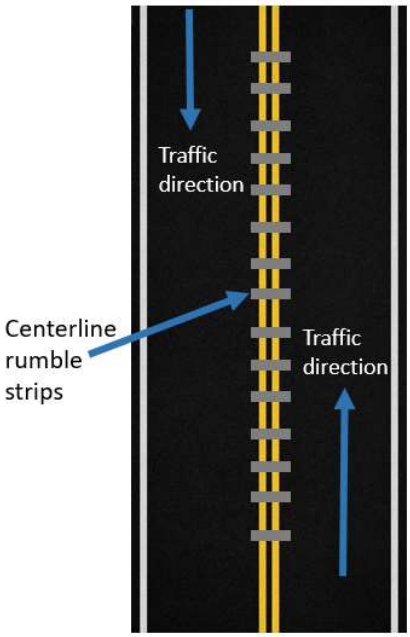

Figure 3-Road diagram for installation of a centerline rumble strip.

Numerous studies have been conducted on the effectiveness of using centerline rumble strips to reduce opposite direction crashes [23-32]. Torbic et al. (2009) compiled the results from individual state studies and past NCHRP reports in NCHRP report 641 to evaluate the design and application of centerline rumble strips. A summary of the individual reports from each state taken from NCHRP report 641 can be found below in Table 4 [23].

Table 4. Compilation of effectiveness numbers for centerline rumble strips for different collision types. Presented originally in Torbic et al. (2009) [23].

State/Location	Type of Facility	Type of Collisions Targeted	Percent decrease (–) or percent increase (+) in target collision frequency from application of shoulder rumble strips (standard deviation)	Type of analysis
California	Rural two–lane roads	Head-on (total)	-42%	Naïve before–after
		Head-on (fatal)	-90%	
Colorado [26]	Rural two–lane roads	Head-on	-34%	Naïve before–after
		Sideswipe	-36.5%	
Delaware [27]	Rural two–lane roads	Head-on	-95%	Naïve before–after
		Drove left of center	-60%	
		PDO	+13%	
		Injury	+4%	
		Fatal	N/A	
		Total	-8%	
Minnesota [28]	Rural two–lane roads	Total	-42%	Cross-sectional comparison
		Total(fatal and severe injury)	-73%	
		Head-on/opposite-direction sideswipe/ single vehicle run off road to the left(all severities)	-43%	
		Head-on/opposite-direction sideswipe/single vehicle run off road to the left(fatal and severe injury)	13%	
Missouri [29]	Rural two–lane roads	Total	-60%	Naïve before–after

Nebraska [30]	Rural two–lane roads	Cross-over crashes	-64%	
Oregon [31]	Rural two and four lane roads	Cross-over crashes	-69.5%	Naïve before–after
			-79.6%	Before-after with comparison group
Multistate [32]	Rural two–lane roads	Total	-14% (8-20%)	Empirical Bayes(EB) before-after
		Injury	-15% (5-25%)	
		Frontal/Opposite-direction sideswipe(total)	-21% (5-37%)	
		Frontal/Opposite-direction sideswipe(injury)	-25% (5 – 45%)	

Of particular importance for estimating the overall benefit of centerline rumble strips is the effect on head-on crashes. These studies have shown that centerline rumble strip installation reduced head-on crashes between 34 – 95% [23]. Averaging over each of these studies, head-on crashes were reduced by 65% [23]

Besides the crash reduction resulting from centerline rumble strips, the effect on driver behavior and potential negative effects must also be analyzed. One interesting effect of CRS that has been seen in several studies is an increase of lateral distance of vehicles from the centerline on roads with a CRS compared to roads without one [33-38]. CRS does not appear to make a significant difference in vehicle speeds as shown by the results of five studies [28, 33, 35, 36, 38]

There have been many concerns over the use of CRS however, many of them have been later shown to be unfounded. Some of the objections to the installation of CRS include additional maintenance requirements, high noise generation, the possibility that they inhibit passing maneuvers, or that they affect motorcyclists adversely [23].

Addressing the issue of additional maintenance, Neumann et al. (2008) reported that current states using CRS had reported any additional maintenance [9]. Torbic et al. (2009)

reported similar findings stating that the concerns of maintenance crews over the installation of CRS were largely unfounded [23].

The concern over the noise generated from the CRS has a basis in truth. To be an effective crash reduction measure, a CRS must generate enough noise and/or vibration to accurately alert the driver to an encroachment. In a study about the effects of CRS, some residents claimed to be able to hear this noise up to 1.2 miles away [39]. However, what is essential to the user acceptance of CRS is not necessarily the noise magnitude but the perceived irritation level of residents close to roads with CRS installed. In a survey of nearby residents, Gardner et al. (2006) found that the majority deemed the noise level to be acceptable/tolerable and the potential safety impacts outweighed the noise level [40].

One claimed issue with CRS is that they could affect motorcyclists adversely. During installation of CRS on roads throughout the state, Pennsylvania surveyed motorcyclists and found no major concerns over the use of CRS [9]. In a full study about the effects of centerline rumble strips on motorcyclists, Miller (2008) concluded that centerline rumble strips posed no additional risk to motorcyclists. This finding was supported by other studies [38, 41, 42].

While many of concerns over centerline rumble strips have been shown to be unsupported after implementation, one study found unexpected driver behavior upon encountering a centerline rumble strip. Noyce and Elango (2002) observed that drivers encountering centerline rumble strips did not always steer their vehicle back to the right as would be expected [43]. Upon encountering a centerline rumble strip, 27% of drivers steered to the left, the opposite of the intended response. In a later study, Noyce et al. (2006) proposed several different designs for centerline rumble strips in order to reduce this counterintuitive driver behavior [44].

As shown through numerous studies, centerline rumble strips have been proven to be effective at reducing head-on and opposite-direction crashes. However, centerline rumble strips require an initial infrastructure expenditure and cannot be used on all roads or in all locations such as on bridges, through intersections, divided roads, extremely narrow roads, roads with bad pavement, and unpaved roads [45].

1.4.4 SUMMARY OF INFRASTRUCTURE BASED SOLUTIONS

Table 5 below summarizes the benefits found from each infrastructure-based solution. As can be seen, the most effective infrastructure based method to reduce crashes on two lane rural roads in terms of installation time and cost is through the installation of centerline rumble strips. Other solutions require a high initial capital expenditure and can span multiple years.

Table 5. Summary of crash reduction effectiveness by solution

Solution	Effectiveness	Comments
Widen the Road	10% – 39% [7]	Long time frame(> 2 years) High relative cost
Implement 2+1 Roadway Design	22% - 55% (in Europe) [17]	Moderate time frame(1- 2 years) High relative cost
Centerline Rumble Strips	34 – 95% [23]	Short time frame(< 1 year) Low relative cost

1.5 Active Safety Systems

Another method of preventing or reducing the number of cross centerline crashes are vehicle based countermeasures. Vehicle based solutions are available anywhere as compared to infrastructure based solutions where the road must have been treated with the countermeasure prior to the crash. These vehicle-based solutions are often referred to as active safety systems or driver assistance systems. Some common driver assistance systems include antilock brakes [46],

intersection assistance systems[47, 48], automated emergency braking [49], lane departure warning [50-54], lane departure prevention [54], and blind spot monitors [55].

1.5.1 LANE DEPARTURE WARNING AND PREVENTION SYSTEMS

Of particular interest to cross-centerline and run off the road crashes are lane departure warning (LDW) and lane departure prevention (LDP) systems. Although specific activation criteria are typically proprietary, a LDW system works by alerting a driver when the system detects that the vehicle is moving out of the original lane and is not using a turn signal [56]. While the specific alert delivered can vary based on the OEM, the alert is generally either visual (icon in the dashboard), audible (beeping), or tactile (steering wheel or seat vibration) [56]. The primary purpose of this system is to alert distracted drivers and help reduce crashess involving the inadvertent crossing of a lane line. LDP provides the same alert as LDW but can also provide automatic steering or one sided braking input to guide the car back to the original travel lane if no action from the driver is taken. Another version of LDP, called lane keeping assist (LKA), is used to maintain a car's position in the center of a lane. Similar to LDP systems, a LKA system can provide a steering input to nudge the car back towards the center of the lane if the LKA system detects that the vehicle is nearing the lane edges. An illustration of a LDW/ LDP system in action is displayed in Figure 4.

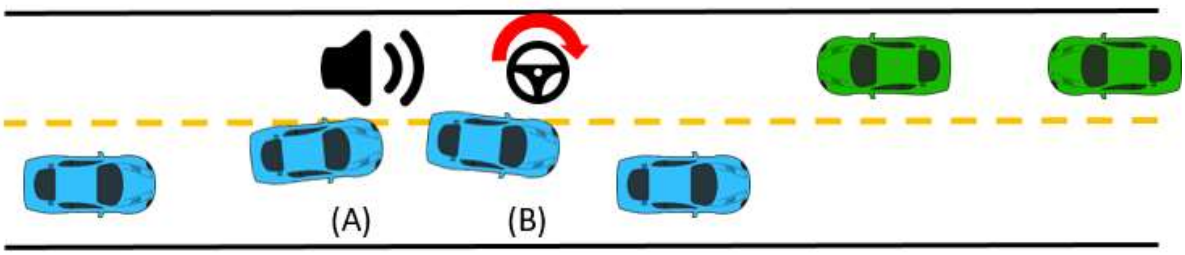

Figure 4. A) The vehicle begins to cross over the lane line and a warning is given to the driver. B) Either the driver takes steering action or the LDP system automatically initiates steering.

A key factor that affects the performance of driver assistance systems is driver acceptance of these features. Drivers have the capability to turn off lane departure warning and lane departure prevention systems. A common reason for turning off these systems is driver annoyance at frequent activation. One study performed by the Insurance Institute for Highway Safety (IIHS) investigated driver acceptance of LDW systems in comparison to another driver assistance system, forward collision warning (FCW) [57]. While FCW systems were enabled in nearly all vehicles, LDW systems were found to be disabled in 66% of the cars investigated [57]. Improving driver acceptance of LDW and LDP systems is essential to improving potential benefits of these technologies. To better tailor active safety systems to match driver expectations, multiple studies have been conducted to monitor driver braking and steering during normal driving [13, 58-63].

Several studies have investigated the effectiveness of LDW in preventing road-departure crashes [50, 54, 56]. In these studies, the primary objective was the impact on road departure crashes. The potential effectiveness of LDW in preventing cross-centerline crashes was not considered. Gordon et al. (2010) reported a LDW effectiveness of 13 – 31.5% using the advanced crash avoidance technologies (ACAT) methodology to evaluate a hypothetical LDW system [56]. Using data from 2007 – 2011, Gorman et al. (2013) estimated crash reduction benefits of 20.3% and a reduction of serious injuries of 25.8% [50]. More recently, Scanlon et al. (2015) estimated benefits of 26.1% in all crashes and a 20.7% reduction in serious injury crashes using 2012 NASS-CDS data [54].

One major limitation of LDW systems is the dependence on roadway infrastructure. Current LDW systems require painted lane markings in order to activate and determine when a vehicle is leaving the original travel lane. Scanlon et al (2015) took roadway infrastructure

parameters, such as lane marking presence and shoulder width, into account in an estimation of LDW benefits using NASS/CDS data [64]. Using current conditions for roadway infrastructure, he estimated crash reduction benefits of 28% for a LDW system [64]. However, in a best-case scenario where all lane markings were present and shoulders were expanded to a standard 3.6m width, he estimated crash reduction benefits of 72% [64]. The drastic difference between the two estimates illustrates the impact of roadway infrastructure on the performance of a LDW system.

To date, many papers on the benefits of LDW have only focused on run off road right side departure crashes because these crashes occur much more frequently than head-on and cross-centerline crashes. Using data from 2004 – 2008, Jermakian et al. (2010) estimated that LDW technology would apply to 73,000 - 94,000 single vehicle crashes annually versus 9,000 - 10,000 head-on crashes [65].

However, LDW also has the potential to function as a crash avoidance measure for cross-centerline and run off to the left crashes also. This means that application of a LDW system could have substantial benefits for mitigating opposite direction head-on crashes if at least one vehicle crossed a centerline or lane line prior to the crash.

1.5.2 HEAD-ON CRASH AVOIDANCE SYSTEMS

Until recently, there have only been a few studies on designing driver assistance systems specifically for head-on crash prevention. In a report to Congress in 2011, NHTSA reported the need for a new data element in the National Automotive Sampling System (NASS) accounting for the presence of a head-on crash avoidance system [66].

Researchers at Dynamic Research Inc. have evaluated a safety impact methodology using a pre-production head-on crash avoidance assist system (HCAAS) [67-70]. This system used yaw rate sensors to detect when a vehicle was experiencing a lateral drift and radar to detect an

oncoming vehicle. The HCAAS was primarily designed for opposite direction crashes where the driver was distracted prior to the crash. In order to alert the driver to the impending crash, the HCAAS uses an audible warning as well as automatic application of a small amount of steering torque to the wheel [69]. This steering torque was not enough to control the vehicle but was used as a haptic means of alerting the driver. Once the HCAAS system deemed a crash imminent, primarily through the use of radar, the system could also apply braking to reduce the delta-V of the crash [69]. A diagram of the sequence of events leading up to the cross-centerline crash with a HCAAS system is shown in Figure 5.

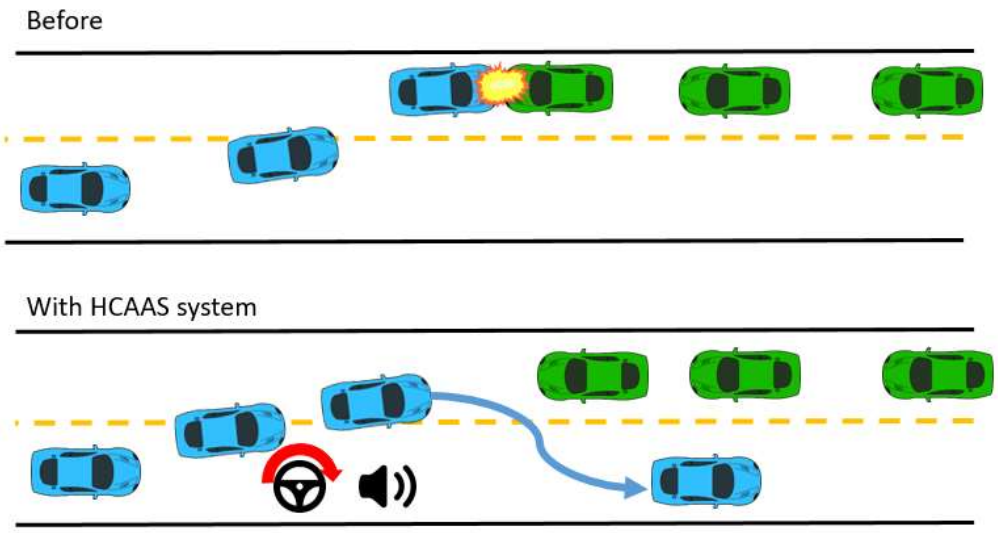

Figure 5. Sample HCAAS crash scenario. Originally the vehicle 1 (blue) impacts the vehicle 2 (green) head-on. With a HCAAS installed and operational on vehicle 1, the system activates steering and provides a warning to the driver as the vehicle is drifting over the centerline. The driver reacts to the warning and steers to avoid the crash.

In applying this system to "Same Trafficway, Opposite Direction crashes" and the 2009 nationwide US light passenger vehicle fleet, Zellner et al. (2015) estimated a 2.6% reduction in all severity crashes and an 11.3% reduction in fatalities [70]. This is lower than the benefits found in other driver assistance systems like LDW discussed previously.

1.6 Research Objective

The objective of this research was to estimate the potential safety benefits of lane departure warning on cross-centerline crashes. As we have seen previously, cross-centerline crashes are a severe crash mode due to the high speeds of both vehicles. While past research has primarily focused on LDW systems and run-off-road crashes, an LDW system has the potential to help alleviate this crash mode. This study contains a process for reconstructing and simulating crashes with a LDW system installed, estimations of the crash benefits of a LDW system if installed on every vehicle in the US vehicle fleet, and an estimation of the potential injury benefits of a LDW system.

1.7 Structure

This thesis presents the simulation models that were used in order to reconstruct and simulate crashes with a LDW system. As part of this, each building block of the simulations is presented in a separate chapter culminating with an estimation of crash and injury benefits of a LDW system. This first chapter presented background on cross-centerline crashes and current active safety systems. Chapter 2 presents the data sources used in this study and the reason why each was used. The process for reconstructing cross-centerline crashes is examined in Chapter 3 and Chapter 4. These chapters describe how the vehicle trajectories, vehicle speed, and driver actions, were modeled prior to the crash. Using this information, the final crash simulations were built and are discussed in Chapter 5. Details from these crash simulations in Chapter 5 are used to estimate the injury benefits discussed in Chapter 6. Finally, Chapter 7 presents a summary of the findings from this study.

2 Data Sources

2.1 Introduction

This study was based on multiple sources of U.S. crash data. This section aims to provide a brief introduction and rationale for the use of each data source in this study.

2.2 NMVCCS

The National Motor Vehicle Crash Causation Survey (NMVCCS) was a crash investigation program sponsored by the National Highway Traffic Safety Administration (NHTSA). The primary objective of the study was to collect data on pre-crash vehicle actions and conditions with the intent of using the information to evaluate potential crash avoidance technologies [71].As such, the focus of this study was on passenger vehicles and light trucks. Minimal information was collected for other types of vehicles. Cases for NMVCCS were investigated from 2005 to 2007 forming a total case set of 6,949 crashes in 24 primary sampling units (PSUs) across the United States. Of these, approximately 1,479 crashes were training cases that were used to teach investigators how to properly code all elements of a crash. The remaining 5,470 cases formed a nationally representative sample with each case assigned a national sampling weight representing the number of similar crashes in the United States that occur annually. At each crash, NMVCCS investigators had to be on-scene prior to the scene being cleared of vehicles and debris [71]. Being on-scene so soon after the crash allowed investigators to create detailed scene diagrams depicting the each vehicle's final rest position and their estimated movements prior to the crash. Additionally, witnesses and involved occupants were able to be questioned. The wide amount of information available to the NMVCCS investigators on-scene also allowed them to determine critical factors that led up to the crash.

Throughout this study, cross-centerline crashes from NMVCCS formed the main simulation set in this study. The reason this crash database was used as the primary data source in this study was twofold: 1) trained investigators were on-scene prior to the crash being cleared. This lends credibility to the accuracy of the prepared scene diagrams for each crash. In other crash databases, like NASS/CDS, investigators can come any time after a crash has been cleared, often any time from a week to a month after the crash, and subsequently attempt to prepare a scene diagram from the evidence left behind. 2) NMVCCS was used was due to the investigators determining the critical factors that led up to the crash. When simulating a LDW system, these critical factors were used to determine the driver capability to react to a lane departure warning.

2.3 NASS/CDS

The National Automotive Sampling System (NASS) was established in 1979 in an effort by NHTSA to increase traffic safety [72]. The Crashworthiness Data System (CDS) was one part of NASS that aimed to form a nationally representative case set of crashes in the United States. NASS/CDS was composed of 24 teams of trained investigators located in different parts of the United States. Approximately 4,000 - 5,000 crashes were investigated every year until 2015 when data collection officially ended [72]. For each case, investigators prepared scene diagrams, conducted interviews with observers and crash participants, and documented the scene and surrounding evidence. To be included in this database, at least one vehicle involved in the crash had to be towed away. Additionally, at least one vehicle involved in the crash had to be a passenger car or light truck. When possible, the delta-V for each vehicle was found using the WinSmash code [73-76]. Like NMVCCS, each case in this dataset was assigned a sampling weight to make the database nationally representative.

The main use of the NASS/CDS database in this work was to use the event data recorder (EDR) data recorded as part of the investigations. As cases for NMVCCS were investigated from 2005 – 2007, there are only a small amount of vehicles that were equipped with EDRs. The large number of cases in NASS/CDS provided enough EDR equipped vehicles for use in this study. For the purposes of this study, NASS/CDS data from years 2000 – 2015 was used.

2.4 Injury Severity

A secondary use for the NASS/CDS database in this study was to determine injury benefits of a LDW system. In NMVCCS, injury outcomes were determined from the police reports and evaluated on the KABCOU scale. The KABCOU scale is used by police officers on the scene of the crash to evaluate occupant injuries. The KACOU scale has 5 levels: K – Killed, A – Incapacitating, B – Non-Incapacitating, C – Possible Injury, O – No Injury, and U – Unknown Injury.

Medical data in NASS/CDS is not coded using the KABCOU scale. Instead, NASS/CDS investigators use the medical records of each occupant in the crash to assess the severity of occupant injuries using the Abbreviated Injury Severity (AIS) scale. The Association for the Advancement of Automotive Medicine (AAAM) developed the original AIS scale in 1969 in order to classify the threat to life associated with injury [77]. The AIS scale has been regular updated since then with the most recent updates occurring in 2008 and 2015.While the KABCOU scale provides a quick method of assessing occupant injuries, the AIS scale provides more detail through coding the type, location, and severity of each injury. There are 7 levels for the injury severity: 1 – Minor, 2 – Moderate, 3 – Serious, 4 – Critical, 5 – Critical, 6 – Maximum, and 9 – Not further specified.

Compton et al. (2005) performed an analysis comparing KABCOU scores to AIS score in NASS/CDS data and found that generally the KABCOU scores were accurate when compared to the AIS scores [78]. However, in some instances, Farmer et al. (2003) illustrated that police officers using the KABCOU tended to overestimate occupant injury levels [79]. A common mistake was coding an injury as "incapacitating" when the injury was only rated as minor on the AIS scale. As KABCOU is an injury assessment performed by police officers on-scene, we can expect that AIS scores are more indicative of the actual occupant injuries.

In this research, injury risk curves developed from NASS/CDS medical records using the AIS scale were used to determine the potential injury benefits of a LDW system [80].

2.5 EDR Records

Event data recorders (EDR) are commonly referred to as the "black boxes" of cars [81, 82]. While the data elements differ by OEM, EDRs typically record up to 5 seconds of pre-crash vehicle kinematics and up to 300ms of crash data. Common pre-crash data elements recorded by EDRs include vehicle speed, brake application, accelerator application, yaw rate and steering wheel angle [83]. Event data recorders function using a circular buffer which means that EDRs always record data but the data is only saved if a deployment or non-deployment event occurs [83]. One example of a deployment event is when an airbag deploys during a crash. Non-deployment events occur when an airbag is not deployed but an acceleration threshold is crossed leading the EDR to store the data prior to the activation event [83]. If no activation event occurs for an EDR, no data is recorded.

As part of each NASS/CDS and NMVCCS case, investigators downloaded the EDR data if the vehicle was equipped with an EDR. Because the NMVCCS crash investigations were conducted only a few years after the introduction of EDRs, far fewer of the cases in NMVCCS

had EDRs installed compared to NASS/CDS. For this study, only EDR records from NASS/CDS were used.

There were specific filters used to select EDR records to ensure the quality of the data. To ensure the recorded data was associated with the initial impact from the crash, records were only included if the EDR recorded an airbag deployment or a non-deployment event with a greater than 5 mph delta-V. A threshold of 5 mph was chosen for the delta-V as this value tends to result in significant vehicle damage and is unlikely to occur from subsequent events in the crash sequence. To ensure that the first event in the EDR corresponded to the primary impact event, the most severe impact in the crash had to be the first one. Additionally, as the primary data elements for use in this study were the pre-impact speed and braking application, both of these data elements had to have been successfully recorded for 5 seconds prior to the crash. EDRs that recorded less than 5 seconds were excluded. These filters have been used before to successfully analyze EDR records and examine pre-crash vehicle kinematics [84].

EDR records in this study were used as the basis for a model estimating the approach speed of a vehicle prior to a cross-centerline crash. This model aims to extrapolate the approach speed of a vehicle based on the impact speed and environment factors. This was necessary in order to form a full speed profile of both vehicles prior to the crash. The knowledge of pre-impact speeds and vehicle kinematics that EDRs provide was essential to forming this approach model.

3 Reconstructing Cross-Centerline Crashes

3.1 Introduction

Knowledge of each vehicle's movements and speed prior the crash was essential in reconstructing and the subsequent simulation of the crash. In this study, a complete crash reconstruction consisted of two pieces of information: knowledge of the full vehicle trajectory prior to the crash and the vehicle speed profile prior to the crash. Using this knowledge, crashes can be simulated to determine whether an LDW system could have prevented or mitigated a cross-centerline crash. This section describes the process that was used to reconstruct all of the crashes used in this study.

3.2 Trajectory Reconstructions

The main objective of trajectory reconstruction was to determine the path of each vehicle prior to the crash. The primary data source for trajectory reconstructions was the scene diagram drawn by the NMVCCS investigators. As the NMVCCS investigators were on the crash scene prior to the scene being cleared, they were able to accurately determine each vehicle's final rest position. By accurately documenting the final rest position, crash scene debris, and closely inspecting each vehicle, scene investigators can determine an approximate impact point and heading at impact for both vehicles. Common evidence found on a crash scene includes broken headlights, broken glass, puddles of oil or gasoline, and skid marks. Each of these pieces of evidence guide the crash investigator when drawing the scene diagram. Another source of information for the scene diagram are witness and involved occupant interviews. These interviews provide details on the approximate motion of the vehicles prior to the impact. To estimate each vehicles pre-crash motion, the investigator takes into account witness interviews, impact position, and the vehicle inspections, and extrapolates backwards to known positions. For

example, in a cross-centerline crash, scene investigators are able to estimate based on witness interviews that both vehicles were traveling in their appropriate lane prior to the crash.

As can be seen in Figure 6, the investigators drew a vehicle image at each point along the vehicle's trajectory prior to the crash. These scene diagrams were then stored as scaled drawings in Easy Street Draw (A-T Solutions Inc.). Some select scene diagrams were stored in Microsoft Visio. The process that follows applies to these scene diagrams as well.

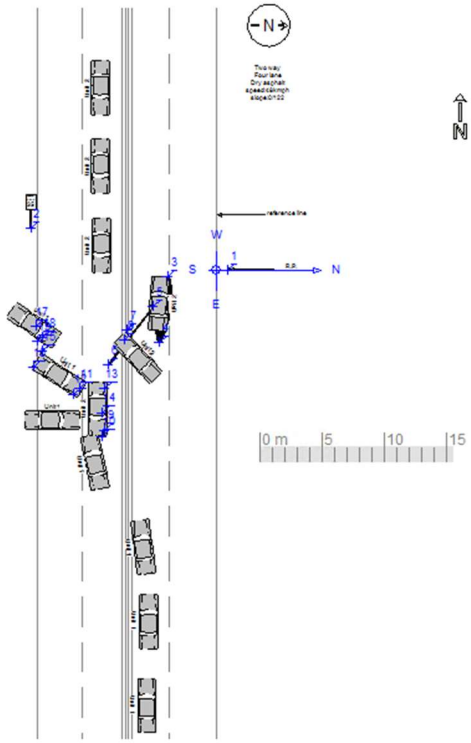

Figure 6. Scene diagram from NMVCCS case #2005012695762. Vehicle 1 travels north, crosses the centerline, and impacts Vehicle 2 head-on.

Previous attempts at performing trajectory reconstructions have performed measurements using offsets from known objects on the scene diagram such as the boundary of an intersection [48]. This method uses a set point on the scene diagram as the origin point for the global reference frame. Having a clear global reference frame is necessary in order to reconstruct the movement of all moving vehicles and accurately determine where one of them crossed the

centerline. The approach of this thesis was to import the scene diagram into AutoCAD and use the AutoCAD coordinate system. By default, AutoCAD incorporates a world coordinate system that researchers can use to identify each feature of a scene diagram in a global reference frame. When a new AutoCAD file is created, a world coordinate system is generated with an automatic origin point of (0, 0). To prepare the scene diagrams, researchers first drew a ruler on the scene diagram using the built in measurement tools in Easy Street Draw or Visio. Then, the scene diagram was imported into AutoCAD and, using the ruler drawn beforehand, the appropriate scaling factor was applied. As the scene diagram depicts the movements of each vehicle prior to the crash, the front-center of each vehicle position shown on the scene diagram was marked as a point. The start and end point of each of the lane markings shown were also marked as points with respect to the AutoCAD coordinate system origin.

This method of recording vehicle trajectory resulted in a point at each vehicle position shown prior to and including impact. However, we also wanted to know the most likely path the vehicle took between these discrete points. Our approach was to determine a "path to point" variable that described the motion of the front center of the vehicle in between each of the vehicle positions recorded earlier. This could either be straight or curved. An example is shown in Figure 7. This description allowed a continuous description of each vehicle's movement between the discrete vehicle positions recorded.

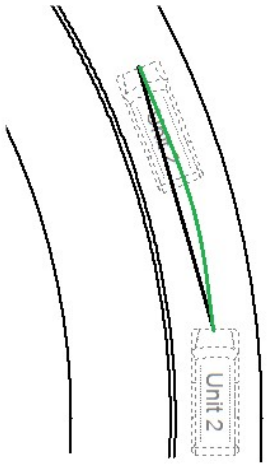

Figure 7. Depiction of the path to point. The black line represents a straight path while the green line represents a curved path. In this scenario, the green path is the most likely vehicle path.

The vehicle heading was also recorded for each vehicle position shown on the scene diagram. The vehicle heading was measured using dimensions in AutoCAD. In the case that the vehicle heading did not match the measured trajectory, we assumed the vehicle heading on the scene diagram was drawn wrong. In this case, the vehicle heading was changed to match the vehicle trajectory. An example of where this occurs can be seen in Figure 8. In this case, the scene diagram shows a lane departure angle of 3 degrees. However, the trajectory of the vehicle indicates that the vehicle actually has a lane departure angle of 8.4 degrees. In a physical sense, the vehicle heading and trajectory must match while the vehicle is tracking on the road. For reconstruction of these crashes, the vehicle heading was matched to align with the vehicle trajectory.

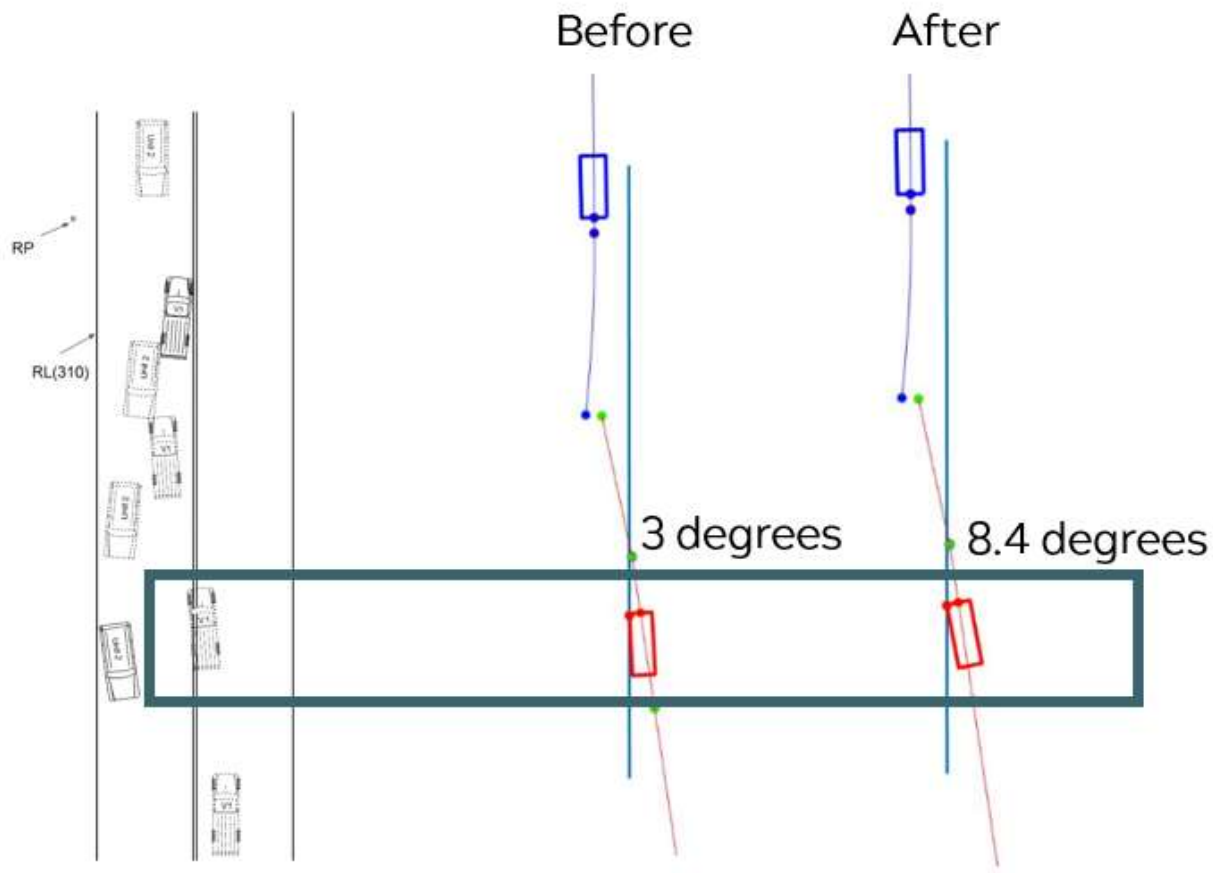

Figure 8. NMVCCS Case Number: 2006005289522. Example of where the heading of the vehicle as drawn on the scene diagram does not match the recorded vehicle trajectory.

A complete list of the measurements collected for each case is shown in Table 6.

Table 6. All measurements collected along with the source of the measurement.

Type	Necessary Measurements	Source
Vehicles	Front Center of vehicle (x,y)	AutoCAD
	Heading (deg)	AutoCAD
	Path to point (straight/curved)	Researcher Judgement
Lane Markings	Start Point (x,y)	AutoCAD
	End Point (x,y)	AutoCAD

	Path to Point (straight/curved)	Researcher Judgement
	Radius of Curvature (meters)	Easy Street Draw

Figure 9 displays an example of a completed measurement file. The full protocol for conducting measurements is attached in the

Appendix. Measurements were performed for all cases in the dataset.

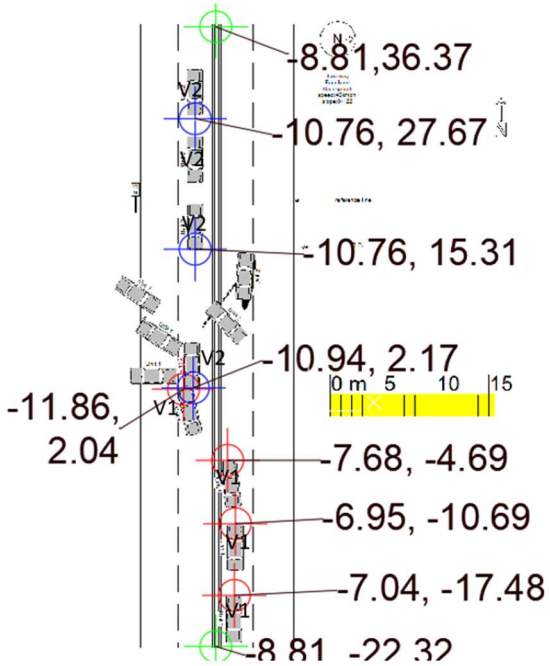

Figure 9. NMVCCS scene diagram from case #2005012695762 after annotation with measurements. Red points are the front center of vehicle 1. Blue points are the front center of Vehicle 2. The green points mark the start and end points of the lane lines.

MATLAB was used to reconstruct the vehicle trajectories from the recorded data elements in AutoCAD. Vectors were used to describe the vehicle path from the data points recorded on the scene diagram. If the path to point was described as straight, the vehicle was assumed to travel in a straight line in between the points. For the purposes of describing a curved path between points, a circle was fit in between the points. An iterative process was used to find the radius of curvature that fit between two points. This process assumed that the vehicle was tangent to the circle and consequently, that the center of the circle was perpendicular to the vehicle heading at the first point. At each point, the distance between the proposed circle center and both of the points was calculated. If the distance between the points was equal, that was assumed to be the

circle radius. Figure 10 shows this process visually.

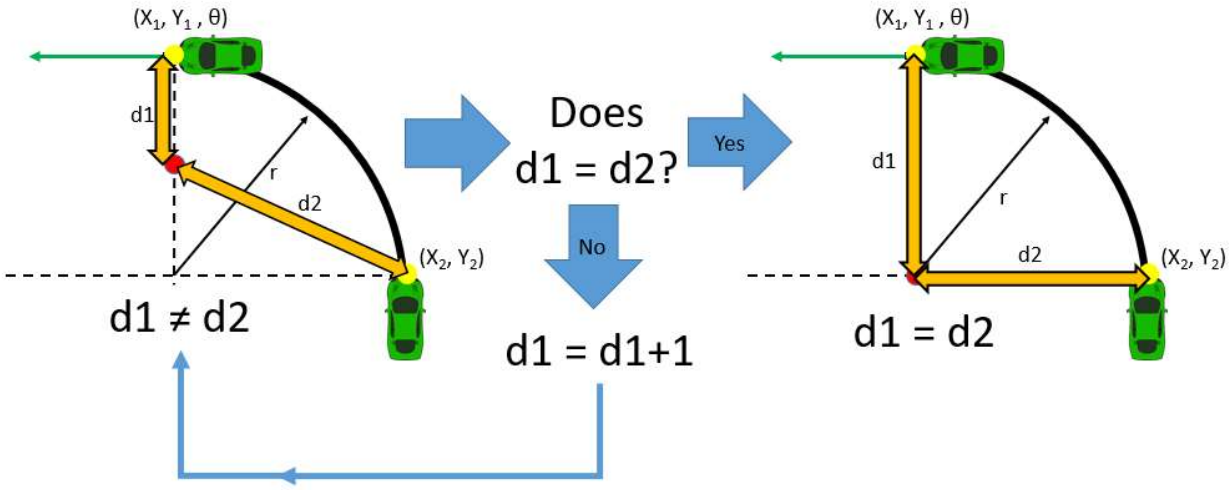

Figure 10. Process to fit a circle between two vehicle position points. X and Y represent the vehicle position at both points and θ represents the heading of the vehicle. In this scenario, r is the radius of the circle and is unknown.

This process had to be used because the radius of the circle between the two points was not known. In the case of lane lines, if the lane line was curved, the radius of curvature was measured and recorded. This meant that the method presented above was not necessary to represent the lane lines. A sample trajectory reconstruction is provided in Figure 11. The green dots indicate the measured trajectory points for vehicle 1 (in red). The blue dots indicate the trajectory points for vehicle 2 (in blue).

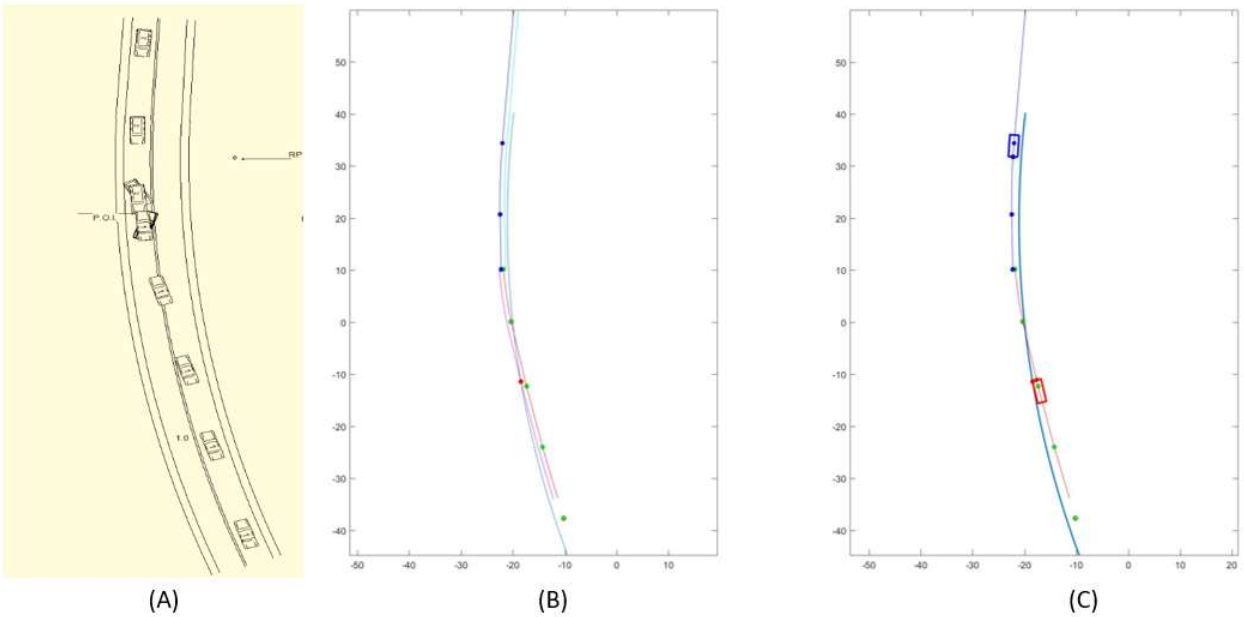

Figure 11. NMVCCS case number 2005011269043. (A) Original NMVCCS scene diagram. (B) Vehicle trajectory reconstruction in MATLAB. (C) Vehicle animation with accurate vehicle dimensions.

3.3 Speed Reconstruction

The speed profile of the vehicle was developed by estimating the impact speed and the approach speed of the vehicle and interpolating between them. Figure 12 shows the phases of a cross-centerline crash. The first phase is the approach phase and the crash ends at the impact phase. An approach model developed using EDR data was used to determine the approach speed given the impact speed. This model is discussed in more detail in Chapter 4. This section describes the process used to reconstruct the speed of the vehicle during the impact phase.

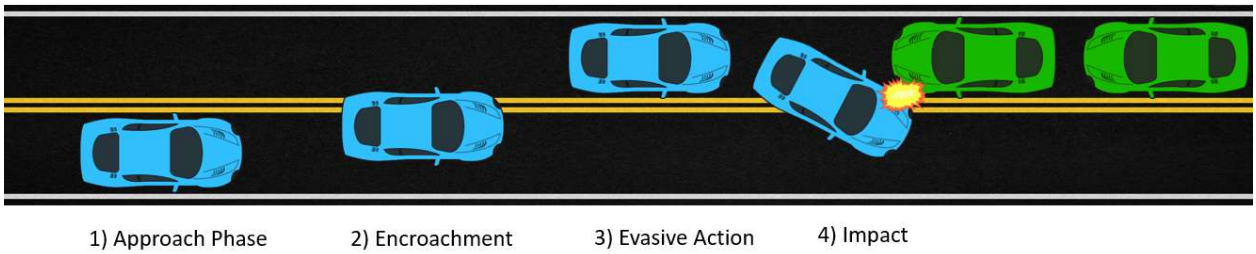

Figure 12. Phases of a cross-centerline crash. This section describes the process of reconstructing the impact speed for all cases.

The impact speed of both vehicles was determined using the crash simulation software PC-Crash 10.0. PC-Crash uses an impulse-restitution model and models forces around a point of intersection between the two vehicles [85]. This study used PC-Crash to conduct 2D crash reconstructions. Vehicle models were placed at the point of impact and simulated to match the final rest positions shown on the scene diagram. The built in collision optimizer within PC-Crash was used to run the simulations and minimize the error in trajectory post-impact. The impact model and collision optimizer function have both been validated in previous studies [86, 87].

All of the crash reconstructions using PC-Crash were performed using a team of researchers. Researchers would download the scene diagram from NMVCCS and use the diagram as the main source of information for the PC-Crash reconstructions. The scene diagram was first imported into PC-Crash and scaled appropriately.

Using the scene narrative and coded information, the make and model of each vehicle was determined. The PC-Crash vehicle database includes the Canadian Vehicle Specifications database. This database was used to import a 3D model of each vehicle involved in the crash. Each vehicle model accurately represented the vehicle dimensions, weight, and vehicle characteristics [85]. Each vehicle model was added and modified to account for the occupants' weight. Intermediate and rest positions were then placed to account for both vehicles' movement post-impact. The surface friction was also modified depending on the surface condition of the road at the time of the crash.

The collision optimizer with the built in genetic algorithm was used to simulate the crash and account for the post-impact movement of both vehicles. Researchers could manipulate the initial impact speed, braking level of both vehicles, and could add custom steering in order to

make the simulation more representative of what was thought to have occurred. A full description of the reconstruction process using PC-Crash is provided in the Appendix.

3.4 Heavy Vehicle Crashes

3.4.1 Motivation

The reconstruction methodology described above has a primary limitation in that the methodology does not deal with special vehicles or rollovers. In this study, a special vehicle was defined as a vehicle that did not appear in the Canadian Vehicle Specifications database in PC-Crash. Examples would include motorcycles, school buses, and tractor-trailers. Heavy vehicles, such as a school bus or tractor-trailers, were specific objects of interest because crashes with a heavy vehicle account for a significant portion of all crashes. Heavy vehicles were also expected to cause more severe injuries due to the large differences in weight and stiffness in a crash between a heavy vehicle and a passenger vehicle. In an active safety study involving straight crossing path intersection crashes, Scanlon et al. (2016) discovered 34 heavy vehicle crashes which represented 8,136 crashes nationwide [48]. In this simulation case set of cross-centerline crashes, heavy vehicle crashes accounted for 5 cases representing 2,181 crashes nationwide. The purpose of this reconstruction methodology was to develop a reconstruction method in order to reconstruct these crashes and subsequently, to validate the methodology.

3.4.2 Reconstruction methodology

Heavy vehicle crashes were selected in this study using the BODYTYPE variable in NMVCCS. In NMVCCS a value of < 49 for the BODYTYPE variable indicates that a vehicle is a passenger vehicle or light truck. Initially heavy vehicles were selected by ensuring the BODYTYPE was between 50 and 79. This eliminated motorcycles, all-terrain vehicles, and

other vehicles such as snowmobiles. Then each case was manually reviewed in order to ensure that there was a model in PC-Crash that could accurately simulate the non-passenger vehicle in the case.

The heavy vehicle descriptor used in this paper refers to any vehicle that had a gross vehicle weight rating of greater than 4,536 kgs. This is the cutoff used in the NMVCCS coding manual for discerning passenger vehicles and light pickups from heavy vehicles [88]. The heavy vehicle category included vehicles such as single unit straight trucks, motorhomes, school buses, and tractor-trailers (18 wheelers). To accurately identify the heavy vehicle, a VIN decoder service was used along with coded make and model information and photos of the heavy vehicle on-scene and after the crash [89].

All heavy vehicle crashes were reconstructed using PC-Crash version 10.0. As originally stated in Section 3.3 Speed Reconstruction, the basic process for reconstruction used the scene diagram with vehicle models and modeled both vehicle's movement from the impact point to the rest position. However, because there was no base vehicle model for heavy vehicles, our approach was to start with a custom vehicle model and then modify the vehicle model to fit the specific characteristics of the heavy vehicle in the crash. Custom vehicle models are provided in PC-Crash as generic versions of common objects and vehicles on the road [85]. Each model is customizable to match specific vehicle characteristics. For the purposes of heavy vehicle reconstructions only the following models were used: Truck_2axle, Truck_3axle, Truck_3axle (Semitractor), Truck_4axle, and Trailer models. The majority of reconstructed cases used the Truck_2axle model with custom specifications. Other than the insertion of a custom vehicle, all other steps of the PC-Crash reconstruction protocol were followed.

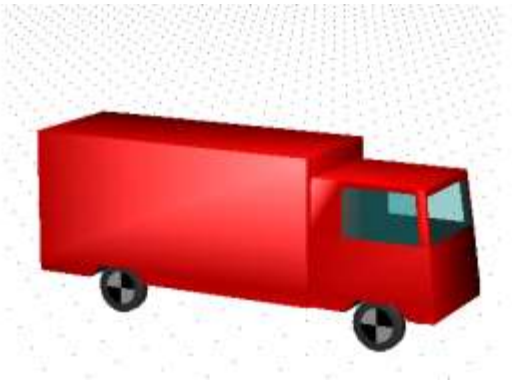

Figure 13. Generic truck_2axle model in PC-Crash. This model was commonly used with custom specifications for heavy vehicle crash reconstruction.

As the stiffness of a heavy vehicle is much higher than the stiffness of most passenger vehicles, the most important characteristic to accurately simulate was the weight of the heavy vehicle. The weight and other specifications of the heavy vehicle such as length, width, and wheelbase, were found and recorded from specification sheets found online. An example specifications sheet for a GM School Bus is shown as an example in Appendix A2 [90]. The development of these heavy truck models involves approximations. Often, the exact specifications of a heavy vehicle with custom modifications cannot be determined. In these cases the closest model found, using pictures to compare, was used.

3.4.3 VALIDATION

The reconstruction methodology was validated by comparing PC-Crash reconstructions with EDR data when available. For validation purposes, EDRs from NASS/CDS were used. As discussed in Chapter 2, EDRs provide a recording of pre-crash vehicle kinematics. Cases were selected from the NASS-CDS database instead of NMVCCS due to the larger EDR dataset available in NASS-CDS. For case selection, one of the vehicles involved in the crash had to have an EDR installed and the EDR must have recorded pre-crash velocity. To select for heavy

vehicle crashes, each crash had to involve a vehicle with a value for the NASS/CDS variable, BODYTYPE, between 50 and 79. This range of NASS/CDS body types included vehicles such as school buses and tractor trailers, but excluded non-relevant vehicles such as motorcycles.

Multiple crash scenarios were used in order to select the maximum number of crashes for validation. All intersection crashes, such as straight crossing path and left turn across path, were included as well as cross-centerline crashes. These scenarios were chosen because this reconstruction methodology was used in the reconstruction of those crash types.

The vehicle impact speed was determined from linear extrapolation using the EDR speed data. This method was used to account for the uncertainty between when the crash occurred and when the EDR started recording. EDRs record data continuously while a vehicle is in motion, but only save the data in the event of a crash. This poses problems when determining impact speed as different OEMS have different methods to designating the time when the event occurs. Toyota EDRs record the vehicle speed as t=0 at the moment of the crash. However, when a crash occurs for a GM EDR, the last vehicle speed is recorded as t = -1 seconds prior to impact. With the exception of Toyota EDRS, this linear extrapolation method was used as an approximation for impact speed in order account for the difference in timelines between the EDR data and the actual crash timeline.

In each case, the two earliest recorded data points taken prior to the crash were used to extrapolate forward to a point at ½ the EDR sampling rate. As an example, if a GM EDR recorded velocity at 1 Hz, the impact speed would be extrapolated from a time at t=-2 seconds and t=-1 seconds to find the speed at t=-0.5 seconds prior to the crash..

Note that in heavy vehicle crashes, we only had access to the EDR data from the passenger vehicle. As NASS-CDS is primarily focused on passenger vehicles, investigators are

not required to fully inspect heavy vehicles, take pictures, or download the EDR data from the heavy vehicle.

3.4.4 RESULTS

The initial dataset contained 14 crashes in NMVCCS involving heavy vehicles. In three cases, a heavy vehicle experienced rollover. These crashes could not be reconstructed. A total of six additional cases were excluded because they did not fit the cross-centerline crash scenario. These crashes were either wrong side of the road crashes or sideswipe crashes. This resulted in a total of 5 heavy vehicle crashes representing 2, 181 crashes nationwide. Table 7 presents the reconstruction results for the NMVCCS dataset.

Table 7. NMVCCS heavy vehicle reconstruction results

Case Number (NMVCCS)	Vehicle 1 Make/Model	Vehicle 2 Make/Model	Vehicle 1 maximum KABCOU Injury Level	Vehicle 2 maximum KABCOU Injury Level	V1 Impact Speed 1 (kph)	V2 Impact Speed (kph)	V1 Delta-V (kph)	V2 Delta-V (kph)
2006005290002	Oldsmobile Cutlass	Chevrolet Series 3500	Injury, severity unknown	No injury	80	41	-59.8	-23.6
2006005496962	Chrysler Sebring	Chevrolet Single Unit Straight Truck	Injury, severity unknown	No injury	63	30	-44.4	-9.4
2006076597143	Dodge Grand Caravan	Freightliner Motorhome	Non-incapacitating injury	No injury	49	53	-13.8	-6.2
2007002585051	Nissan Frontier Crew Cab	Freightliner 106 Medium Duty M2	Incapacitating Injury	Possible Injury	135	65	-64.8	-7.2
2007011583249	Ford Taurus	Chevrolet C7 7000 Medium Duty Truck	Non-incapacitating injury	No injury	24	0	-23.8	0.03

In four out of the five crashes involving a heavy vehicle, the driver of the heavy vehicle was uninjured while the driver of the other vehicle suffered some level of injury. There are clear

differences in average impact speed and delta-V experienced between the passenger vehicles and the heavy vehicles. Passenger vehicles tend to be traveling faster than heavy vehicles and experience much greater delta-V values than the heavy vehicles experience. Although this is a very limited dataset, the greater delta-V was to be expected due to the drastic differences in weight between a heavy vehicle and a standard passenger vehicle such as a sedan.

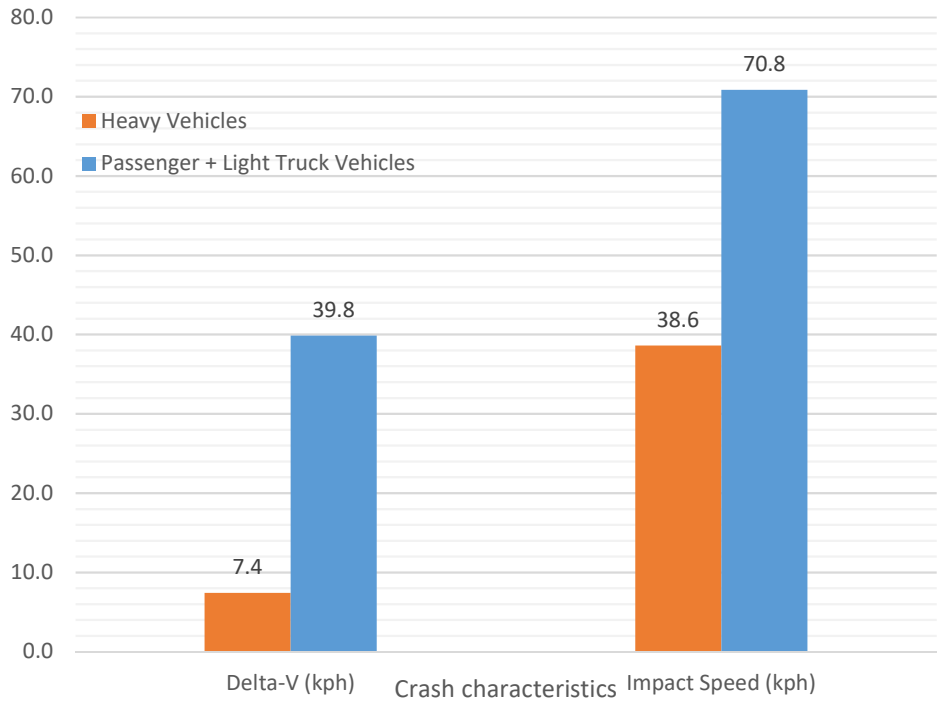

Figure 14. In this limited dataset, passenger vehicles travel faster and experience much high delta-Vs than heavy vehicles.

For validation of the heavy vehicle reconstruction methodology, cases were selected from the NASS-CDS database. A total of 30 cases were initially selected where an EDR equipped passenger vehicle was involved in a crash with a heavy vehicle. A brief summary of the dataset, the vehicle models involved, and the maximum injuries in each crash is presented in Table 8.

Table 8. Summary of database contents

NASS/CDS Case Id	Passenger Vehicle Make/Model	Heavy Vehicle Make/Model	Most Injured Occupant Position	Maximum AIS score in passenger vehicle
155010315	2005 Pontiac J-2000	2002 Kenworth T8	Right Front Passenger	2
173009112	2002 Oldsmobile Intrigue	2004 Freightliner Columbia 120	Driver	3
510016863	2012 Dodge Avenger	2002 Freightliner CST120	Driver	1
511018040	2011 Buick Regal	2009 Ford E-450 Ambulance	Driver	1
530013817	2004 Oldsmobile Alero	2007 Ford E-450	Driver	1
666014459	2009 Chevrolet Caprice	1999 International Harvester Model 9400 Tractor with Trailer	Driver	4
688017183	2007 Chevrolet Caprice	2011 Ford F450	Driver	3
689019504	2015 Chevrolet Colorado	1995 International 4700 Truck	Driver	0
748014910	2010 Chevrolet C Series pickup	2004 Freightliner Ambulance	Left Rear Passenger	1
762014945	2009 Chevrolet Aveo	2007 Mack CF	Right Front Passenger	6
768015264	2002 GMC Jimmy	Ford E-450 Ambulance	Driver	1
769014899	2011 Ford Fusion	1996 International Harvester 2654	Driver	0
771015341	2000 Pontiac Grand Am	2006 International Harvester 9400	Driver	*NA*
773014695	2011 Ford Escape	1998 Kenworth W9 Series	Driver	4
782013483	2002 Cadillac Deville	1987 Peterbilt 379	Driver	4
782014468	2003 Chevrolet C/K-series Pickup	2005 International	Driver	1

		Harvester 3300 Bus CE PB 105		
785013793	2006 Pontiac Grand Prix	2001 Chevrolet C6 Medium Duty	Driver	0
835016784	2004 Chevrolet C/K-series Pickup	2009 Freightliner	Driver	1
914020578	2014 Jeep Grand Cherokee	2001 Mack Truck	Driver	3
923018882	2013 Ford Mustang/Mustang II	2001 Isuzu NPR	Driver	1
958020609	2009 GMC Arcadia	2006 Gillig Bus	Driver	1

Table 9 shows a breakdown of the 9 excluded cases. The final dataset contained 21 cases representing 3,561 crashes nationwide.

Table 9. Composition of excluded cases for validation

Number of Cases	Exclusion Reason
3	Unreadable scene diagrams
1	Right roadside departure prior to crash (non-relevant crash scenario)
1	Cross-median crash (non-relevant crash scenario)
1	Vehicle lost traction
1	No model for the passenger vehicle
1	Underride crash
1	EDR recorded deceleration greater than 1g (unrealistic deceleration value)

To investigate the severity of these crashes the impact speeds and average delta-V values were found. The average speed of the passenger vehicle in these heavy vehicle crashes was 46 kph (28 mph) with an average delta V of 27 kph (17 mph). In comparison, the average delta V that the heavy vehicles experienced was 10 kph (6 mph) or about a third of what the passenger vehicles experienced.

The occupant injuries were also looked into as part of this investigation. As can be seen from Figure 15, the most common result from impacting a heavy vehicle was an MAIS 2 injury, which is classified as a "moderate injury". A total of 40% of the cases reported a MAIS 2 injury. In slightly over 30% of the crashes in this dataset, the maximum injury in the light passenger vehicle was a serious-to-fatal injury (MAIS 3+). There were 3 fatalities.

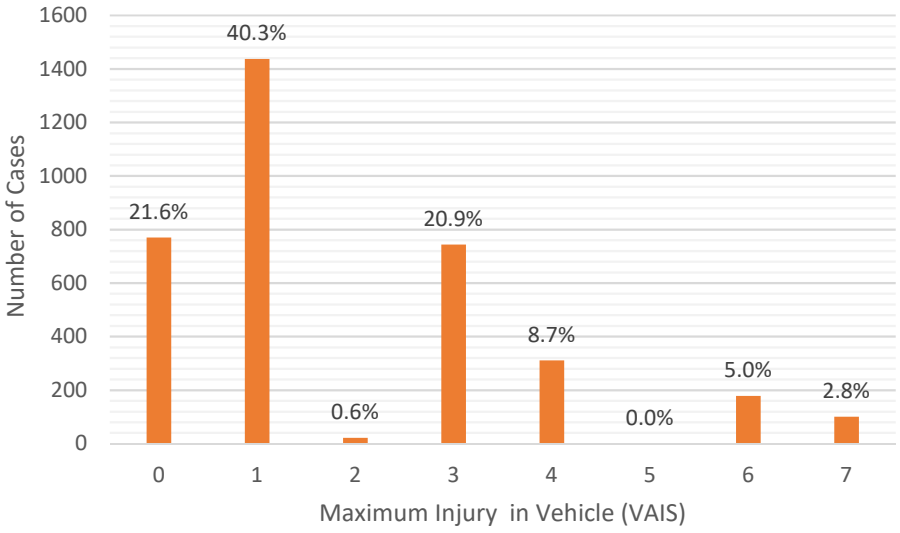

Figure 15. Injury distribution in heavy vehicle crashes

This indicates that, while the impact speeds may not be high, the significant mass difference between heavy vehicles and passenger vehicles lends itself to higher proportions of serious injury crashes. There are two possible reasons for this. As shown previously, passenger vehicles experienced a greater delta-V in these crashes than the heavy vehicles. Several papers have shown an increase in delta-V to be associated with a higher injury risk [80, 91]. Another possibility results from the difference in stiffness between a heavy vehicle and a passenger vehicle. The smaller stiffness coefficient for the passenger vehicle leads to a greater probability of large deformation and intrusion into the occupant department. The greater deformation in the

passenger vehicle compared to the heavy vehicle could result in greater passenger vehicle occupant injuries.

Comparing the EDR speeds with the final PC-Crash simulations allowed an estimation of the accuracy of this reconstruction method. Using a weighted average, the PC-Crash simulation reported impact speeds 20% different than the EDR reported. The weighted median error was 19%. Figure 16 illustrates a scatter plot comparing the EDR reported speed with the PC-Crash speed.

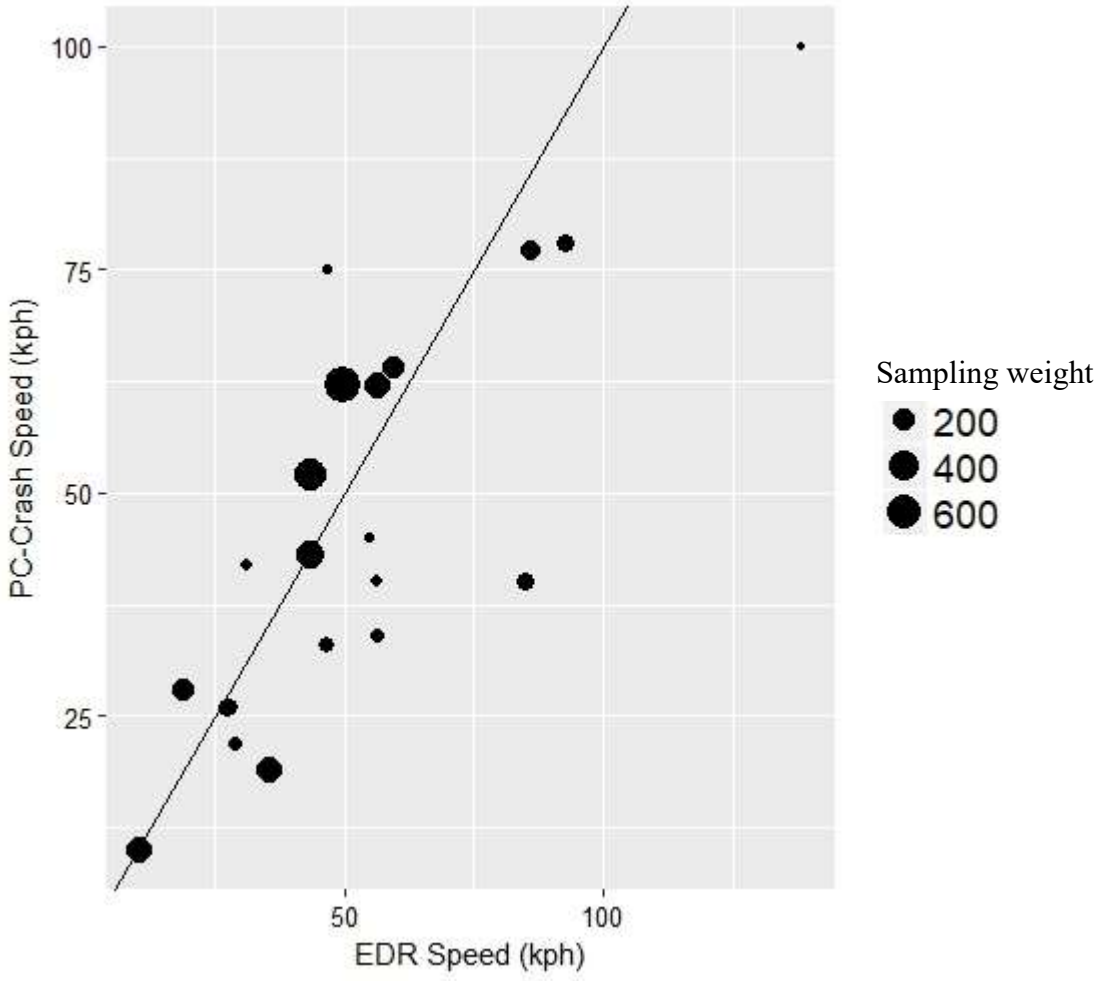

Figure 16. Comparison of the EDR speed and the final PC-Crash simulation impact speeds. The black line depicts a Y=X fit. If the PC-Crash simulated impact speeds were exactly equal to the EDR reported speeds, every point would be on that line.

Some of this error may lay in the modification of the custom vehicles. While every attempt was made to model the heavy vehicles as accurately as possible, there may be some discrepancies between specification sheets and actual vehicle weight. A good example of this can be found in the case of a semi-tractor hauling a trailer. Clearly, there are major differences in how a semi-tractor drives with a full trailer versus an empty trailer.

Note here, that this validation method used NASS-CDS crashes where the investigators did not have to be on the scene prior to the crash being cleared. Additionally, NASS-CDS investigators do not have to complete a full investigation for non-CDS applicable vehicles such as tractor-trailers. This means that there is less data available to help identify the heavy vehicle make and model. This is in contrast to NMVCCS where the scene investigator is on-scene for the crash and completes investigations of both vehicles. As this reconstruction methodology has been used primarily with NMVCCS crashes to date, these different investigation methods may lead to higher accuracy of this reconstruction methodology when looking at NMVCCS crashes instead of NASS-CDS.

3.4.5 LIMITATIONS

The primary limitation of this reconstruction methodology lies in determining accurate heavy vehicle specifications. While specification sheets exist online, it can be hard to determine an approximate weight for custom attachments depending on the type and model year of heavy vehicle.

One additional limitation, unique to NASS-CDS and this validation process, is that the investigator was not on-scene to see the final rest positions of both vehicles and document evidence prior to the crash being cleared. This may affect the final scene diagram drawn. As the

scene diagram is the primary data source for PC-Crash simulations, this may affect the accuracy of the simulations and the validation performed here to some degree.

As an initial basis for simulation, this heavy vehicle reconstruction methodology has been shown to be relatively effective. Further work could focus on refining the methodology by using heavy vehicle EDR data. A database formulation of this data is not publicly available currently but private investigators download the data routinely for inspection. Another option for future work could be to build common heavy vehicle models, such as a Bluebird School bus, from scratch using design and specifications sheets. These could then be used instead of the default models in PC-Crash.

3.5 Rollovers

3.5.1 Motivation

Our standard reconstruction methodology could not be applied to vehicles that experienced rollover because the PC-Crash simulations performed previously were focused on the 2D vehicle kinematics and rollovers are fundamentally a 3D phenomenon. However, rollover crashes occur frequently enough in crash simulation sets used for lab studies that there is a need for a way to reconstruct rollover crashes. In our case set of cross-centerline crashes, rollover crashes accounted for 5 cases representing 1, 366 crashes nationwide. This rollover reconstruction methodology was developed to reconstruct these crashes.

3.5.2 Reconstruction methodology

The rollover reconstruction methodology was developed from a combination of the standard reconstruction protocol and a reconstruction protocol used in the NCHRP 17-43 project. The objective of the NCHRP 17-43 project is to create a database of run-off-road crashes with

trajectory measurements and speed reconstructions [92]. NCHRP 17-43 uses the Kildare curves and the roll distance to estimate a trip velocity for rollover events [93]. The Kildare curves assume that the majority of energy in a rollover is dissipated through the vehicle rotation and interaction between the ground and the rolling vehicle [93]. Consequently, trip velocity can be estimated through the roll distance and associated drag factors. Because different vehicles have different properties, there are different curves for pickups, sedans, and small cars. The trip point was defined as the last point the vehicle was on four wheels prior to rollover. The roll distance was the distance from the trip point to final rest.

Figure 17 illustrates how a combination of PC-Crash and the NCHRP 17-43 rollover reconstruction methodology were used to estimate impact speeds.

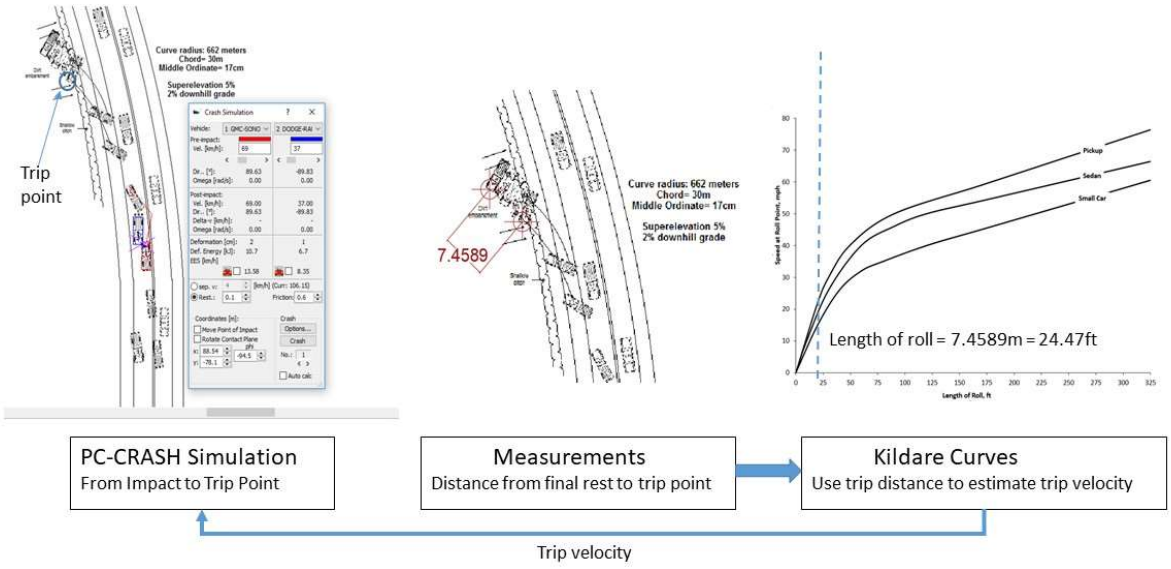

Figure 17. Illustration of the rollover reconstruction methodology process

PC-Crash was first used to obtain a rough estimate of the impact speeds and the post-impact trajectories prior to rollover. In order to approximate the post-impact trajectory prior to rollover in a two-dimensional simulation, an intermediate position was placed at the post-impact vehicle position closest to the trip point. The crash simulation was run first initially to generate a

baseline impact speed for both vehicles and the speed at the estimated trip point was recorded. Next, the rollover event was reconstructed using the trip distance and the Kildare curves. This gave another velocity for the same trip point that was used in PC-Crash. This trip velocity was then used to modify the PC-Crash simulation in order to obtain an agreement between the Kildare curves and the PC-Crash simulation. This combination of Kildare curve usage and PC-Crash enabled impact speed estimation for crashes where one vehicle experienced a rollover event post-impact. To see the full process of how to conduct a rollover reconstruction using this method see the Appendix.

3.5.3 VALIDATION

In order to validate this method of rollover reconstruction, event data recorder data was used. Event data recorders can be used to determine a vehicle's actions prior to a crash as EDRs store pre-crash data for up to five seconds prior to a deployment or non-deployment event. For the purposes of validation, only the speed element of the EDR data was used. Cases were selected from the NASS-CDS database instead of NMVCCS due to the larger EDR dataset in NASS-CDS. For case selection, both vehicles involved in the crash had to have an EDR installed and the pre-crash speed must have been recorded. Additionally, one vehicle had to have experienced a rollover event. Multiple crash scenarios were used during validation. All intersection crashes, such as straight crossing path and left turn across path, were included as well as head-on crashes.

If the vehicle impact speed was not directly recorded at the time of impact, the impact speed was determined from linear extrapolation using the same method described above in Section 3.4.3 Heavy Vehicle Crashes Validation. The impact speeds using the EDR data and impact speeds from the PC-Crash simulation were then compared to determine the overall

accuracy of the rollover reconstruction method. Additionally the trip speeds were compared between the Kildare curves and the final PC-Crash simulation in order to obtain an estimate of the accuracy of the Kildare curves.

3.5.4 RESULTS

The initial dataset contained 8 crashes in NMVCCS involving vehicles experiencing rollovers after a cross-centerline crash. In three cases, a heavy vehicle experienced a rollover. These crashes were not able to be reconstructed because the Kildare curves do not describe heavy vehicle rollovers. This resulted in a total of 5 rollover cross-centerline crashes representing 1, 366 crashes nationwide. Table 10 presents the reconstruction results for this NMVCCS dataset.

Table 10. NMVCCS cross-centerline rollover crashes reconstruction results. Vehicles are designated as either the rollover vehicle (vehicle that experienced rollover) or non-rollover vehicle.

	Rollover Vehicle				Non-Rollover Vehicle			
Case Number	Make/Model	Impact Speed	Delta-V	KABCOU	Make/Model	Impact Speed	Delta-V	KABCOU
2005045706301	Chevrolet S-10	77	41.72	Non-incapacitating injury	Nissan Sentra	10	-30.2	Incapacitating injury
2006002229004	GMC C,K Series Pickup	100	9.79	Non-incapacitating injury	Dodge Caravan	95.3	19.41	Non-incapacitating injury
2006076597586	GMC Sonoma Pickup	105	42.7	Non-incapacitating injury	Dodge Ram Pickup	37	2.37	No injury
2006079624767	Lexus ES 250	93	61.6	Non-incapacitating injury	Volkswagen Touareg	0	-38.6	Non-incapacitating injury
2007004112948	Ford Escape	35	4.12	Non-incapacitating injury	Peterbilt Medium Heavy Tractor-Trailer	30	-4.07	Possible injury

The weighted average impact speed for the vehicle that experienced rollover was 90 kph (56 mph) compared to an average impact speed of 45 kph (28 mph) for the vehicles that did not experience rollover. The weighted delta-V the rollover vehicles experienced was 30 kph (19 mph) versus 1.2 kph (0.7 mph) for non-rollover vehicles. Both of these results indicate that the vehicles that experienced rollover enter into a crash with greater energy than the struck vehicle and suffer a more severe crash impulse than the struck vehicle.

Validation of this rollover reconstruction methodology was performed using EDR data from rollover crashes in NASS/CDS. The initial validation dataset contained 11 cases where both vehicles had an EDR and the speed was recorded prior to impact. However, in one case, a vehicle had an attached trailer and another case had an unreadable scene diagram. Both cases were excluded resulting in a final of 9 cases in NASS/CDS representing 1,031 cases nationwide.

By comparing the EDR reported speed with the final PC-Crash results using this rollover methodology, we can obtain an idea of the accuracy of the methodology. The average difference between the EDR speed and the final simulations in PC-Crash was 3.6 kph. This represented a percent error of 11% indicating that this reconstruction methodology tends to slightly overestimate the EDR-reported speed of the vehicles. As shown below in Table 11, there was one case that represented an outlier to this data with a simulation error of 59.9%. Looking at this case, we can see the simulation predicted an impact speed of 18 kph instead of 7 kph for vehicle 1. While this is a high percent error, in terms of magnitude this is small. This trend is also not evident in other reconstructed crashes using this method.

Table 11. NASS/CDS Rollover reconstruction cases with a comparison between EDR data and PC-Crash simulations.

	EDR Reported Impact Speed (kph)		PC-Crash Simulated Impact Speed (kph)		Simulation Error (%)		Trip Speed (kph)		Trip Speed Error (%)
Case Number	V1	V2	V1	V2	Rollover Vehicle	Non-Rollover Vehicle	Kildare Curves	PC-Crash	
2014-48-115	80.5	32.2	84	43	-4.3%	-33.5%	66	53	24.5%
2013-76-94	19.3	49.9	10	58	48.2%	-16.2%	27.6	13.31	107.4%
2013-48-73	40.3	86.9	61	97	-51.6%	-11.6%	48.9	45.68	7.0%
2010-12-201	66.0	43.5	71	42	-7.6%	3.4%	40.2	36.75	9.4%
2009-49-175	45.9	66.0	46	63	-0.2%	4.6%	16.8	8.51	97.4%
2009-13-256	16.9	70.8	24	67	-41.9%	5.4%	67	64	4.7%
2009-12-202	74.9	94.2	68	90	9.2%	4.4%	61.5	69.2	-11.1%
2008-12-133	7.2	82.9	16	82	-120.8%	1.1%	22.4	48	-53.3%
2006-12-94	66.8	30.6	54	35	19.2%	-14.4%	14.2	16	-11.3%

A scatter plot comparing the EDR impact speed and the PC-Crash impact speed can be seen in Figure 18.

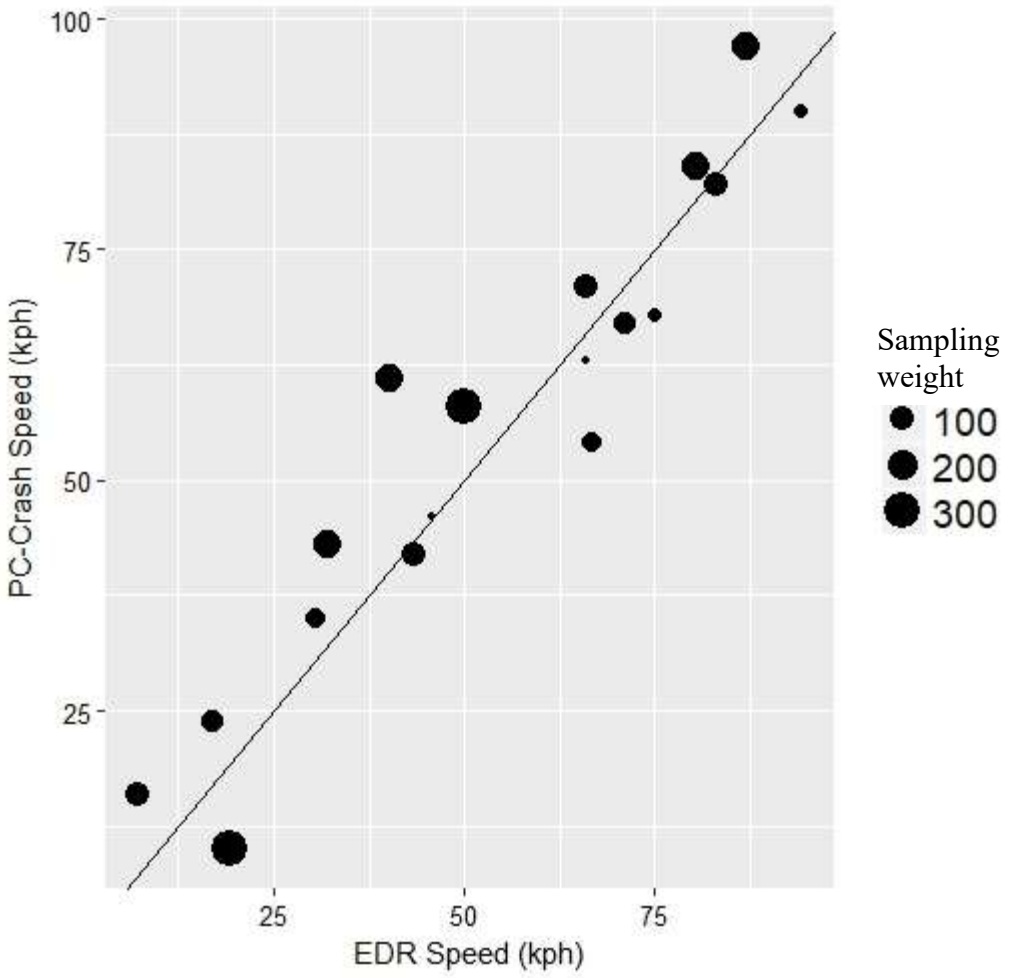

Figure 18. Scatter plot comparing EDR speed to PC-Crash speed in rollover crashes.

An additional comparison was done by comparing the simulated speeds for the vehicle that experienced rollover versus the other vehicle. As the vehicle that experienced rollover is reconstructed differently (using the Kildare Curves) than the other vehicle, we determined if there were significant differences using the Kildare curves versus the original reconstruction method. There was an average error of 10% for the vehicle that experienced rollover versus an error of 12% for the other vehicle. While there are slight differences, there does not appear to be a significant difference in the reconstruction accuracy between the different vehicles.

Recall that the Kildare curves are used to initially estimate the trip speed which provides additional information for the PC-Crash simulations. In this study, it was also of interest to

determine the difference between the trip speed obtained using the Kildare curves and the final trip speed of the final PC-Crash simulation. Although every attempt was made to minimize the error between these during subsequent iterations, there remained residual error in the final PC-Crash simulations. On average, the Kildare curves predicted a trip velocity 32% higher than the PC-Crash simulations predicted. In this scenario, the true value of the trip velocity is unknown so the accuracy of this reconstruction methodology at estimating the true trip velocity is still unclear. Note that in the PC-Crash simulations, the vehicle does not experience rollover whereas the Kildare curves were specifically crafted for vehicles that do rollover. This might account for the differences between the two methods.

The difference between the PC-Crash simulations and the Kildare curve estimate illustrates the importance of using multiple sources of data when reconstructing rollovers. Using this reconstruction methodology, the Kildare curves provide an initial baseline for the reconstruction and afterwards PC-Crash and the collision optimizer are used. This combination of Kildare and PC-Crash allows for a reduction from 32% error for trip speed estimation to 11% error for final impact speed results.

Overall, this validation suggests that this rollover reconstruction method has the capability to reconstruct rollover crashes with a reasonable degree of accuracy.

3.5.5 LIMITATIONS

The rollover reconstruction methodology posed here and the validation process have a number of limitations. As the validation has shown, this rollover reconstruction methodology has errors and approximations regarding trip speed. The primary error inherent in this method lies in using the Kildare curves and incorporating the results from them into the PC-Crash simulation. Additionally, another limitation is that the final PC-Crash simulations are, by definition,

imprecise as the vehicle does not experience rollover in these simulations. Note that the validation process has limitations as well. Using NASS/CDS data for validation introduces an important source of uncertainty. Instead of being required to be on-scene prior the crash being cleared, NASS/CDS investigators can come visit a crash site days or weeks after a crash has occurred. This length of time between the crash and subsequent investigation can lead to inaccuracies in determining the trip point and subsequent roll distance of the vehicle that experienced rollover. Inaccurate trip point positions and roll distances would affect the accuracy of this reconstruction process.

Additionally, note that follow-up efforts to this methodology could attempt to use PC-Crash to completely simulate vehicle rollover. PC-Crash has the capability to reconstruct rollover crashes in their entirety. While there are benefits to this approach, there are also limitations. Rose (2009) found that one of the most significant variables affecting the accuracy of a PC-Crash rollover simulation is accurate reconstruction of the vehicle-ground coefficient [94]. This coefficient is difficult to accurately simulate [94]. In later writings, he suggested reconstructing the vehicle's roll motion and speed based on physical evidence and a constant deceleration rate. Then PC-Crash would be used to simulate the crash from impact to the trip point. This is a similar approach to the one used in the rollover reconstruction methodology presented here.

3.6 Final Crash Reconstruction Dataset

A total of 42 cases consisted of a crash only involving standard vehicles and were reconstructed using the traditional impact speed reconstruction method. A passenger vehicle crash with a heavy vehicle accounted for 5 additional cases. Using the rollover methodology,

five additional cases were added to the dataset for a total of 52 crashes representing 23,014 crashes nationwide. Table 12 presents a breakdown of the total simulation set for this study.

Table 12. Breakdown of final NMVCCS Case set

Crash Scenario	Raw	Weighted
Passenger vehicles + light truck vehicles crash	42	19,467
Impact with heavy vehicle	5	2,181
Vehicle experienced rollover	5	1,366
Total	52	23,014

4 Using Event Data Recorders to Model Driver Actions Prior to Impact

4.1 Introduction

A cross-centerline crash can be divided into four distinct parts: the approach phase, encroachment, evasive action, and impact as shown in Figure 19. During the approach phase, the vehicle is traveling at a normal speed and maintaining lane position. In the encroachment phase, the vehicle moves laterally and begins to cross over the lane line. Having detected the possible impending crash, the driver might initiate an evasive action such as hard braking or steering prior to the crash. This is the evasive action phase. The final phase of a crash is impact where the crossing vehicle strikes another vehicle. To accurately simulate the crash with and without a lane departure warning (LDW) system, the vehicle's position and speed in each of these phases is needed. Scene diagrams from trained NMVCCS investigators who were on-scene prior to the crash being cleared can provide important information on both vehicle's movements prior to and including impact. These positions were measured and position data was collected using the trajectory reconstruction protocol described in Chapter 3.2.

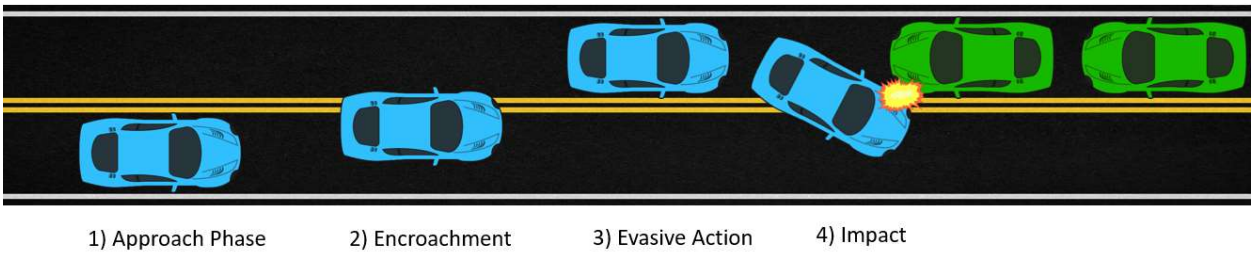

Figure 19. Diagram of a cross-centerline crash depicting the 4 distinct phases of a cross-centerline crash: (1) approach phase, (2) encroachment, (3) evasive action, and (4) impact.

In this project, the impact speed was obtained using a variety of reconstruction methods as described in Chapter 3. While this provides information about the impact conditions, the speed of the vehicle during the approach and encroachment phases must still be estimated. Because

vehicle speed during the pre-collision phase is highly dependent on the actions of the driver, reconstruction of pre-collision vehicle kinematics is very challenging.

One way to determine the speed of the vehicle prior to impact is by downloading the event data recorder (EDR). EDRs record data continuously but only save the data prior to a triggering event such as an airbag deployment. EDR data has previously been used in safety impact methodologies to reconstruct vehicle trajectories [95].

4.2 Objective

The objective of this study was to develop a statistical model to predict the approach speed and braking magnitude of a vehicle involved in a cross-centerline crash based on the impact speed, vehicle class, and environmental factors.

4.3 Approach

Our approach was to build an approach model using EDR pre-crash data. Ideally, this calculation would be performed using NMVCCS EDRs to be consistent with our NMVCCS dataset. However, NMVCCS cases were investigated in the early days of EDRs and there were too few cases for this calculation. Instead, EDR data in NASS/CDS was used as a basis for an approach speed model. As this calculation only analyzes the approach phase and does not simulate the entire crash, we can use cases where only one vehicle was equipped with an EDR. This greatly increases the size of the available dataset. This same data, where only one vehicle had to have an EDR, can also be used to gather more information on the evasive actions drivers take prior to a cross-centerline crash. Using EDR data, we can determine what evasive actions drivers take, such as braking or steering, and the magnitude of these actions.

The goal of the approach model was to create a relationship between approach speed and impact speed. Given the impact speed, the approach model should output the estimated approach

speed of the vehicle. By linking the approach speed and the impact speed using the approach model, we could determine each vehicle's speed profile prior to impact.

One way to estimate the approach speed given the impact speed is to estimate the level of braking prior to impact. Our approach was to develop two logistic regression models to estimate the probability of heavy or light breaking compared to a baseline of no braking. The braking predictions from these models were used to determine the braking level of the vehicle prior to impact. The braking level was then used in a linear regression model in order to estimate the approach speed given the impact speed and braking level.

4.4 Data Source

EDRs from the National Automotive Sampling System / Crashworthiness System (NASS/CDS) years 2000 – 2015 were the primary data source for this study. Cases were selected based on the crash location (intersection or non-intersection), crash configuration and movements prior to the crash. If the speed limit, crash configuration, or driver age were unknown, the case was eliminated. An LDW system is expected to activate when the leading wheel of a vehicle crosses a lane line so locations with no lane lines were excluded. As usually there are no painted lane lines through intersections, all crashes selected occurred in a non-junction and non-interchange area. In every crash, one vehicle had to cross over the centerline and strike another vehicle that was traveling in its lane. Crashes involving two vehicles traveling in opposite directions in the same lane without the scene diagram showing one crossing over the centerline were excluded. Both vehicles also had to be tracking and under control prior to the crash. In each crash, at least one vehicle had to have been equipped with an EDR.

EDR records were only included if they recorded either a deployment event or a non-deployment event with a maximum longitudinal delta-v of greater than or equal to 5 mph. This

filter was to ensure the non-deployment event was associated with the impact and not through a separate event such as being towed away [84]. Additionally, the EDR must have recorded speed and braking data for at least 5 seconds.

To further verify the quality of the recorded EDR speed and braking data, deceleration values were computed over each second prior to the crash using Equation 2.

$$a = \frac{v_2 - v_1}{t_2 - t_1} \tag{2}$$

As Nerijus et al. (2007) reported a maximum possible deceleration for vehicles between 0.75 – 0.95g, if the computed deceleration was greater than 1g, the case was excluded [96].

4.5 Determining Pre-Crash Driver Behavior

The first step was to determine the approach speeds of each vehicle. The approach speed of the vehicle was assumed to be the speed of the vehicle at 5 seconds prior to the crash. The implicit assumption is that there no evasive actions occurred earlier than 5 seconds prior to impact. The vehicle impact speed was determined depending on the OEM of the EDR. As discussed previously, there is uncertainty between when the EDR started recording the vehicle speed and when the crash actually occurred. While Toyota records the impact speed (t = 0 seconds), other OEMs use different methods to designate the first recorded speed when the EDR deployed. The coarse recording rates EDRs use, which can range from 1 Hz (most common currently) to 10 Hz, also adds to this uncertainty between the crash timeline and the EDR time. To address this, the two recorded data points closest to impact were used to extrapolate to a point forward at ½ the EDR sampling rate. For an EDR recording at 1 Hz, this method would use points at t = -2 and t = -1 and estimate the speed at t = -0.5. This would then be called the impact speed. An example of EDR data in a cross-centerline crash scenario can be seen in Figure 20.

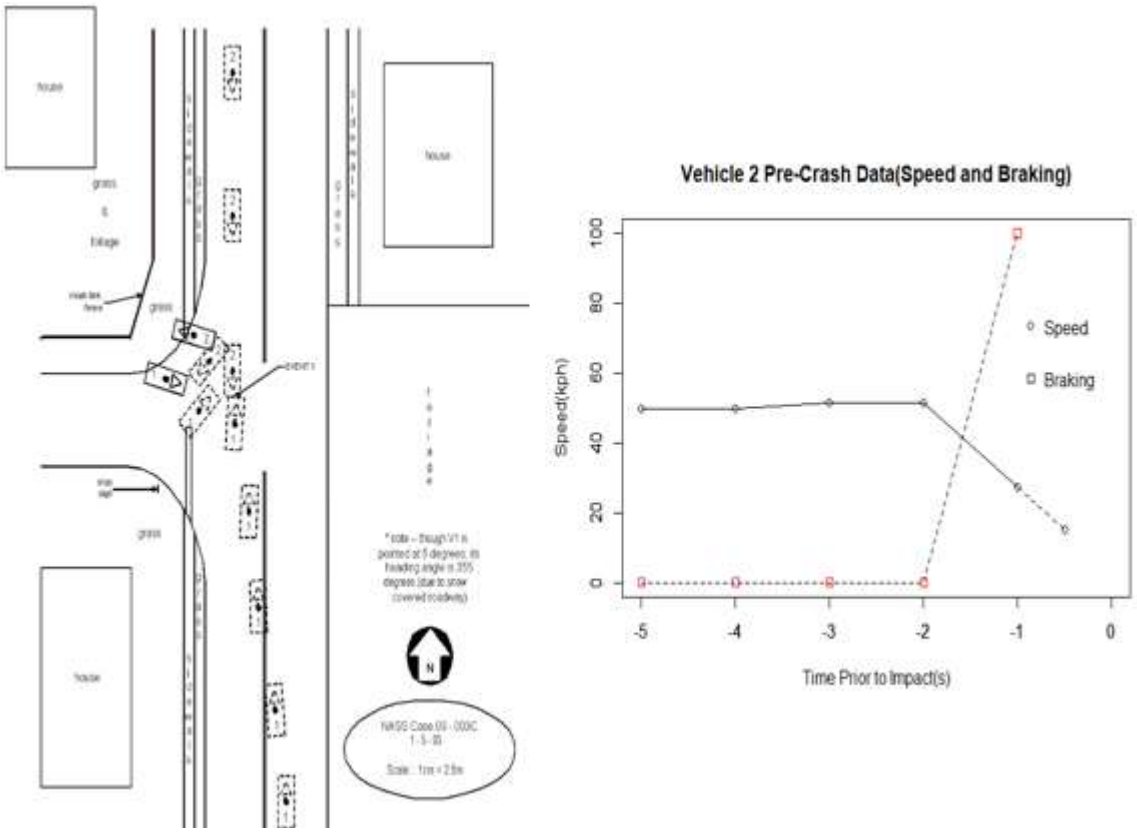

Figure 20. NASS/CDS case number 168005837. Scene diagram of cross-centerline crash. Vehicle 1(traveling north) crosses over the centerline and impacts V2. Data from the EDR in vehicle 2 is shown on the right side. Vehicle 2 applies the brakes (brake status shown in red) at t=-2 seconds resulting in a decrease in speed. The extrapolated impact speed is shown as a point at t=-0.5 seconds

A secondary aim of this study was to investigate driver's evasive actions prior to a centerline crash. Common evasive actions include braking and steering. EDRs record brake application as either on or off. EDR pre-crash yaw rate data was used to estimate evasive steering maneuvers when available. Because yaw rate is only recorded in new generation EDRs, the steering analysis was only possible on a subset of overall EDR dataset. A threshold of 4 deg/sec was used to classify an evasive steering maneuver. This threshold has been used during the 100 Car Naturalistic Driving Study to identify crashes or near crashes in naturalistic data [97].

4.6 Development of the Approach Model

The approach of this study was to estimate the braking level of a vehicle prior to impact and use the braking level and impact speed to estimate the approach speed. During movement, a vehicle has three options relating to speed: to brake, stay at a constant speed, or to accelerate. These three levels were used initially to characterize the vehicle's pre-crash movement. To account for the possible presence of evasive braking prior to a crash, braking was split into two levels: heavy braking (possibly evasive) or light braking. Each vehicle was assigned one of these braking levels using the average deceleration over the 5 seconds prior the crash. Table 13 below indicates the cutoffs used for each level.

Table 13. Deceleration thresholds for braking levels

Braking Level	Lower Bound (g's)	Upper Bound (g's)
Heavy Braking	N/A	-0.2
Light Braking	-0.2	-0.05
No Braking	-0.05	N/A

Two logistic regression models were used to estimate the possibility of the vehicle performing heavy braking and light braking respectively. No braking was set as a baseline for both models. The dependent variables tested were the impact speed, speed limit, driver age, crash configuration (head-on or sideswipe), and vehicle designation. The vehicle designation had two values: encroaching or non-encroaching and was used to determine which vehicle crossed over the lane line. Our hypothesis was that the encroaching vehicle and the non-encroaching vehicle might have different pre-crash actions.

The approach speed model was then developed to predict approach speed given the impact speed and braking status of the vehicle prior to impact. As impact speed was also used to determine the braking level of the vehicle, an interaction variable between impact speed and braking was initially tested within the model.

4.7 Model Validation

In order to evaluate the braking level model, two fold cross validation was used. The dataset was split into 2 approximately similar parts using the sample function in R. The model was initially trained using one section of the overall dataset and then validated using the other section. This enabled an overall accuracy metric for the braking level models and the approach speed model to be obtained.

4.8 Results

A total of 155 vehicles from NASS/CDS with EDR's were selected in this study representing 39,261 vehicles in cross-centerline crashes nationwide. The dataset included more non-encroaching vehicles (61.1%) than encroaching vehicles (38.9%). All cases in the dataset had braking and speed data. 19 vehicles within the 155 vehicles also recorded yaw rate in addition to braking and speed. Table 14 presents the dataset composition.

Table 14. Summary of NASS/CDS EDR Data Source

	Unweighted		Weighted	
Vehicle Designation	Count	% of Total	Count	% of Total
Encroaching	72	46.4%	15,267	38.9%
Non-Encroaching	83	53.6%	23,993	61.1%
Recorded Data				
Speed + Braking	155	100%	39,261	100.00%
Speed + Braking + Yaw Rate	19	12.3%	7,522	19.2%
Total	155	100%	39,261	100.00%

4.8.1 EVASIVE MANEUVERS PRIOR TO A CROSS-CENTERLINE CRASH

An initial analysis of braking maneuvers was conducted on the entire dataset of 155 vehicles. This analysis examined braking and speed data which was available for all cases. The weighted results broken down by the class of the vehicle are shown in Figure 21. The

proportions are roughly equal between the encroaching and non-encroaching vehicles. In this dataset, only the encroaching vehicles accelerated prior to the crash.

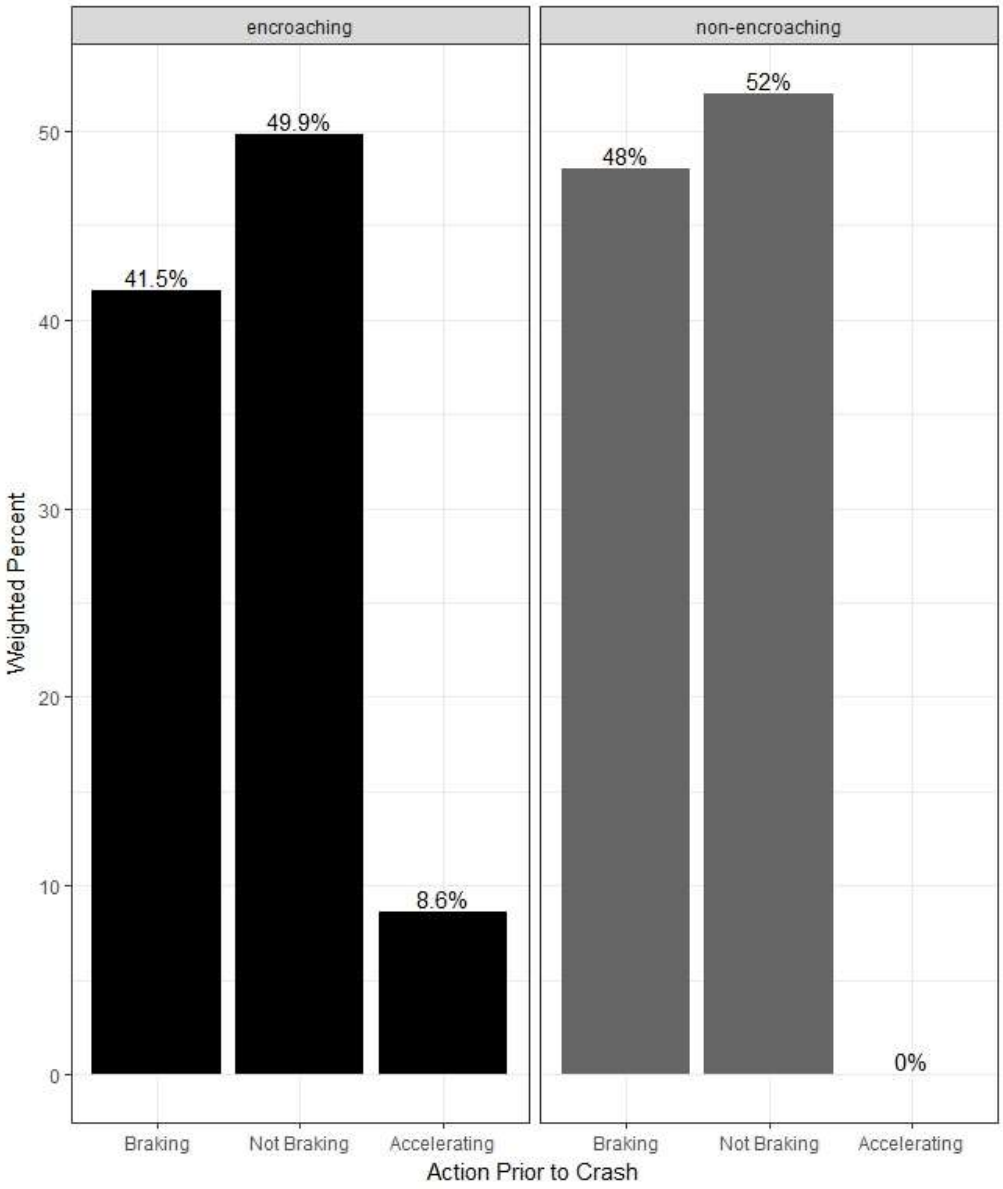

Figure 21. Analysis of driver speed behavior prior to impact.

Although overtaking or conducting a passing maneuver has been shown to only be a factor in a minor percentage of centerline crashes, overtaking is one scenario that would explain the encroaching vehicle acceleration [9]. To investigate this claim further, the PREMOVE variable was inspected. NASS/CDS use the PREMOVE variable to describe the actions and speed of the

vehicle prior to the crash. As can be seen from Figure 22, only 0.5% of vehicles were passing or overtaking another vehicle. This indicates that overtaking may not explain the acceleration of the encroaching vehicles in this dataset.

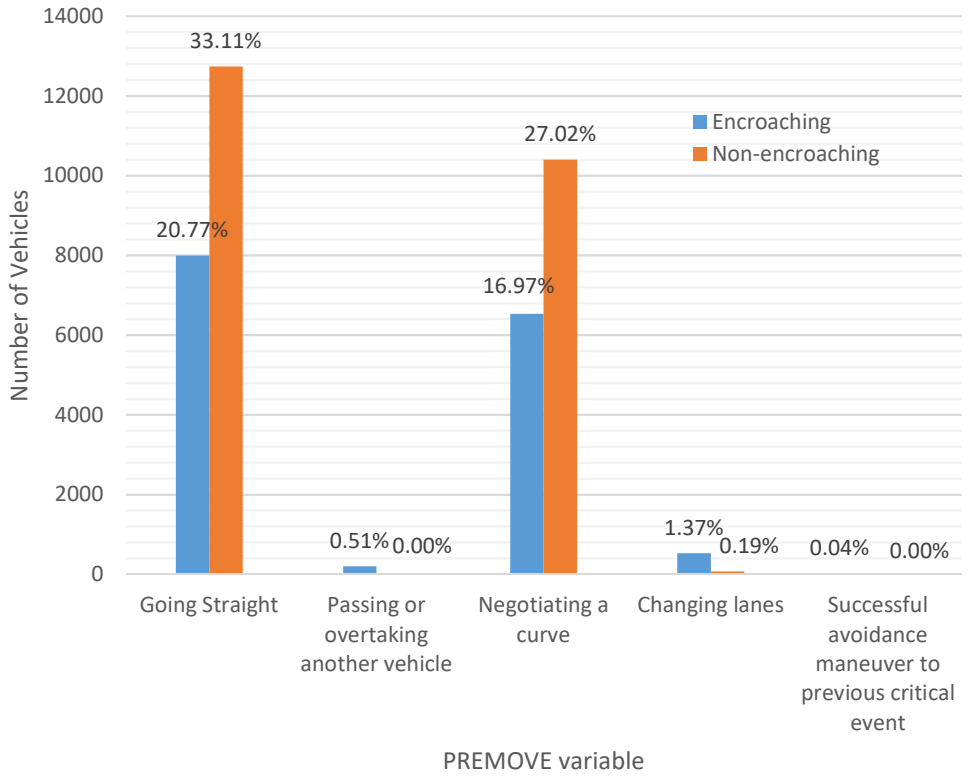

Figure 22. Illustration of the pre-crash motions of each vehicle separated by encroaching and non-encroaching.

An additional analysis was conducted on the smaller subset of 19 vehicles that had yaw rate data which represented 7,522 vehicles nationwide. This additional data allowed the full range of evasive actions drivers to be examined. However, this data is limited by the small number of cases. As shown in Figure 23, the most common evasive action for both vehicles was a combination of braking and steering.

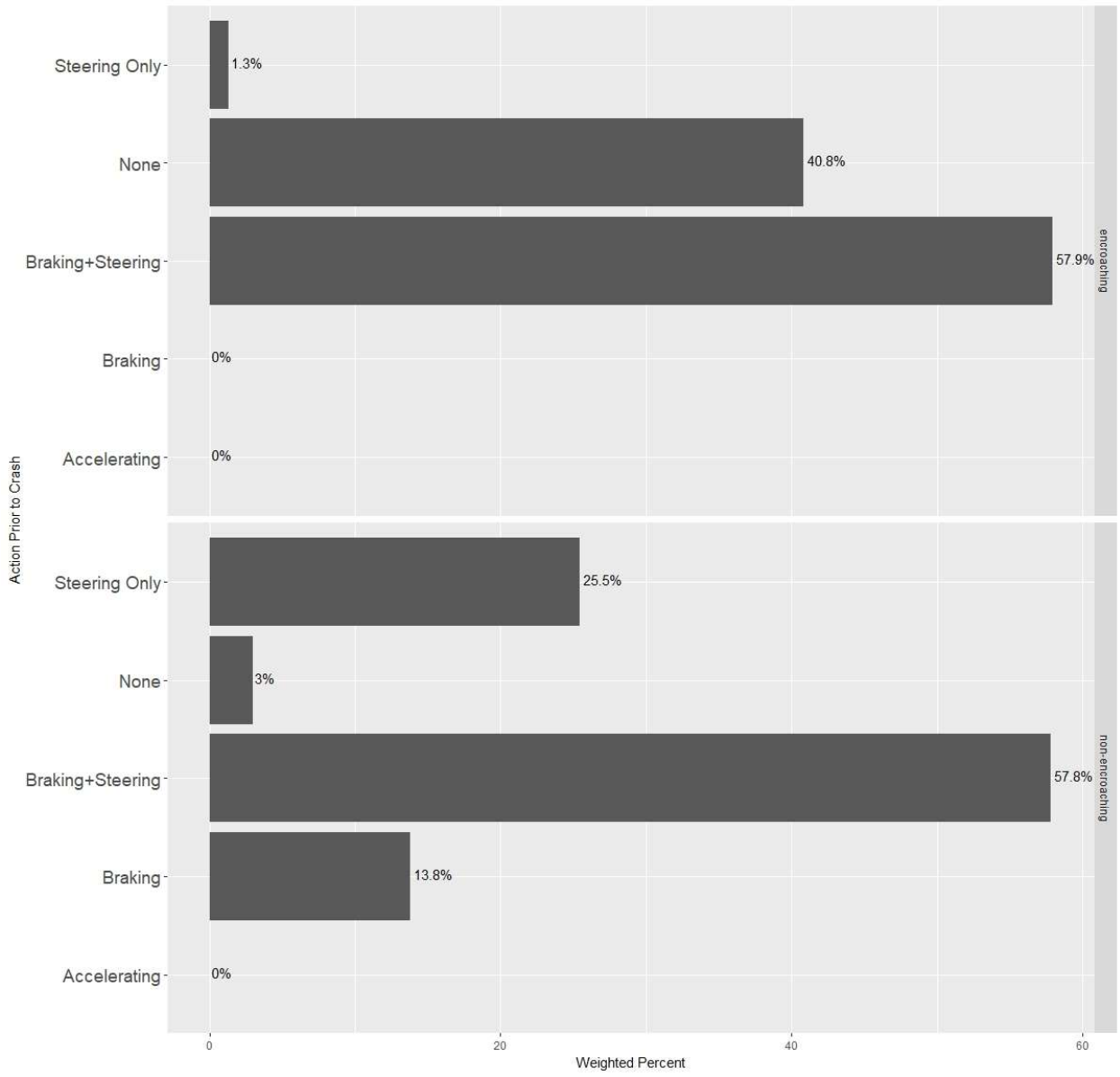

Figure 23. Driver actions prior to impact. Data drawn from the 19 cases that had both braking and steering data.

Comparing Figure 21 to Figure 23, a similar number of encroaching vehicles took no evasive actions prior to a crash at 40.8% and 49.9% respectively. One possible reason for these crashes occurring is driver distraction or driver inattention of the encroaching driver, these drivers might not be aware of the impending crash [2].

Of the original 19 vehicles with steering data, 13 of the vehicles representing 5,811 vehicles nationally (77% of the steering dataset) initiated an evasive steering maneuver. The data

was heavily made up of non-encroaching vehicles which accounted for 11 of the 13 vehicles. Figure 24 below illustrates the evasive steering direction broken down by the vehicle class. In this dataset, the encroaching vehicle only steered right while the non-encroaching vehicle was split nearly 50-50 in terms of direction.

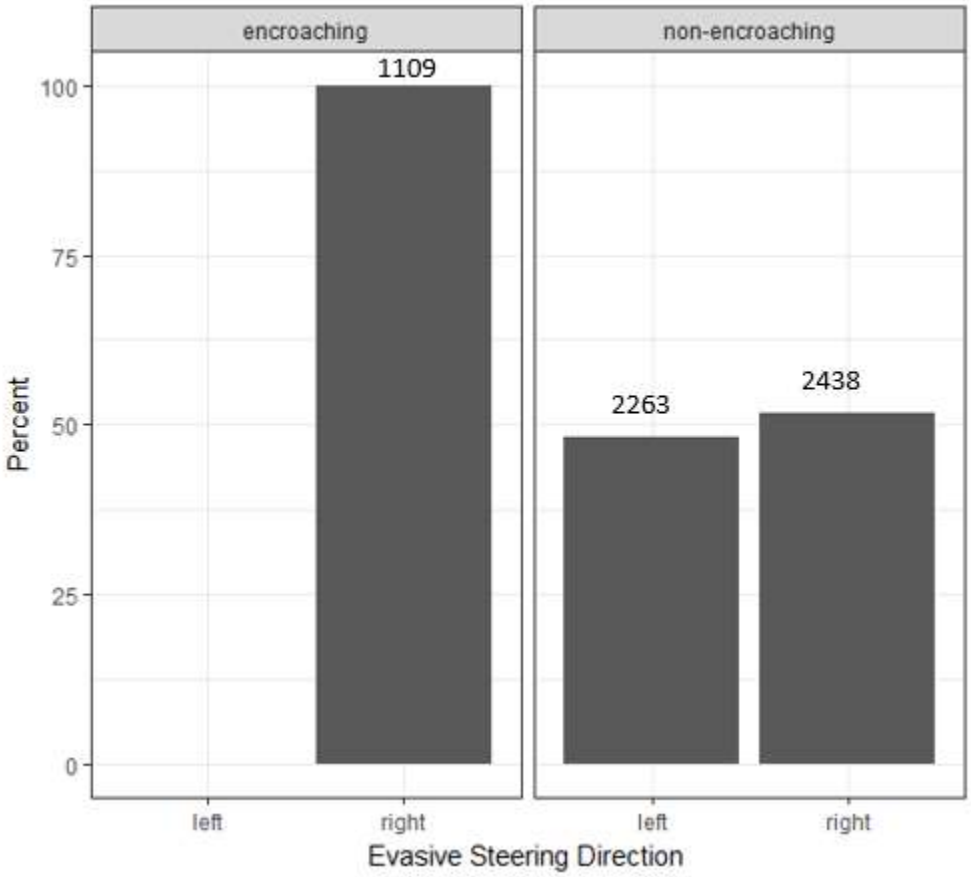

Figure 24. Analysis of steering direction in cross-centerline crashes. Conducted on 13 vehicles that initiated an evasive steering maneuver. Labels illustrate the representative number of vehicles.

To impact a vehicle traveling the opposite direction in the United States, the most likely scenario involves a driver crossing over the lane line to their left. Encroaching drivers might realize that a head-on crash is imminent and attempt to steer right to get back into their original lane where they can resume driving. In contrast to this, non-encroaching vehicles start out traveling in their original lane but are faced with a vehicle approaching them head-on. This results in a quick choice made by the driver about which way to steer. This data suggests that

non-encroaching drivers weigh the options of steering left or steering right approximately equally. However, these observations are based on a small sample size and should be revisited when additional EDR data becomes available.

4.8.2 *Effect of Speed Limit and Pre-Impact Braking*

As speed limit was one of the variables thought to influence the travel speed of a vehicle, the range of speed limits present and relationship to travel speed was investigated. The lowest speed limit in this study was 40 kph (25 mph) and the highest speed limit was 105 kph (65 mph). Figure 25 shows the distribution of approach speeds found at different speed limits. As can be expected, as the speed limits increase, the travel speed increases.

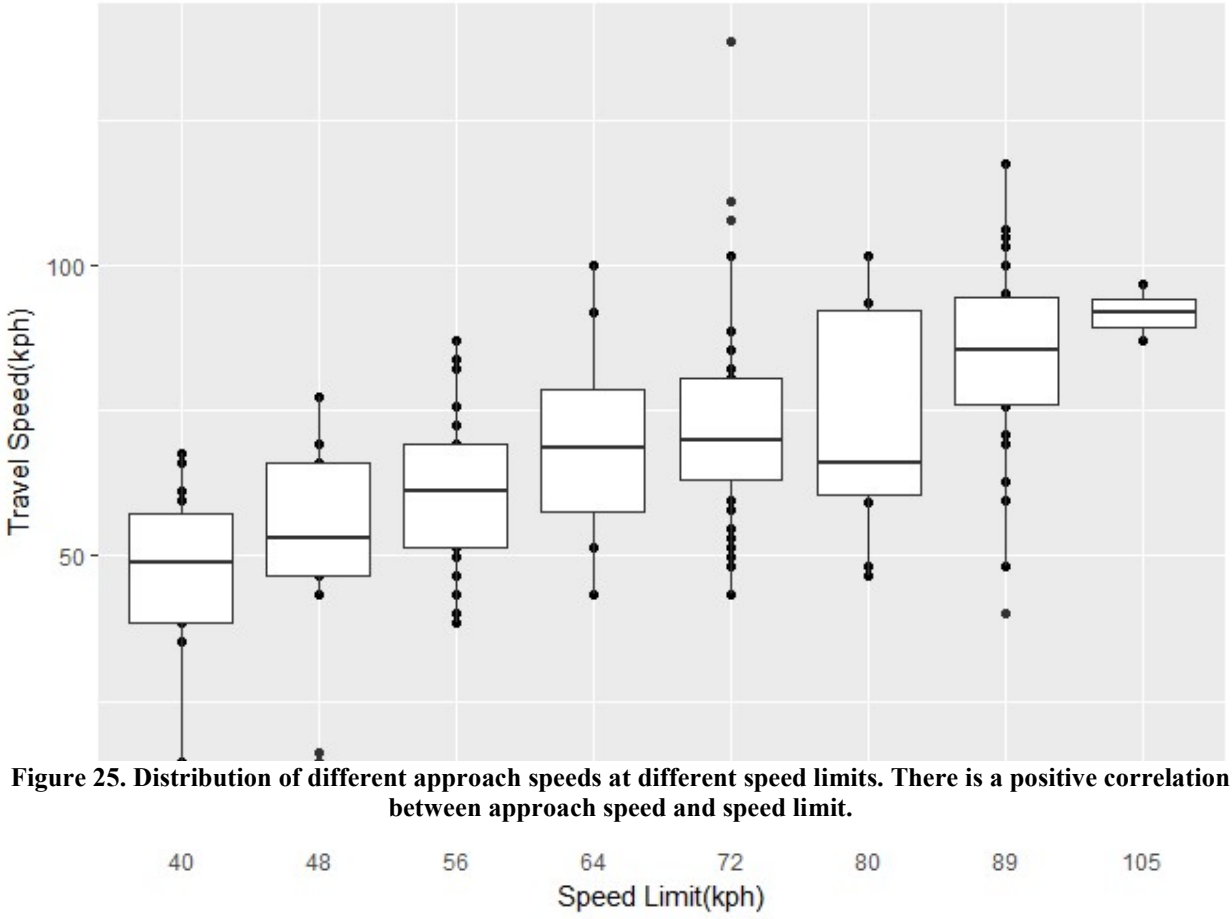

Figure 25. Distribution of different approach speeds at different speed limits. There is a positive correlation between approach speed and speed limit.

The range of acceleration undergone by each vehicle was also investigated using a weighted cumulative distribution plot. Figure 26 shows the majority of the deceleration each vehicle experienced was between -0.2 and 0g.

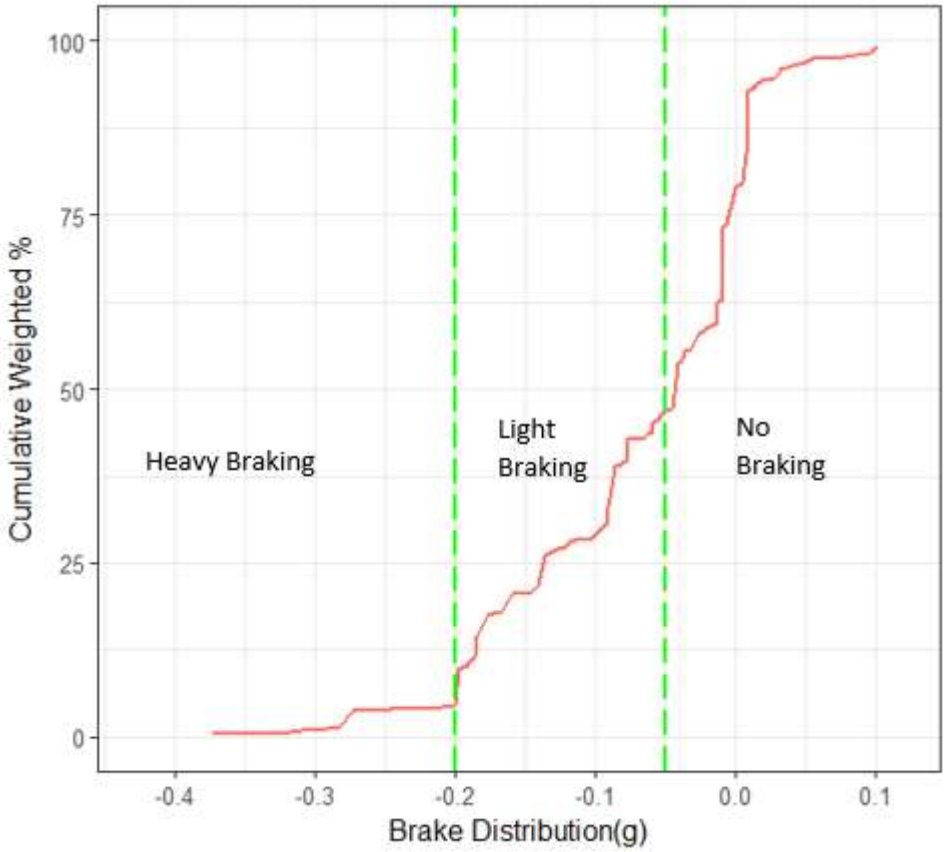

Figure 26. Distribution of deceleration prior to impact.

4.8.3 BRAKING LEVEL MODEL

Recall that the first goal of the approach model was to estimate the braking level of a vehicle. The final forms of the heavy and light logistic models used to estimate braking level are shown in Equation 3 and Equation 4 below. The same input variables were used for both models.

$$\log\left(\frac{p}{1-p}\right) = B_0 + B_1(impact\ speed) + B_2(struck) + B_3(crashtype) + B_4(senior) + B_5(young) \quad (3)$$

$$\log\left(\frac{p}{1-p}\right) = B_0 + B_1(impact\ speed) + B_2(struck) + B_3(crashtype) + B_4(senior) + B_5(young) \quad (4)$$

Where p was the predicted probability of heavy or light braking, impact speed was the speed of the vehicle at impact, struck represented the class of the vehicle, crashtype was either 1 or 0 representing a head-on crash versus a sideswipe respectively, and $senior$ and $young$ were variables used to represent the driver age. If the vehicle was the non-encroaching vehicle, the struck variable would have a value of 1 and if the vehicle was the encroaching vehicle, the struck variable would have a value of 0. $Senior$ was defined as 1 if the driver was older than 65 and $young$ was defined as 1 if the driver was younger than 20. Otherwise both variables were set to 0.

Table 15 below shows the values for the coefficients for heavy braking logistic regression model. This model represents the probability that the vehicle experienced heavy braking prior to impact.

Table 15. Coefficients and p-values for heavy braking model

	Coefficient	Coefficient Value	P-Value
Intercept	B_0	0.92	3.69E-12
Impact Speed	B_1	-0.13	< 2e-16
Struck	B_2	0.67	6.34E-08
Crash Type	B_3	-1.27	< 2e-16
Senior	B_4	0.42	0.0264
Young	B_5	0.42	0.0279

The same variables that were used to predict heavy braking were used to predict the possibility of light braking. The coefficients and p-values for the probability of light braking are shown in Table 16. In this model the struck variable is not significant. The other variables in the light braking model may account for its effect rendering it insignificant.

Table 16. Coefficients and p-values for Light Braking Model

	Coefficient	Coefficient Value	P-Value
Intercept	B_0	1.76	< 2e-16
Impact Speed	B_1	-0.051	< 2e-16
Struck	B_2	-0.00015	0.996
Crash Type	B_3	-0.11	7.05E-05
Senior	B_4	1.69	< 2e-16
Young	B_5	1.21	< 2e-16

The heavy and light logistic regression models were used together to predict the braking level of the vehicle prior to impact. For both logistic regression models, a threshold of 0.5 was used to determine if the vehicle initiated heavy or light braking. If the light braking model indicated light braking occurred, then we assumed that the driver initiated light braking prior to the crash. This same process was used with the heavy braking model. In the event that both of the models returned true indicating both heavy and light braking, it was assumed that only heavy braking was conducted.

Figure 27 below shows a plot of the logistic regression illustrating the braking probability at different impact speeds. As can be seen, the probability of heavy braking is higher at low impact speeds while light braking is found across a range of impact speeds. This is due to the difference between the impact speeds and approach speeds. In this dataset, there was a weighted average approach speed of 58 kph. Using an example to clarify, if a vehicle involved in a cross-centerline crash had an impact speed of 8 kph, it is highly likely that the vehicle was traveling faster than 8 kph before the crash occurred. The low impact speed indicates that the vehicle braked prior to the crash.

The dashed green line represents the probability cutoff of 0.5 used in this study. Above this line, the logistic regression models would return 1 indicating heavy or light braking.

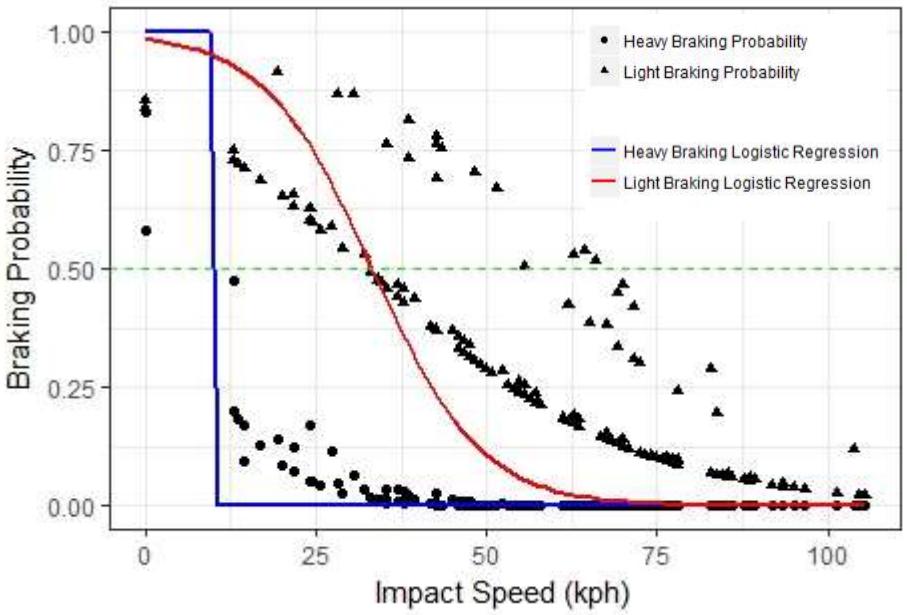

Figure 27. Logistic regression plot indicating braking models performance

These braking level models were tested using 2-fold cross validation. Together, the models correctly predicted different braking levels of a vehicle in 75% of the cases. Through further analysis, we found that of the 55 wrong predictions, 89% were only one level off. For example if the true level was Heavy Braking, the prediction would indicate Light Braking. The most common mistake made was predicting no braking when the true level was Light Braking. This suggests that these braking level models underestimate the true vehicle braking level.

4.8.4 APPROACH MODEL

The linear model for approach speed used the predictions from the braking level model along with the impact speed, speed limit, and an interaction term between the impact speed and the braking level model in order to predict the traversal speed. The full model is shown below in Equation 5.

$$Approach\ Speed = B_0 + B_1(Impact\ speed) + B_2(Heavy\ Braking) + B_3(Light\ Braking) + B_4(Impact\ speed) * (Heavy\ Braking) + B_5(Impact\ speed) * (Heavy\ Braking) \quad (5)$$

Where $Heavy\ Braking$ was either 1 or 0 depending on whether the vehicle experienced heavy braking prior to impact. This was determined using the heavy braking logistic regression model discussed above. $Light\ Braking$ was similarly 1 or 0 depending on the probability of light braking that the light braking logistic regression model produced. Two interaction terms were also included between Impact Speed and Heavy Braking and Impact Speed and Light Braking. Table 17 below shows the coefficients along with the p values for each variable.

Table 17. Coefficients of approach speed model

	Estimate	P-value
(Intercept)	4.26	0.092
Impact Speed	0.93	< 2e-16
Heavy Braking	46.85	< 2e-16
Light Braking	22.13	0.0027
Impact Speed:Heavy Braking	-0.018	0.78
Impact Speed:Light Braking	-0.028	0.85

Interaction terms between impact speed and the Heavy and Light Braking variables were thought to be needed due to the use of impact speed in the logistic regression models used to develop those variables. The p-values of these interaction terms were not significant however, leading to elimination of these terms in the final model. The final model for approach speed is shown below in Equation 6 which includes impact speed, heavy braking, and light braking.

$$Approach\ Speed = B_0 + B_1(Impact\ speed) + B_2(Heavy\ Braking) + B_3(Light\ Braking) \quad (6)$$

Table 18 below gives the coefficients and p values of the final approach speed model.

Table 18. Coefficients of the final approach speed model

	Estimate	P-value
(Intercept)	4.74	0.128
Impact Speed	0.92	< 2e-16
Heavy Braking	46.27	< 2e-16
Light Braking	20.93	1.05e-12

Shown in Figure 28, validation was performed through a plot of predicted speeds using the approach model versus the actual travel speed.

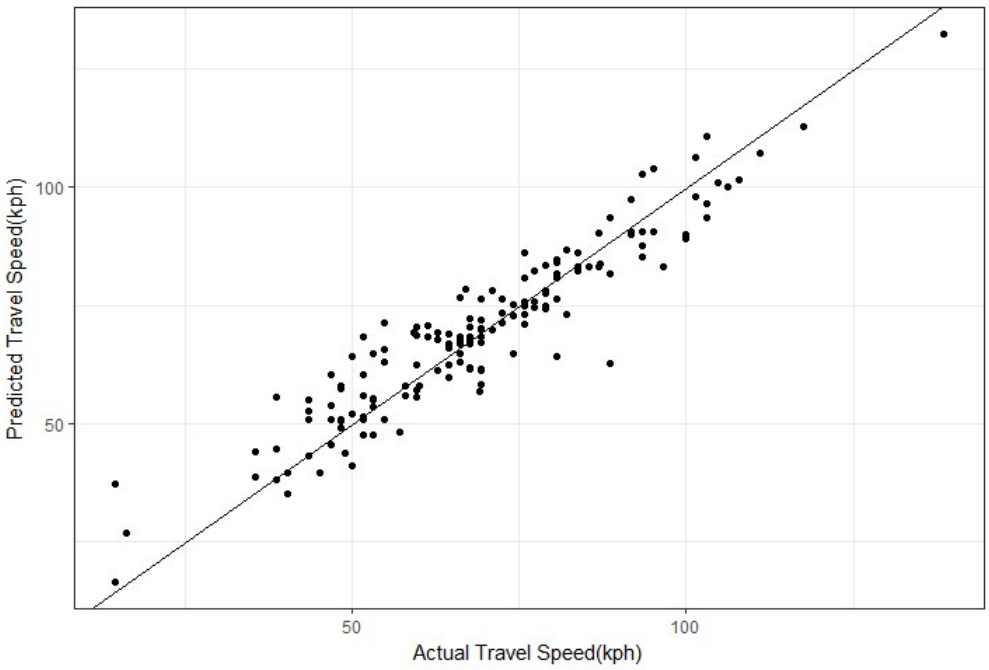

Figure 28. Plot of actual approach speed versus the predicted approach speed. There is good correlation between the model results and the actual results.

Further analysis examined the percent difference between the predicted approach speed and the actual approach speed of the vehicle. It was found that 50% of the predicted speeds were within 7.5% of the actual speed and 90% were within 20.1% of the actual approach speeds of the vehicle.

4.9 Conclusion

This study used pre-crash data from EDR's and related crash factors such as vehicle encroachment, crash type, and driver age, in order to predict the presence of heavy or light braking of a vehicle prior to a crash using logistic regression models. The vehicle impact speed and presence of heavy or light braking were then used to predict the approach speed of a vehicle using a linear regression model. The logistic regression models were validated using two-fold cross validation while the R^2 value was used to evaluate the linear regression model. Results show good comparisons between the predicted approach speeds and the actual vehicle approach speeds. This approach model was applied in order to predict approach speeds and develop realistic speed profiles for vehicles in the NMVCCS simulation dataset.

5 Crash Benefits of LDW Systems Applied to Cross-Centerline Crashes[1]

5.1 Introduction

Lane departure cross-centerline crashes occur when a vehicle drifts out of their lane and into a lane with a vehicle traveling in the opposite direction. While not as frequent as road departure crashes, cross over to left crashes account for 44% of injured occupants in non-junction vehicle-to-vehicle crashes despite only accounting for 5% of these total crashes [1]. In 2010, cross-centerline crashes accounted for 2711 fatalities [1]. Previous studies have shown that overtaking is not a major cause of these crashes on two lane opposite direction roadways. Instead, up to 65% of these fatal head on crashes involve vehicles drifting over the centerline which could indicate driver inattention [2].

Lane departure warning (LDW) is an active safety system that uses sensors to detect when a vehicle is inadvertently moving out of its lane. LDW is not activated if the driver indicates a purposeful lane departure, e.g. when using a turn signal. After detecting a departure, LDW systems deliver an audible, visual, or tactile warning to the driver to alert the driver to the departure. While LDW systems only provide an alert to the driver, lane departure prevention (LDP) systems can automatically generate a steering impulse to guide the vehicle back into its lane if the driver does not react to the warning. Several papers have investigated the potential benefits of fleet wide LDW systems applied to road departure crashes [50, 52, 54].

Less has been reported on the effectiveness of LDW for prevention of cross-centerline crashes. Zellner et al. (2015) evaluated a pre-production head-on crash avoidance system using

[1] Parts of the work shown in this study have been part of a previously published peer-reviewed manuscript: Holmes, D., Sheroni, R., & Gabler, H. C. (2018). *Estimating Benefits of LDW Systems Applied to Cross-Centerline Crashes*. Paper presented at the SAE WCX World Congress Experience 2018, Detroit, Michigan.

the Advanced Crash Avoidance Technology (ACAT) - II safety impact methodology [70]. This preproduction system detected impending head-on collisions using a combination of radar and lateral acceleration measurements. Upon receiving a warning, the driver applied steering to avoid the crash. To accurately characterize pre-crash driver evasive steering, prior tests from a driving simulator were used. The system discussed in Zellner et al. (2015) activates based on a threshold of time to collision to the oncoming vehicle provided certain pre-impact conditions are met [70]. In contrast, the hypothetical LDW system discussed in this study activate upon a vehicle crossing a lane line. The different activation criteria between these systems can lead to a difference in benefits found in regards to cross-centerline crashes.

5.2 Objective

The objective of this study was to quantify the number of crashes avoided or modified if every vehicle in the US vehicle fleet was equipped with a LDW driver assistance system.

5.3 Methodology

This study was approached in four separate parts that are discussed in more detail below. Initially, cross-centerline crashes were selected from NMVCCS. Path measurements were taken and each crash was reconstructed in PC-Crash in order to find the impact speed. Then a LDW model was applied and the crash outcome was recorded with and without a LDW system installed.

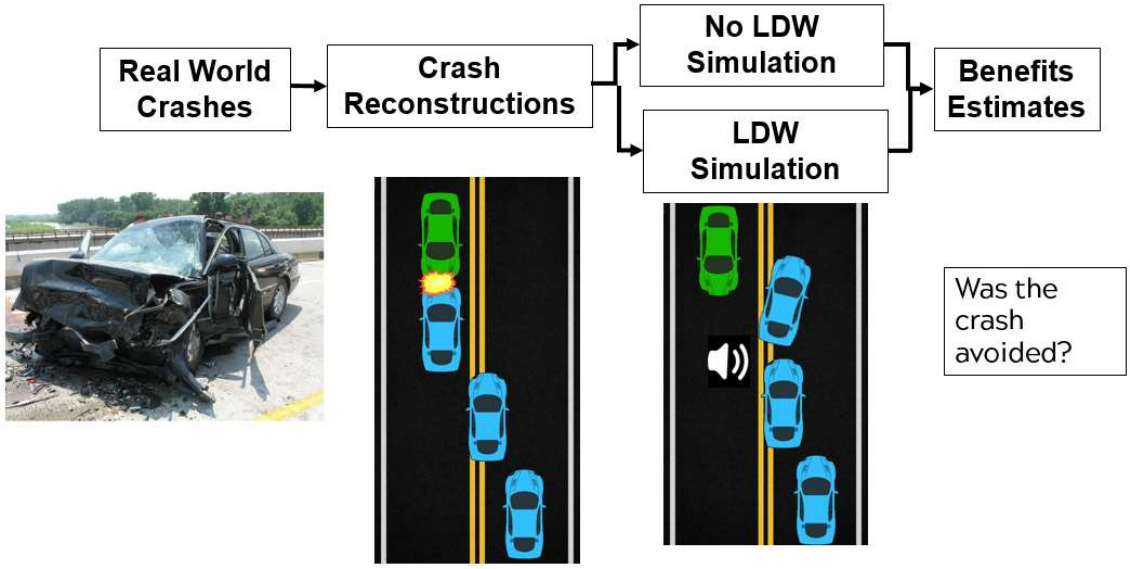

Figure 29. General methodology to estimating crash benefits of LDW systems.

5.3.1 DATA SOURCE

Real world collisions were extracted from the National Motor Vehicle Crash Causation Survey (NMVCCS). NMVCCS was a crash investigation program sponsored by the National Highway Traffic Safety Administration (NHTSA) that collected data from selected crashes occurring from 2005 – 2007 [88]. This dataset is commonly used to evaluate potential benefits of driver assistance systems due to the additional information on pre-crash scenarios and critical reasons for the pre-crash event leading up to the crash.

For this specific study, cases were selected based on the crash location, crash configuration and the vehicle movements prior to the crash. The target crash scenario was a non-divided road crash with a centerline lane departure being the primary movement prior to the crash. To exclude intersections, all crashes selected occurred in a non-junction and non-interchange area. In every crash, one vehicle had to cross over the centerline and strike another vehicle that was traveling in the opposing lane. Crashes involving two vehicles traveling in opposite directions in the same lane without the scene diagram showing one crossing over the

centerline were excluded. Only cases where both vehicles were tracking and under control prior to the crash were included. If the encroaching vehicle had lost control prior to the crash, a LDW system would have provided little benefit.

5.3.2 *CRASH RECONSTRUCTIONS*

As discussed previously in Chapter 3, path and speed reconstructions were performed on each crash initially selected. The focus for path reconstruction was primarily on reconstructing each vehicles trajectory prior to the crash. Path reconstruction was performed using the scene diagram drawn by the NMVCCS investigators who were on-scene prior to the crash being cleared. In order to ensure a global frame of reference, which makes reconstructing the movement of both vehicles easier, AutoCAD was used. When a new AutoCAD file is created, the program automatically generates a global reference system. The global reference system within AutoCAD was used instead of attempting to set an origin for a reference system somewhere on the scene diagram.

Once the trajectory of the vehicle was known through path reconstructions, the speed of the vehicle had to be reconstructed. While this was done using different methods depending on if a vehicle experienced rollover or there was a heavy vehicle involved, primarily PC-Crash was used to reconstruct the impact speed. PC-Crash uses an impulse-restitution model and models forces around a point of intersection between the two vehicles [85]. Using the scene diagram, representative vehicle models were placed at the impact location shown and the crash was simulated. The objective of the simulation was to minimize the difference between the post-impact vehicle motion in the PC-Crash simulation and the post-impact vehicle motion shown on

the scene diagram. This was done using the built-in collision optimizer in PC-Crash. The collision optimizer function has been validated in previous studies [86, 87].

While PC-Crash provided information about impact speed and brake application after the crash, the pre-crash speed of the vehicle needed to be determined in order to develop the full speed profile of the vehicle prior to the crash. For this objective, an approach speed model was developed using data downloaded from EDRs in NASS/CDS. This model is discussed fully in Chapter 4. The objective of this approach model was to estimate the approach speed using known factors of the crash such as impact speed, crash configuration, and speed limit. The approach speed was assumed to be the recorded speed of the vehicle at 5 seconds prior to the crash. The approach speed was initially estimated to be a function of impact speed, braking level, vehicle class (encroaching or non-encroaching vehicle), and the speed limit. To find the braking level, a deceleration profile for each vehicle was calculated. Using the average deceleration, each vehicle was classified as having a braking level of heavy braking, light braking, or no braking. After creating two logistic regression models to predict the probability of heavy or light braking relative to no braking, the impact speed and braking level were used to predict the approach speed of the vehicle. While the approach model was developed using NASS/CDS data, this model was applied to the NMVCCS cases selected. Each database had the necessary data elements used within the approach model. This allowed estimation of the approach speeds of both vehicles in the NMVCCS case set.

Each vehicle's impact speed (speed at time = 0 seconds) was estimated from PC-Crash. Using the approach model, the approach speed (speed at time = -5 seconds) of each vehicle was estimated. In order to generate the full vehicle speed profile, the difference between the approach speed and the impact speed was modeled by assuming a jerk of 11.0 m/s^3 down to a maximum

deceleration. This value for jerk was chosen based on the typical magnitudes experienced by drivers during conflict situations [98]. The maximum vehicle deceleration was chosen based on road conditions [99]. In this study, three road conditions were considered as shown in Table 19.

Table 19. Maximum deceleration values for different road conditions

Road Condition	Maximum Deceleration Value(g's)
Dry	0.8
Wet	0.4
Icy	0.3

Figure 30 illustrates the vehicle speed profile used in the simulations. The approach speed was determined using the approach model, the impact speed determined from PC-Crash, and the max deceleration was determined from the road condition at the time of the crash.

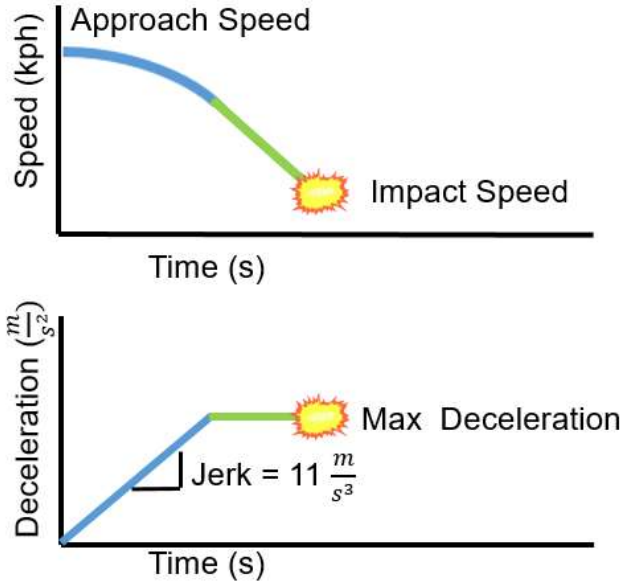

Figure 30. Vehicle speed profile used in simulations

If the impact speed was greater than the estimated approach speed, we assumed that the approach speed was equal to the impact speed and the driver did not take any evasive actions prior to the crash.

5.3.3 LDW SIMULATION

The LDW system was assumed to activate when the leading wheel of the vehicle touched the lane line. For an LDW system, the driver capability to react to the warning was also considered using the critical reason leading to the crash. The critical reason for each crash was assigned by NMVCCS investigators on scene as the immediate reason for the critical pre-crash event [88]. If the critical reason was the driver experiencing heart attack/physical impairment of ability to act, we assumed that the driver would not have been able to react to the LDW alert.

A critical reason when the driver was sleeping was was more difficult to account for. The coded value in NMVCCS for critical reason used to describe this was "sleeping, that is, actually asleep" which is described in the NMVCCS coding manual as when the driver is no longer consciously in control of the vehicle [88]. While that the driver was experiencing a level of sleepiness prior to the crash, it is difficult to know the exact level. The driver could have been drowsy enough to relinquish control of the vehicle, experienced a micro-sleep episode, or have been fully asleep. After the crash, investigators may be unable to distinguish between these levels of sleepiness.

In the case of drowsy drivers and drivers experiencing micro-sleep episodes, two studies have illustrated that a LDW system has a significant effect on awakening these drivers. Kozak et al. (2006), investigated drivers who were deprived of sleep for 23 hours prior to the testing [100]. That experiment showed that the addition of a LDW alert (in any tactile, visual, or audible manner), nearly halved the reaction time of drowsy drivers.

In a simulator study performed by Rimini-Doering et al. (2005), the effect of an LDW alert on sleepy male drivers was studied [101]. Several hundred micro-sleep episodes were observed during the study. The authors concluded that the addition of a LDW system

significantly reduced the frequency and severity of lane departure events even when the driver was experiencing micro-sleep prior to the warning.

In order to account for this uncertainty in sleepy driver response to a LDW alert, two simulations were run. In one simulation, the sleeping driver was assumed to react to the LDW alert with the standard reaction times used in this study. In another simulation, the sleeping driver did not react to the LDW alert. These simulations were used to present the upper and lower bounds for the potential benefits of a LDW system.

In all other situations where the driver was not physically impaired or sleeping, the driver was assumed to react to the LDW after some reaction time. Different studies have taken multiple approaches to modeling this driver reaction time. When determining LDW benefits in road-departure crashes, Scanlon et al. (2015) used two equally weighted driver reaction times of 0.38 and 1.36 seconds as a way to model the variability in reaction time across the driver population [54]. These were chosen as upper and lower bounds based on a study performed by Suzuki and Jansson (2003) in a driving simulator to investigate driver response to different LDW alerts [102]. Suzuki and Jansson tested 4 different alert methods: a monaural beep sound, stereo beep sound, steering vibration, and pulsing steering torque. In their study, every driver responded in some way to the alert. Two different conditions were tested. In the first condition, the subjects were not aware of the meanings of the warnings [102]. In the second condition, the subjects were made aware of the warning meaning and encouraged to try the system performance prior to the start of the study. Across all four alert methods, reaction times ranged from 0.38 seconds in the unaware condition (drivers not aware of the meaning of the alerts) to 1.36 seconds when all drivers were aware of the meaning of the alerts [102].

As previously discussed, Kozak et al (2006) found an average driver reaction time of

0.67 seconds based on a study of drowsy drivers' time to steering after receiving a LDW warning [100]. While both studies evaluated similar methods of delivering a LDW alert, Kozak et al (2006) specifically tested drivers deprived of sleep for 23 hours prior to the study [100]. For this study, the two driver reaction times of 0.38 and 1.36 seconds from Suzuki and Jansson (2003) were used to encompass the variance in reaction time across the national driver population in the United States.

To model the driver's response after receiving a lane departure warning and faced with an oncoming vehicle, it was assumed that the driver conducted an evasive steering maneuver and kept a constant speed. In this study, evasive steering was modeled using a steering radius that was a function of velocity and surface friction as shown in equation 7.

$$R = \frac{v^2}{\mu g} \tag{7}$$

Where R is the steering radius, v is the velocity of the vehicle at the point evasive maneuvering occurs, μ is the surface friction, and g is the acceleration due to gravity. This equation was derived by determining the maximum possible lateral force available between the tires and the road while the car is turning. In essence, this is the best case scenario for a LDW system. Using this formula assumes that the driver steers his vehicle at the limit of traction on the road in order to avoid the crash. We assumed a linear ramp up to this maximum acceleration over a period of 0.5 seconds. Figure 31 shows the lateral acceleration function used to model the driver steering after a LDW alert. The maximum lateral acceleration was determined from the surface condition as previously shown in Table 19.

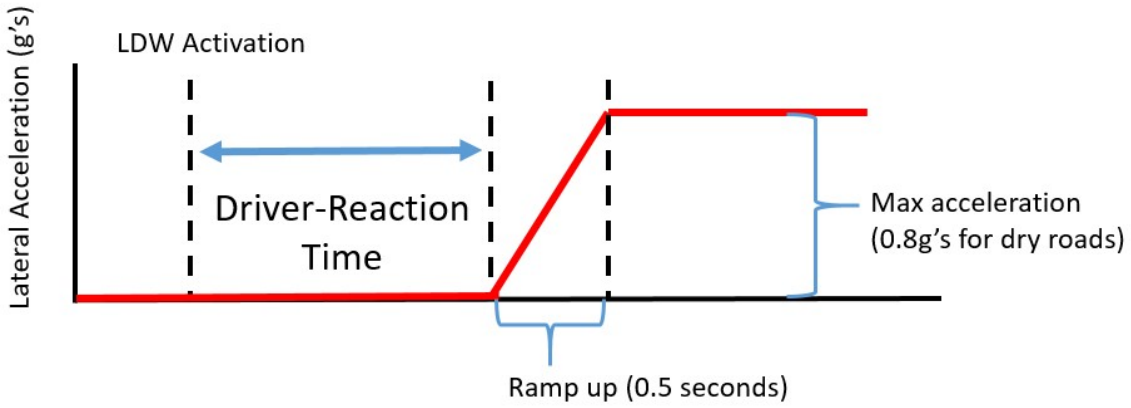

Figure 31. LDW lateral acceleration ramp function.

In the LDW simulation, the non-encroaching vehicle was assumed to maintain its original trajectory. This means that if the non-encroaching vehicle performed an evasive maneuver prior to the crash, it was assumed to perform the same action during the LDW simulations. Figure 32 illustrates an example of how this LDW system would function in a cross-centerline crash scenario. As described above, the difference between the initial approach speed and impact speed is modeled using a jerk of 11 m/s^3 initially. However, once the driver reacts to the alert, the vehicle speed remains constant throughout the evasive steering maneuver.

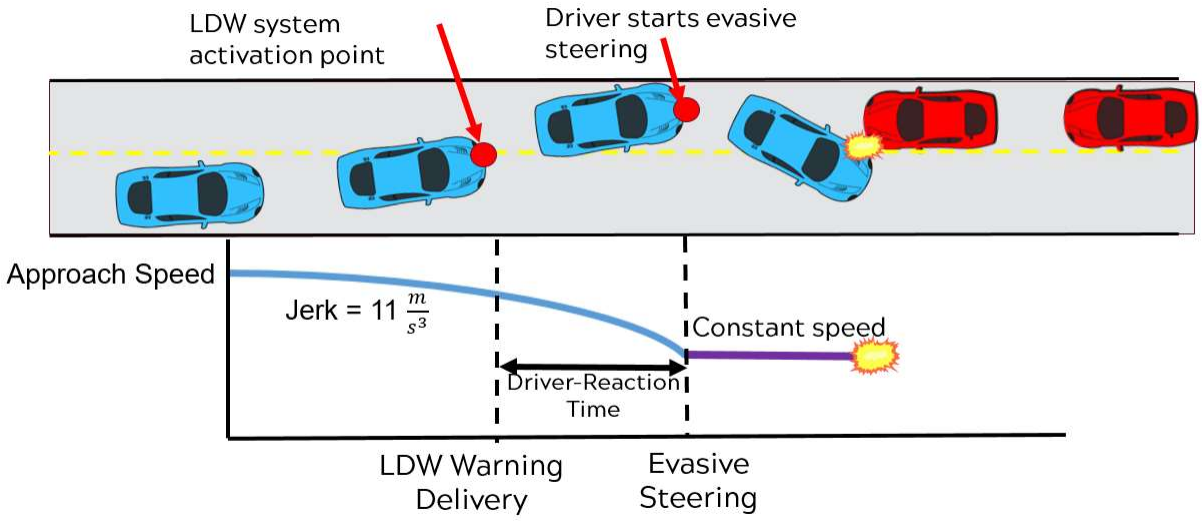

Figure 32. Diagram of LDW system activation criteria and speed profile of the vehicle throughout the simulation.

Each crash was first simulated as the crash originally occurred to generate a baseline. The simulations were then run again with the encroaching vehicle equipped with a LDW. The fleet wide benefits for both systems were calculated as a ratio between the weighted number of avoided crashes and the total weighted number of crashes.

5.4 Results

5.4.1 Passenger Vehicle LDW Dataset Composition

Using the criteria described before to identify a cross-centerline crash, initially 75 cases involving passenger vehicles were selected from NMVCCS representing 35,943 crashes nationally. From this initial dataset, 33 cases were excluded for lack of lane lines, inability to reconstruct, or non-relevant scenarios. A full breakdown of the excluded cases is presented in Table 20.

Table 20. Detailed count of exclusion reasons for passenger vehicle crashes

Exclusion Reason	Number of Cases
No lane lines at point of lane departure	6
Multiple moving vehicles	18
Not relevant	6
No impact location	1
Scene diagram scaling(couldn't be reconstructed)	2
Total cases excluded	33
Initial NMVCCS cases	75
Final case count	42

Table 21 provides the composition of the dataset. The most common road alignment in this dataset was curved roads accounting for 61.7% of the dataset when both curve directions were combined. Previous studies have shown that cross-centerline crashes are more likely to occur on curved roads and especially curve to the right roads as encroaching vehicles depart from their

lane while traveling around the curve [1].

Cross-centerline crashes are commonly thought to happen mainly on two lane roads [1]. In our dataset, over 75% of the cases in this study occurred on 2 lane roads. The most common speed limit in our dataset was 56 kph (35 mph) accounting for 39.1% of the dataset. In this sample, most speed limits ranged from 48 kph to 89 kph (30 – 55 mph).

Table 21. Data composition. Distribution of road alignment, number of lanes, speed limits, day/night, and weather conditions

Road Alignment	
Straight	38.3%
Curve right	27.1%
Curve left	34.6%
Number of Lanes	
2	78.1%
3	3%
4	11.1%
Speed Limits (kph)	
40	0.4%
48	7.2%
56	39.5%
64	13.4%
72	29.1%
80	2.8%
89	7%
97	0.2%
105	0.5%
Day/Night	
Daylight	79.4%
Dark	12.8%%
Dark, but lighted	6.1%
Dawn	0%
Dusk	1.7%
Weather Conditions	
Clear	86.4%
Cloudy	10.5%
Rain	3.1%

One factor of interest in lane and road departures is the lane departure angle. The lane departure angle influences the vehicles lateral speed at lane departure which governs how

quickly the vehicle can return to its original travel lane. This study used data from the project NCHRP 17-43 in order to provide a frame of reference for the lane departure angles found here. NCHRP 17-43 looked at all roadside departures (left and right) in NASS/CDS 2012 – 2015 [103]. This dataset represents over 385,000 road departure crashes nationwide. Figure 33 illustrates the distribution of lane departure angles in this cross-centerline dataset compared to the road departure angles in NCHRP 17-43 year 2012 - 2015. The median departure angle varied slightly with a weighted median departure angle of 8 degree for cross-centerline crashes and a weighted median departure angle of 11 degrees for the 17-43 dataset.

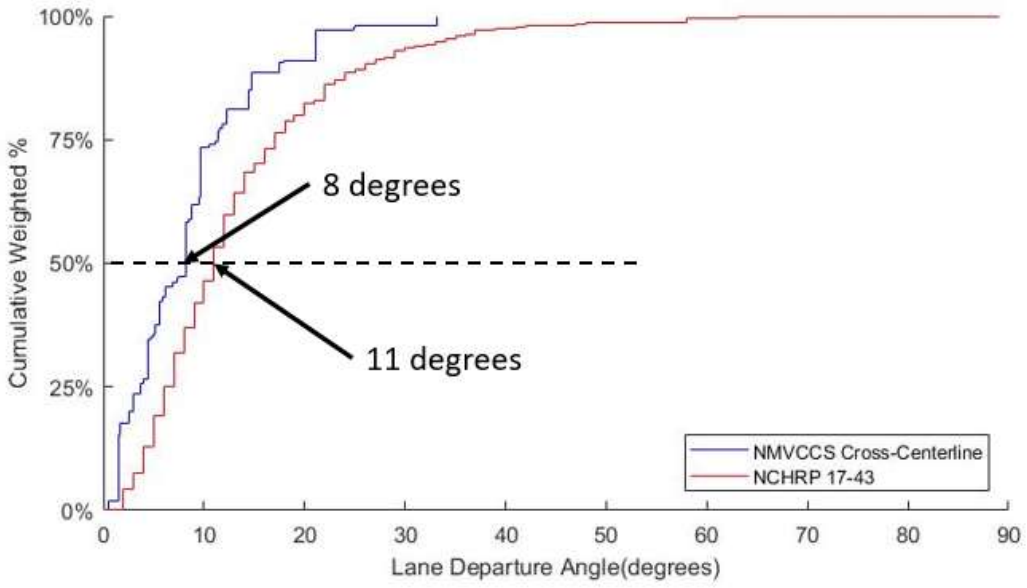

Figure 33. Comparison of lane departure angle in the cross-centerline dataset and road departure angle from NCHRP 17-43.

The approach speed of the vehicles was investigated as well. One factor that makes cross-centerline crashes severe is the high closing speeds of both vehicles. The effect of the approach model was also of interest. Figure 34 shows a comparison between the impact speed and approach speed. The median impact speed was 58 kph (36 mph) while the median approach speed was 68 kph (42 mph). Note that the approach model was not used in all cases. If the

impact speed was greater than the predicted approach speed, the vehicle was assumed to be traveling at a constant speed prior to impact. This occurred in 21 cases. In 16 out of these 21 cases, the vehicle was traveling faster than the posted speed limit. As can be seen from Figure 34, the approach model had the greatest effect in generating realistic approach speed values for low impact speed crashes.

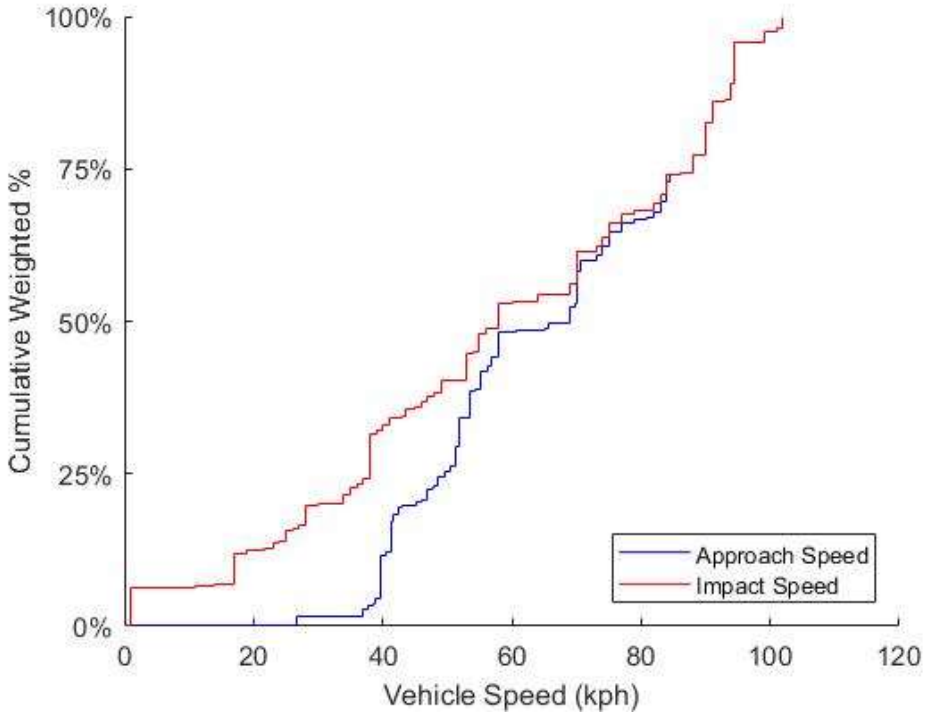

Figure 34. Distribution of approach speed compared to impact speed for both vehicles

The driver's capability to react to a LDW alert was determined through the use of the "Critical Reason" variable in NMVCCS. The unweighted distribution of critical reasons is shown in Figure 35. The most common critical reason for the crash (10 cases) was the driver sleeping. Two simulations were run in order to adequately account for the variability in sleepy driver's reaction to a LDW alert. One simulation assumed that a sleeping driver would react while the other assumed that an LDW system would have no effect. These simulations were used to present bounds for the potential effectiveness of an LDW system. In 7 cases, the driver was

physically impaired/unable to act prior to the crash. In these 7 cases, the drivers were assumed to not react to the LDW alert.

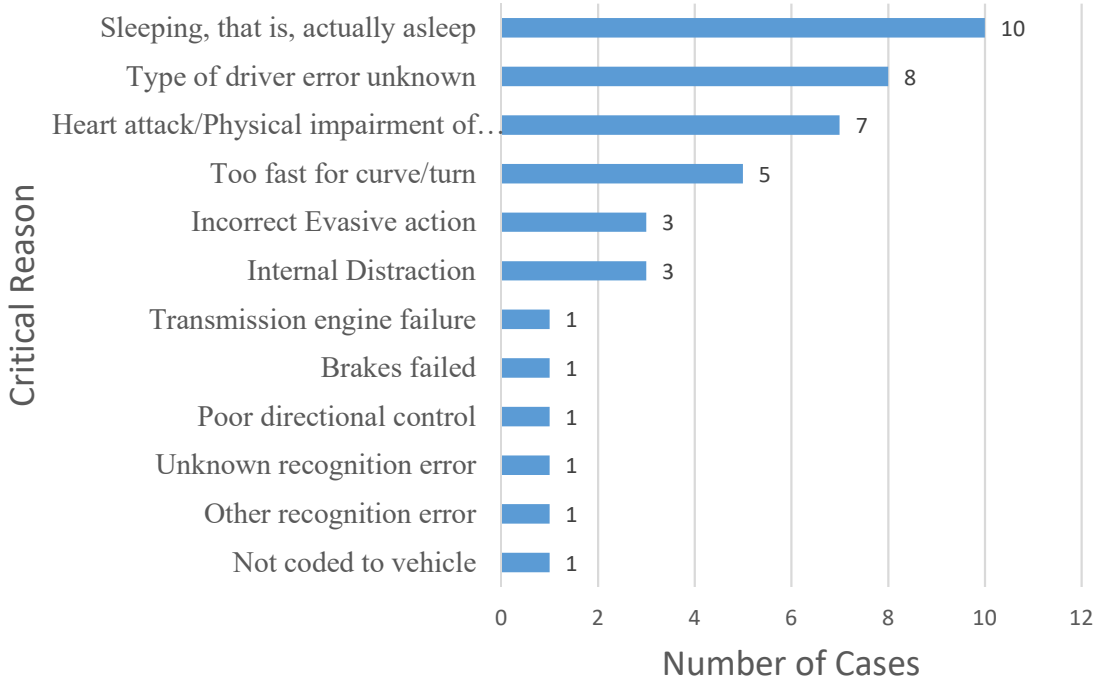

Figure 35. Critical reasons for the cross-centerline crash

Looking at the critical reasons in more detail, we can see that in a number of cases there were vehicle-related failures such as the brakes failed or the engine failed. In these cases, lane departure warning systems are unlikely to help as well. The reason we did not take into account these vehicle related failures into these simulations is due to the small sample size of this study. The small sample size makes these vehicle related failures seem like a greater issue and may not be representative of the actual causes of these cross-centerline crashes. From the literature review presented in Chapter 1, there is little to support the prevalence of vehicle related failures in this dataset. There is literature to support that driver distraction and/or drowsy or sleeping drivers play a role in these crashes [1, 2]. A future study may look at the causes behind cross-centerline crashes with a greater number of cases.

5.4.2 *Passenger Vehicle LDW Benefits*

Using the LDW model described previously, this study estimated that between 22 - 30% of cross-centerline lane departure crashes could be potentially avoided completely if every vehicle in the US passenger vehicle fleet was equipped with a LDW system. In these cases, drivers had enough time to react to a lane departure warning and successfully steer out of the way of the oncoming vehicle. An estimated 18 - 24% of crashes had a modified impact location after activation of LDW. In these cases, the driver of the encroaching vehicle was able to react to the warning but was unable to completely avoid an impact with the other vehicle. In some of these crashes the crash configuration was significantly changed from what occurred originally possibly resulting in different occupant injuries.

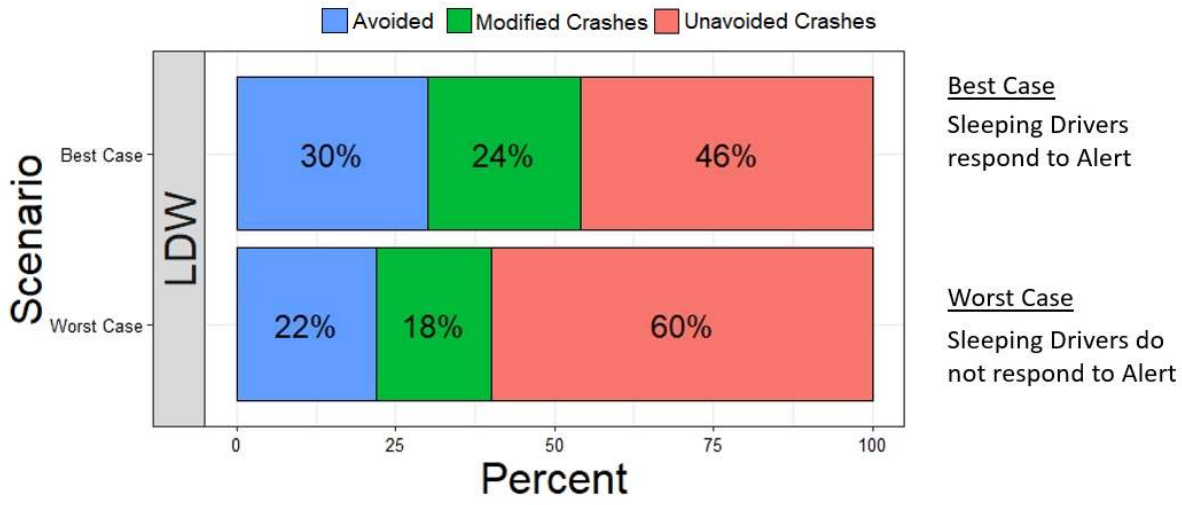

Figure 36. Visual description of LDW estimated crash benefits.

To look closer into the effects of a LDW system, the delta-V values of the crash were investigated. The weighted average delta-V across the original 42 cases was 30 km/hr. In the LDW simulations, every crash that was avoided was assumed to have a delta-V of 0. For all

other crashes, the crash was simulated in PC-Crash and the delta-V was assumed to be the change in velocity over the first 300 ms of the crash. Looking at all of the crashes, including the ones that were avoided with a LDW system, the weighted average delta-V was 20 km/hr. This represents a 33% reduction in delta-V.

By only looking at the crashes that were modified by the installation of the LDW system, we can determine if a LDW system increases or decreases the delta-V. There is also the possibility in some of these cases that an LDW system and the subsequent driver steering could change the crash configuration enough to injure the driver more so than if the LDW system had not been installed. Figure 37 illustrates an example of this. In (A) the driver impacts another vehicle with full frontal frame engagement. Several crash tests include variants of this crash configuration and OEMs specifically design to protect the occupants in the event of this crash [104]. In (B) we can see that, because of the driver initiating evasive steering, the collision is transformed from a frontal collision to a side impact. Side impacts may induce higher severity than the original full frontal engagement head-on crash [105, 106].

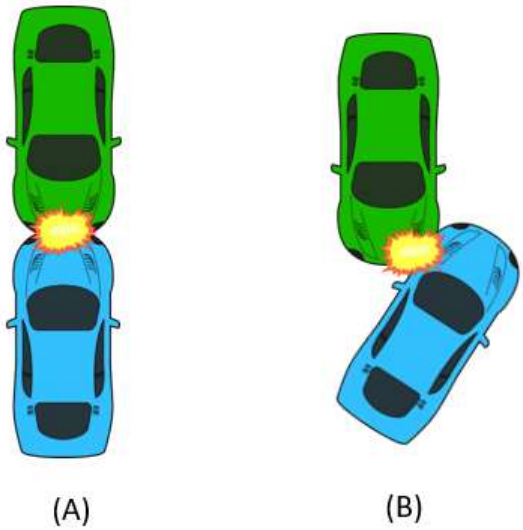

Figure 37. Difference in crash configuration when driver initiates evasive steering. (A) Without LDW system. (B) With LDW system

In this dataset, the original subset of crashes that became modified crashes with a LDW system installed originally had a weighted delta-V of 26 kph. With an LDW system, these crashes were modified resulting in an average weighted delta-V of 15 kph. This represents a 42% reduction in delta-V from the original crashes. This indicates that a LDW system might mitigate the severity of a crash even if the use of the LDW system is unable to completely avoid a crash.

5.4.3 *Heavy Vehicle and Rollover Crashes dataset composition*

Putting the heavy vehicle and rollover reconstruction methodologies described in Chapter 3 to use, 18 cases were selected that involved either a heavy vehicle or a vehicle that experienced a rollover post-impact. From these 18, 8 cases were excluded for the reasons detailed in Table 22.

Table 22. Exclusion reasons for heavy vehicle and rollover cases

Exclusion Reason	Number of Cases
Heavy vehicle experienced rollover (cannot reconstruct using Kildare curves)	2
Not relevant	5
Impact with motorcycle	1
Total cases excluded	8
Initial NMVCCS cases	18
Final case count	10

None of the cases that involved the rollover of a heavy vehicle could be reconstructed using the current reconstruction method. The current method relies on the Kildare curves which use trip distance, vehicle mass, and vehicle type in order to estimate the trip speed prior to the rollover event. While there are Kildare curves for small cars, pickups, and sedans, there is no curve for heavy vehicles.

After measurements and reconstructions using PC-Crash and the Kildare curves, 10 cases remained representing 3,547 of crashes nationwide. To investigate the dataset composition further, the body type composition of the vehicles was analyzed. Figure 38 illustrates the distribution of body types across the dataset. Passenger cars represented the largest portion of the passenger vehicles, accounting for 1,492 vehicles. The most common body type among the heavy vehicle class was a single unit straight truck. During reconstructions, the cases involving a single unit straight truck were easier to reconstruct than others due to the pre-built custom models that PC-Crash has of single unit trucks.

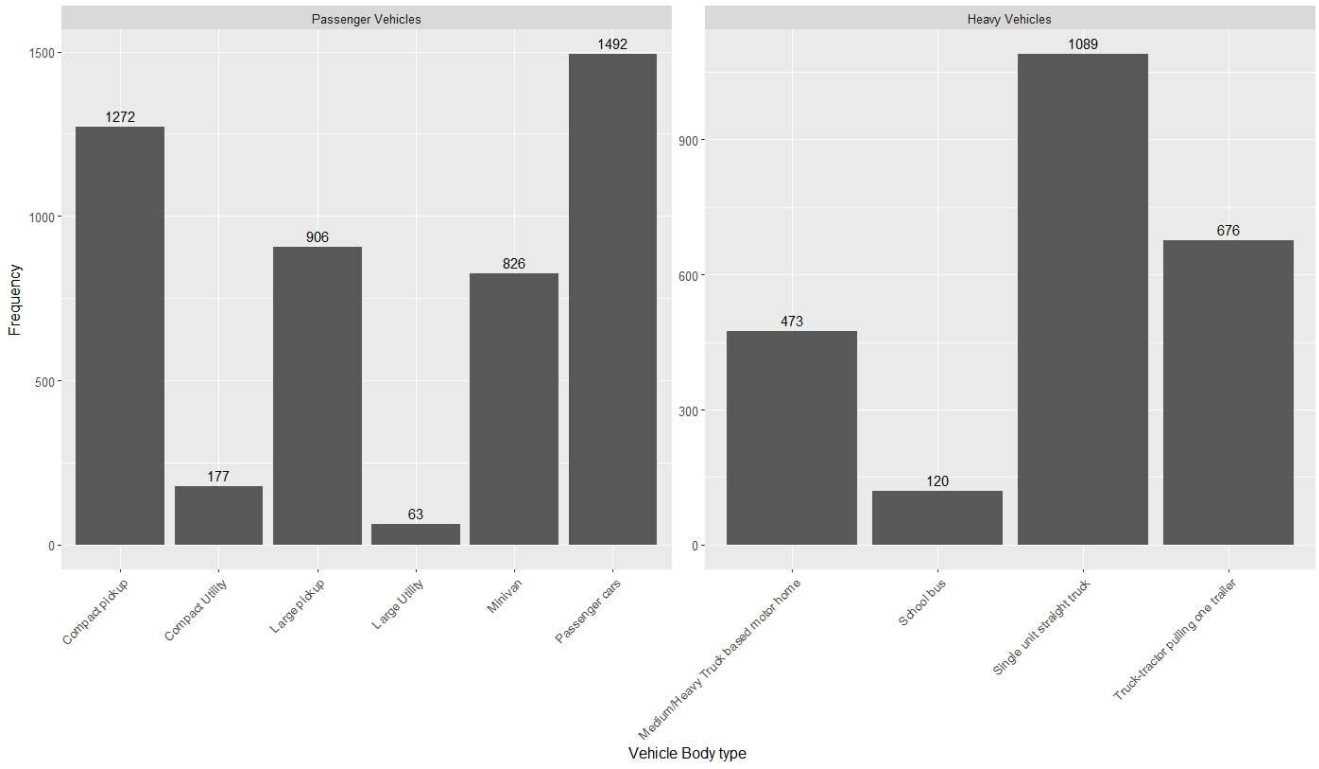

Figure 38. Body type distribution of vehicles reconstructed using special reconstruction methodology.

Rollover and heavy vehicle crashes are especially of interest to prevent because of the typical high severity of the crash. Table 23 illustrates the average impact speed of the encroaching vehicle and the delta-V of rollover and heavy vehicle crashes in comparison with the entire dataset. As can be seen, rollover crashes had higher impact speeds with an average

impact speed of 88 kph (55 mph) compared to 72 kph (45 mph) for all crashes. Note also that most heavy vehicle crashes occur at similar speeds to regular crashes. While these crashes occurred at similar speeds, we expected that these crashes had more severe injuries due to the mass difference between a heavy vehicle and a passenger vehicle.

Table 23. Comparison of impact speed and delta-V across the datasets used in this study.

	# of Cases (weighted)	Average Impact Speed of Encroaching Vehicle (kph)	Average Delta-V (kph)
All Crashes	52 (23,014)	72	30
Crashes, non-roll, non-heavy vehicle	42 (19,467)	71	30
Rollover	5 (1,366)	88	29
Heavy vehicle	5 (2,181)	71	28

Investigating the hypothesis that rollover and heavy vehicle crashes result in more severe injuries than regular crashes, Figure 39 shows the maximum injury experienced in the encroaching vehicle on the KABCOU scale. While non-rollover non-heavy vehicle ("regular") crashes were dominated towards incapacitating injury levels and below, heavy vehicle and rollover crashes tended to be more severe than regular crashes.

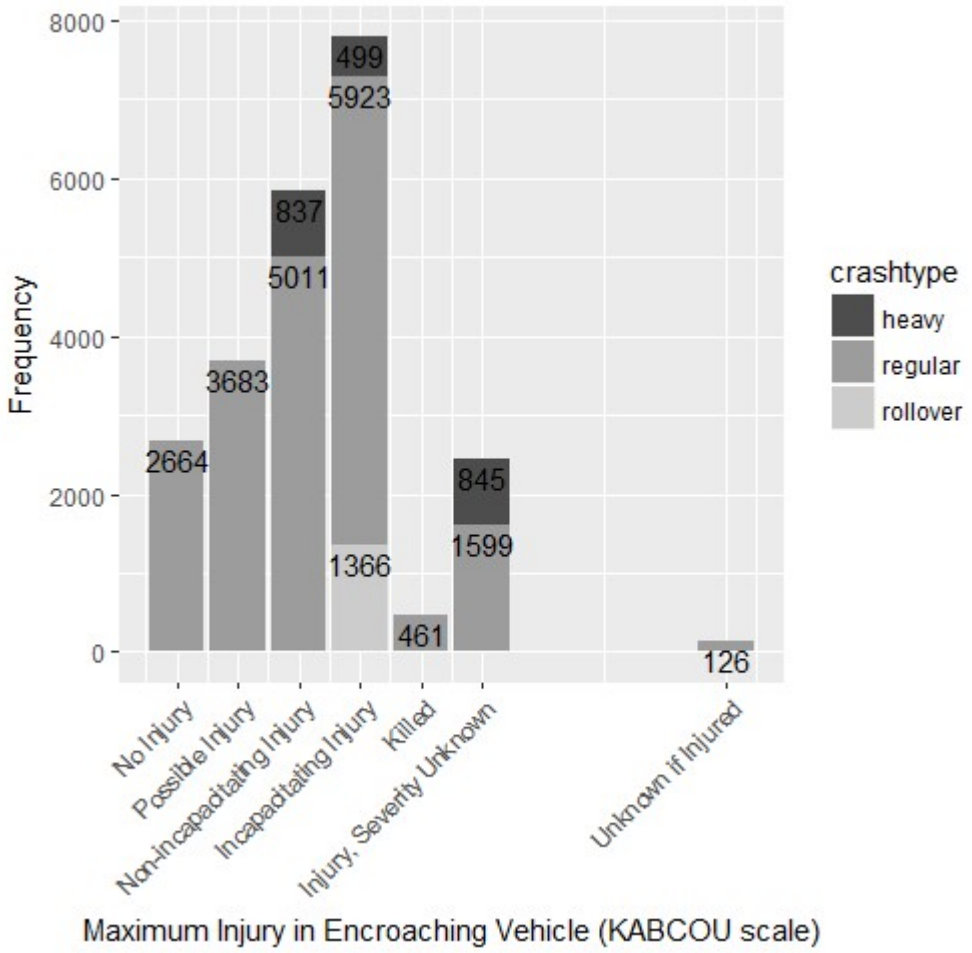

Figure 39. Injury comparison between rollover, heavy vehicle, and passenger vehicle crashes.

To look at the reason behind the crashes, the critical reason variable was used. The distribution can be seen in Figure 40. As can be seen, one driver was sleeping and two additional drivers were physically impaired prior to the crash.

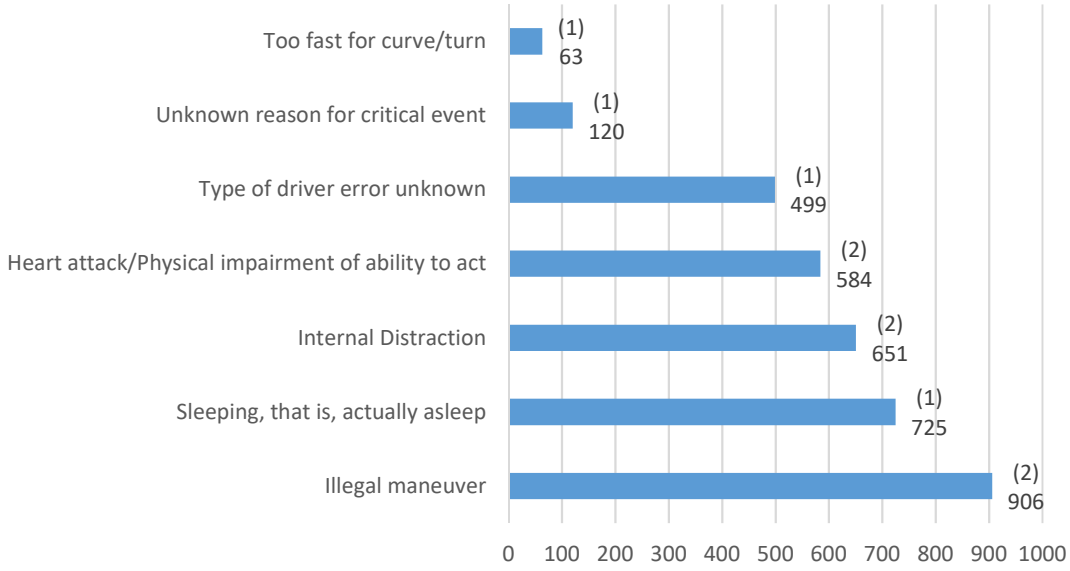

Figure 40. Critical reasons behind crash for rollover and heavy vehicle crashes. Raw number of cases is shown in the parentheses.

5.4.4 Heavy Vehicle And Rollover LDW Crash Benefits

With a LDW system installed, 18% of crashes were avoided in heavy vehicle and rollover crashes. Modified crashes ranged from 17% - 27% due to the fact that one driver was sleeping prior to the crash. This range is presented to represent the best case scenario, where the driver wakes up and reacts to LDW alert, and the worst case scenario, where the driver does not react prior to the crash. Using these numbers and the national weighting factors, the benefits based on the original dataset can be updated with a larger dataset (42 cases vs 52 cases with rollover and heavy vehicle crashes included). When combined with the overall case set and appropriately weighted according to the size of the respective datasets, 21% to 28% of crashes were avoided based on if a sleeping driver would react to a LDW alert or not. In 18% – 24% of crashes, the crash configuration was changed due to the installation of a LDW system. From the original benefits discussed previously, we see a slight decrease by including these cases. With the original non-rollover non-heavy vehicle dataset, an LDW system would result in an estimated

22 – 30% of cross-centerline crashes being avoided. With this larger dataset containing heavy vehicles and rollovers, an LDW system is estimated to avoid 21 – 28% of crashes.

5.5 Discussion

To put the crash benefits presented above into context, the benefits estimated for LDW were compared with the benefits of centerline rumble strips. Rumble strips are perhaps the most direct comparison to a LDW system as they both alert the driver upon crossing a lane line, albeit in different ways. Several studies have shown that centerline rumble strips are effective at preventing head-on and sideswipe opposite direction crashes, the same crash types simulated here with a LDW system. In one study based on state data from Minnesota, Pennsylvania, and Washington State, centerline rumble strips were estimated to have a crash reduction factor of 37% for head-on and sideswipe crashes on rural roads [23]. If only considering head-on and sideswipe crashes that resulted in an injury, the same analysis showed that centerline rumble strips have a crash reduction factor of 45% [23].

While the benefits of centerline rumble strips are larger than the estimated benefits for an LDW system presented here, one primary advantage of a LDW system is that the countermeasure is vehicle based while centerline rumble strips are road based. Consequently, a LDW system for addressing head-on and sideswipe opposite direction crashes is available everywhere unlike centerline rumble strips which require installation and maintenance. As an example, none of the cases in our dataset had centerline rumble strips installed.

Another interesting result found in this study was the amount of time that drivers had from the initial lane departure to the collision. Figure 41 illustrates that over 50% of drivers had more than 1 second to collision which should be sufficient time to react to an alert and possibly avoid the impending crash. In contrast, approximately 30% of crashes had a TTC of 0.32 seconds or

less indicating that these crashes might not be avoidable without automated intervention such as an LDP system.

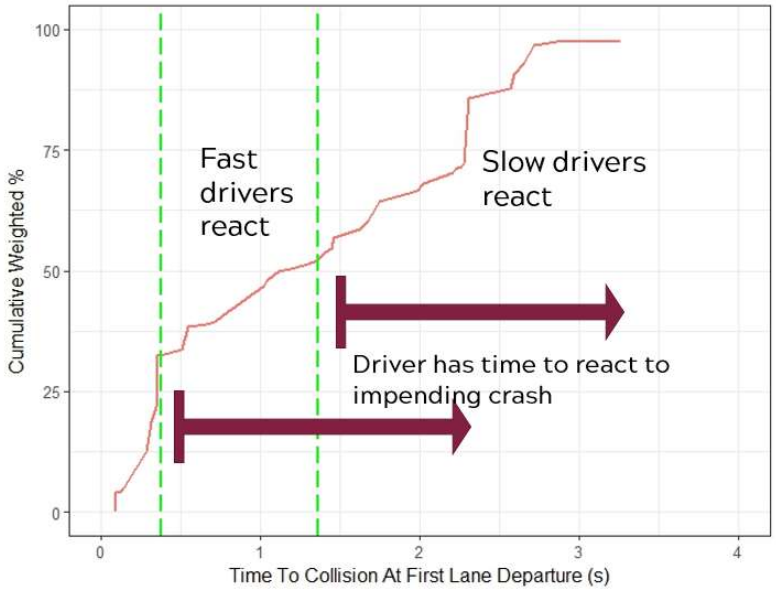

Figure 41. Time to collision at the point of first lane departure. Many drivers had a chance to react prior to the crash.

5.6 Limitations

This primary limitation of this study was the small number of cases the simulation set was based on. While every attempt was made to gather more cases in the form of rollovers and heavy vehicles, this still only resulted in 52 crashes as a basis for the simulations and estimated benefits. This study also used two values for driver reaction time to represent the variability in driver reaction time across the United States. There is the possibility that using only two reaction times might not account for all of the variability inherent in driver reaction time.

One assumption of this study was also that the LDW system was always turned on. In reality, driver acceptance of these systems varies. In many cases, drivers may deactivate these systems. One study has found that LDW systems were deactivated in two-thirds of the cars investigated [57]. Consequently, the benefits of a LDW system are lower than what is presented here.

This study also used a hypothetical model of a LDW system that activated at the moment the leading wheel touched the lane line. The system specifications for activation of production LDW systems are proprietary and may differ from this hypothetical system. Additionally, the only evasive maneuver assumed after LDW activation in this study was steering. It is possible that some drivers may brake and steer or even accelerate trying to avoid the crash. These possibilities were not considered in this study.

One scenario is also possible that, in the event of this evasive steering, the initial head-on impact is avoided but the driver loses control of the vehicle or over reacts to the impending crash. In this case, there is a possibility that the vehicle could impact another object or travel off the roadway to the right resulting in a road-departure crash. This study did not consider that scenario.

6 Injury Benefits of LDW Systems

6.1 Introduction

This chapter projects the injury benefits of a LDW system for use in a future vehicle fleet in 2025. There are multiple methods to estimate injury risk in simulations [91, 107-112]. These can generally be classified as one of two methods: methods involving finite element modeling or statistical methods. Finite element modeling is commonly used to assess occupant injury risk but the development and validation of the model can take time and be computationally intensive [113]. Additionally some of the data elements that finite element models require are not available in NMVCCS. This study used statistical modeling with injury risk curves developed using logistic regression models to estimate the occupant injury risk. Statistical modelling has been used previously to estimate the injury benefits of driver assistance systems [47, 54].

6.2 Methodology

6.2.1 *INJURY RISK MODELING*

This study was based on cases extracted from NMVCCS which investigated crashes from 2005 – 2007 [88]. Because NMVCCS data collection occurred a decade ago, not every vehicle in NMVCCS crashes was equipped with frontal or side airbags. In a future vehicle fleet in 2025, all vehicles would be equipped with frontal and side air bags. This future vehicle fleet was also expected to have the best possible passive safety countermeasures available today. One measure of vehicle passive safety comes from the US New Car Assessment Program (NCAP). Originally mandated in 1973, NCAP was created in order to provide consumers with information on the crashworthiness of a vehicle [114]. In 1994, NCAP changed their reporting system from a technical numbers-based report to a simple 5 star rating system [114]. NCAP runs 4 different

crash scenarios and determines individual star ratings for each of the scenarios. The scenarios are a frontal collision, side barrier collision, side pole collision, and a rollover test. In the frontal collision test, a vehicle crashes into a fixed barrier at 35 mph [114]. In the side barrier crash test, a moving deformable crashes into the vehicle side at 38.5mph [114]. A 5 star rating for frontal collisions represents less than a 10% chance of serious injury in a frontal collision while a 5 star rating for side impacts represents less than a 5% chance of serious injury in a side impact [114]. For the purposes of projecting injury benefits to a future fleet, all vehicles were modelled as if they would be rated 5 stars using the US NCAP star ratings. Bareiss and Gabler (2018) present the methodology and development of a near-side injury risk model using this method in the paper "Preliminary Estimates of Near Side Crash Injury Risk In Best Performing Passenger Vehicles" [80]. Bareiss generated three initial injury risk curves to determine frontal, near-side, and far-side injury risk for front-row occupants. The injury risk curves were developed using data from NASS/CDS from years 2010 – 2015 [80]. This database was used as the data source due to the large amount of medical data collected on each of the occupants in the vehicle. The frontal injury risk model was developed by Bareiss and Gabler and used the same methodology presented in Bareiss and Gabler (2018) [80]. In this study, the frontal injury risk model was used to predict the injury risk of all frontal occupants involved in a frontal impact.

6.2.2 Determining Frontal Injury Risk

Bareiss used a logistic regression model to model the risk of a serious injury for the frontal occupants which was defined as a maximum AIS value of 2 or greater (MAIS2+). The final form of the frontal injury risk model can be found in equation 9.

$$P(MAIS2+) = \frac{1}{1 + e^{-logi}} \tag{9}$$

$$logit_{frontal} = \beta_0 + \beta_1 \cdot \Delta v + \beta_2 \cdot belted + \beta_3 \cdot senior + \beta_4 \cdot male \quad (10)$$

Where,

($MAIS2+$) = Probability of a moderately injured driver (0-1)

β_{0-4} = Model Parameters

Δv = Total change in velocity (km/hr)

$belted$ = 1 if driver was known to be belted / 0 otherwise

$senior$ = 1 if driver age ≥ 65 years, 0 otherwise

$male$ = 1 if driver gender was male, 0 otherwise

One application of the frontal injury risk model is shown for a female belted occupant in Figure 42.

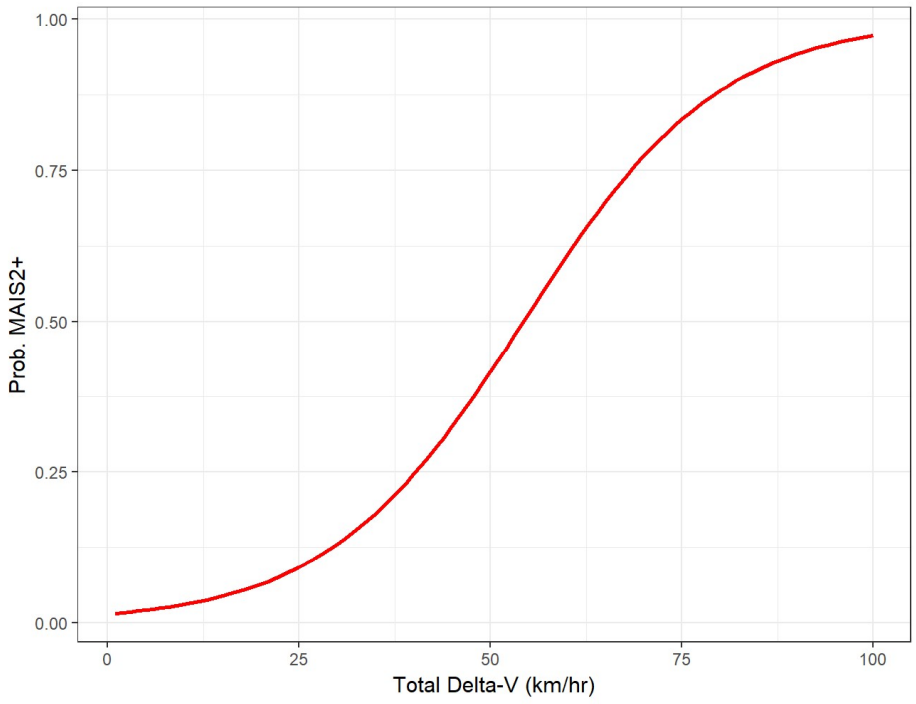

Figure 42. Frontal injury risk curve for a female belted occupant from 13 to 64 years old.

One issue with using this injury risk model on NMVCCS data comes with how belt use data is collected in the data. In NMVCCS, belt use is only reported for the driver using the Police Accident Report. While some EDR models also record belt use, there was not enough EDR data in the NMVCCS case set to account for the missing data. The approach used in this study was to approximate belt use based on frontal occupant population statistics. An analysis of all frontal occupants in NASS/CDS was done in order to determine the approximate percentage of belted vs un-belted. It was found that 81% of frontal occupants were belted and 19% were unbelted. After calculating the injury risk for each occupant in both belted and unbelted scenarios, these percentages were used to weight each injury risk appropriately to obtain a single injury risk value for each occupant.

6.2.3 Determining Injury Benefits

The frontal injury risk model was used initially to estimate the probability of a MAIS2+ injury for each frontal occupant in the dataset. This probability was then multiplied by the case weight in order to determine a nationally representative number of occupants predicted to experience a MAIS2+ injury before the implementation of a LDW system. The frontal injury risk model was then used to predict the probability of a MAIS2+ injury for each case after the implementation of a LDW system. For the LDW system, two simulations were run accounting for different driver reaction times. The injury outcomes of both simulations were weighted equally and the number of MAIS2+ injuries after a LDW system was installed was determined. If the driver was physically impaired, it was assumed that the driver would not be able to react to a LDW alert and consequently, there would be no injury benefits. If the crash was completely avoided, the injury risk was 0 for all occupants involved. For all modified crashes, the new crash configuration was simulated again in PC-Crash and the delta-V value was calculated for each

vehicle over the first 300 ms of the crash. This delta-V value was then input to the injury risk model to determine the updated risk of injury.

6.3 Results

From the original 42 cross-centerline cases (19, 467 crashes), 39 cases had all of the available data for the frontal injury risk model. In two cases, the driver age was unknown because the crash was a hit and run. In the remaining 39 cases, there were a total of 105 front row occupants representing 49, 897 people nationwide. Using the frontal injury risk model to predict injury before the installation of LDW system, it was estimated that 24.6% of the frontal occupants would experience a MAIS2+ injury (defined as a greater than moderate injury on the AIS scale). This corresponded to 12, 261 people. The occupant injuries on the KABCOU scale are shown in Figure 43.

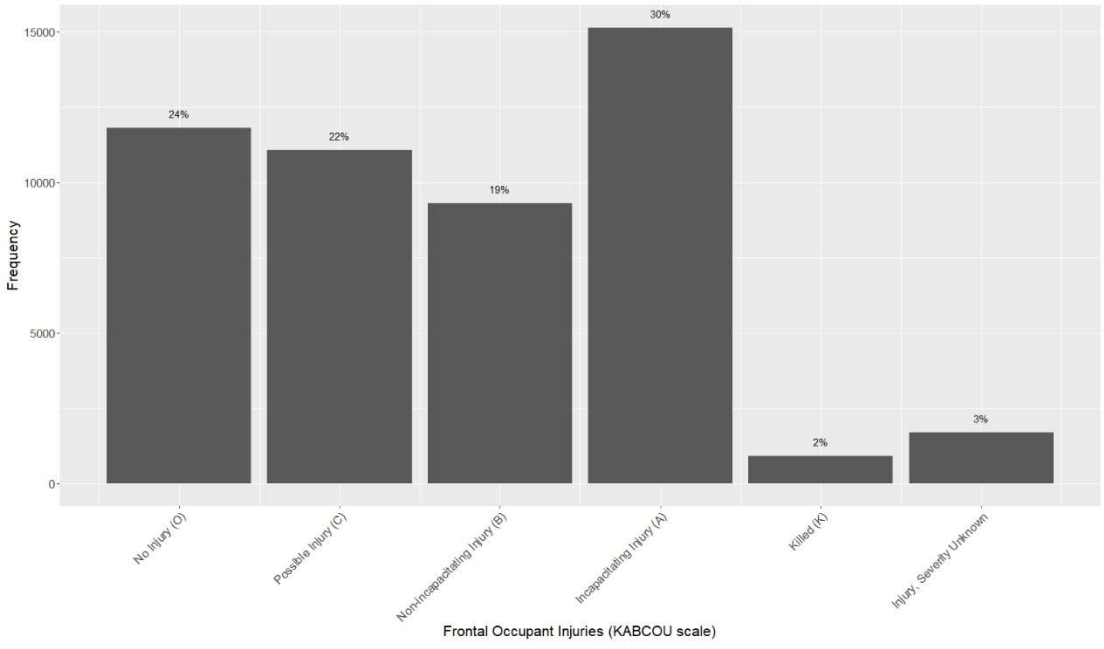

Figure 43. Occupant injuries in cross-centerline crashes displayed using the KABCOU scale.

After running simulations accounting for the effect of a LDW system and different reaction times, it was estimated that 17.6% of occupants would experience a MAIS2+ injury. This is a 29% reduction from the original estimate using the frontal injury risk curves.

Primarily, this can be attributed to the efficiency of lane departure warning systems in mitigating cross-centerline crashes. As seen previously, this system has been shown to prevent between 22 – 30% of cross-centerline crashes. In the crashes that it is unable to fully prevent, an LDW system can lower the average delta-V experienced by approximately 42%. These factors allow this reduction in injuries among front-row occupants.

By assuming a translation between the AIS and the KABCOU scales, we can estimate the injury benefits when compared to the original injury outcomes recorded. Using research performed by Compton (2005), a MAIS2+ injury would most likely be coded as "A" on the KABCOU scale but also could be coded as "B" [78]. We assumed that any score of "K", "A", or "B" on the KABCOU scale corresponded to a MAIS2+ injury. In the original dataset, 51% of the dataset reported an occupant injury of K, A, or B. The injury risk model predicted half of that with only 24.6% of occupants experiencing a MAIS2+ injury. Part of this disparity could be due to including a score of "B" in our definition of MAIS2+ injuries on the KABCOU scale. If we assume that only KABCOU scales of "A" and "K" are MAIS2+ injuries, we see closer results with 32% of occupants experiencing this versus the injury risk model result of 24.6%. However, due to the broadness of the KABCOU scale, it is not reasonable to limit MAIS2+ injuries to only "A" and "K" scores. Still, this significant disparity between what occurred and what the injury risk model estimates indicates that the injury risk model used in this study may need further development to accurately represent injury outcomes in crashes.

Overall, by comparing the results of injury risk model before and after, we see significant injury benefits in cross-centerline crashes due to a LDW system.

7 Summary of Findings

7.1 Goal

This thesis aimed to estimate the potential crash and injury benefits of a hypothetical LDW system in order to guide automakers' decisions when designing these systems. This thesis has presented simulations that are capable of using a LDW model and estimating the potential crash and injury benefits. The research had three main objectives: 1) to characterize cross-centerline crashes in the United States and current prevention methods, 2) to develop a reconstruction methodology for all crashes including rollovers and heavy vehicles, and 3) to develop a simulation model to estimate the potential crash and injury benefits of a LDW model on cross-centerline crashes.

7.2 Cross-centerline crashes in the United States

This thesis performed a literature review in order to determine common characteristics of cross-centerline crashes. The most likely location for such a crash is a narrow undivided curved right two lane rural road that has a high speed limit. There are numerous solutions to preventing cross-centerline crashes but one of the most efficient methods is the installation of centerline rumble strips. Centerline rumble strips function similarly to shoulder rumble strips in that they provide a tactile alert to the driver that they are departing their lane. Numerous studies have shown that centerline rumble strips have an effectiveness of 45% in preventing head-on and sideswipe crashes.

7.3 Development of reconstruction methodology for cross-centerline crashes

This thesis provided a methodology for reconstructing cross-centerline crashes using the scene diagrams and a crash reconstruction software, PC-Crash. Initially, measurements were taken on the scene diagram by trained researchers in order to reconstruct the vehicle trajectory

prior to the crash. In order to estimate the impact speed of both vehicles, each crash was simulated in PC-Crash and optimized to match the post-impact vehicle motion shown on the scene diagram. Rollovers and heavy vehicles were simulated differently in PC-Crash. For heavy vehicles, the approach was to customize one of the built-in custom vehicle models in PC-Crash in order to approximate the heavy vehicle characteristics. To reconstruct a rollover crash this study used a combination of the Kildare curves and PC-Crash. Utilizing information from both sources allowed two estimations of the trip velocity of the vehicle at the same point. By minimizing the error between the PC-Crash reported trip speed and the predicted trip speed from the Kildare curves, an accurate rollover simulation in 2D was able to be created in PC-Crash.

In order to estimate the vehicle speeds prior to impact, an approach model was developed based on event data recorder (EDR) data. Conditions such as impact speed, crash configuration, driver age, and whether the vehicle was encroaching or not, were used to estimate the braking level and, subsequently, the approach speed of the vehicle.

7.4 Estimation of crash and injury benefits of an LDW system

Using the crash reconstructions, this thesis has illustrated an extensive simulation model for a hypothetical LDW system. Using real-world crashes as the basis, the potential crash benefits of a LDW system were found. An LDW system would allow an estimated 29-37% of cross-centerline crashes to be avoided.

Using a frontal injury risk model developed from NASS/CDS data, the potential injury benefits for a LDW system were able to be estimated in a future vehicle fleet in 2025. This future vehicle fleet was assumed to have the best passive safety features available today. Without LDW, the number of MAIS2+ frontal occupant injuries as a result of cross-centerline crashes

was estimated at 24.6%. In this thesis, a LDW system was estimated to decrease this to 17.6%, a 29% reduction.

7.5 Publication Plan

A portion of the research presented in this thesis was published in a peer-reviewed conference publication and is pending application to a journal.

Holmes, D., Sheroni, R., & Gabler, H. C. (2018). *Estimating Benefits of LDW Systems Applied to Cross-Centerline Crashes*. Paper presented at the SAE WCX World Congress Experience 2018, Detroit, Michigan.

7.6 Future Work

This thesis has presented a simulation model and methodology for estimating the crash and injury benefits of a LDW model. One future application of this research could evaluate the LDW model used in this research and compare the LDW model to LDW and LDP systems in current vehicle models. This would allow the realism of the model used in these simulations to be estimated and the model could possibly be updated depending on the real-world system specifications.

The simulation model presented in this thesis also allows easy testing of a hypothetical LDW model in order to optimize the crash and injury benefits of an algorithm. For example, using this simulation model, researchers could test the crash benefits if a LDW system activated before the leading wheel of a vehicle touched the lane line. Additionally, more parameters, such as computational latency, could be added to the LDW model in order to make the model more realistic to real-world systems currently being deployed by OEMs.

Another possibility for this research lies in the rollover and heavy vehicle reconstruction methodology presented within. This methodology could be applied to previous and future crash

and injury benefit studies in order to expand the available dataset for simulation and update the benefits with these additional crashes.

References

1. Kusano, K. and H. Gabler, *Characterization of opposite-direction road departure crashes in the United States.* Transportation Research Record: Journal of the Transportation Research Board, 2013(2377): p. 14-20.
2. Gårder, P., *Segment characteristics and severity of head-on crashes on two-lane rural highways in Maine.* Accident Analysis & Prevention, 2006. **38**(4): p. 652-661.
3. Zaloshnja, E., et al., *Crash costs in the United States by crash geometry.* Accident Analysis & Prevention, 2006. **38**(4): p. 644-651 DOI: http://dx.doi.org/10.1016/j.aap.2005.12.008.
4. Al-Senan, S.H. and P.H. Wright, *Prediction of head-on accident sites.* Transportation Research Record, 1987(1122).
5. Deng, Z., J. Ivan, and P. Gårder, *Analysis of factors affecting the severity of head-on crashes: two-lane rural highways in Connecticut.* Transportation Research Record: Journal of the Transportation Research Board, 2006(1953): p. 137-146.
6. Hosseinpour, M., A.S. Yahaya, and A.F. Sadullah, *Exploring the effects of roadway characteristics on the frequency and severity of head-on crashes: Case studies from Malaysian Federal Roads.* Accident Analysis & Prevention, 2014. **62**: p. 209-222.
7. Zegeer, C.V., R.C. Deen, and J.G. Mayes, *The Effect of Lane and Shoulder Widths on Accident Reductions on Rural, Two-Lane Roads.* 1980.
8. Zhang, C. and J. Ivan, *Effects of geometric characteristics on head-on crash incidence on two-lane roads in Connecticut.* Transportation Research Record: Journal of the Transportation Research Board, 2005(1908): p. 159-164.
9. Neuman, T.R., et al., *Guidance for implementation of the AASHTO strategic highway safety plan*. Vol. 20. 2008: Transportation Research Board.
10. Alexander, H. and P.A. Pisano, *An investigation of passing accidents on two-lane, two-way roads.* Public Roads, 1992. **56**(2).
11. Mohamedshah, Y.M., *Investigation of Passing Accidents Using the HSIS Data Base.* Public Roads, 1992. **56**(2).
12. Draskóczy, M. and T. Mocsári, *Present speeds and speed management methods in Europe.* MASTER project. Espoo, Finland: VTT, 1997.
13. Tignor, S.C. and D. Warren, *Driver speed behavior on US streets and highways.* Compendium of Technical Papers, Institute of Transportation Engineers, Washington, DC, 1990.
14. Johnson, N.S. and H.C. Gabler, *Reduction in fatal longitudinal barrier crash rate due to electronic stability control.* Transportation Research Record: Journal of the Transportation Research Board, 2015(2521): p. 79-85.
15. Johnson, N.S. and H.C. Gabler, *Injury Risk in Frontal Crashes with Guardrail and Guardrail End Terminals.* 2013.
16. Carlsson, A., *Evaluation of 2+ 1-roads with Cable Barriers*. 2009: Statens väg-och transportforskningsinstitut.
17. Potts, I., *Application of European 2+ 1 roadway designs*. 2003: Transportation Research Board.
18. Daniello, A. and H. Gabler, *Effect of barrier type on injury severity in motorcycle-to-barrier collisions in North Carolina, Texas, and New Jersey.* Transportation Research Record: Journal of the Transportation Research Board, 2011(2262): p. 144-151.

19. Gabler, H.C. *The risk of fatality in motorcycle crashes with roadside barriers*. in *Proceedings of the 20th international conference on enhanced safety of vehicles, Lyons, France*. 2007.
20. Daniello, A. and H. Gabler, *Characteristics of Injuries in Motorcycle-to-Barrier Collisions in Maryland.* Transportation Research Record: Journal of the Transportation Research Board, 2012. **2281**: p. 92-98 DOI: 10.3141/2281-12.
21. Daniello, A. and H. Gabler, *Effect of Barrier Type on Injury Severity in Motorcycle-to-Barrier Collisions in North Carolina, Texas, and New Jersey.* Transportation Research Record: Journal of the Transportation Research Board, 2011. **2262**: p. 144-151 DOI: 10.3141/2262-14.
22. Daniello, A. and H.C. Gabler, *Fatality risk in motorcycle collisions with roadside objects in the United States.* Accident Analysis & Prevention, 2011. **43**(3): p. 1167-1170 DOI: 10.1016/j.aap.2010.12.027.
23. Torbic, D.J., et al., *Guidance for the Design and Application of Shoulder and Centerline Rumble Strips*. 2009, Washington, DC: The National Academies Press. 171.
24. Hauer, E., et al., *Accident Modification Factors for Traffic Engineering and ITS Improvements*. 2008, Washington, DC: The National Academies Press. 85.
25. Fitzpatrick, K., *Accident mitigation guide for congested rural two-lane highways*. 2000: Transportation Research Board.
26. Outcalt, W. (2001). *Centerline Rumble Strips*. Retrieved from
27. *CRS: The Delaware Experience*. Retrieved from http://www.deldot.net/static/projects/ rumblestrip/handout.pdf doi:
28. Briese, M. (2006). *Safety effects of centerline rumble strips in Minnesota*. Retrieved from
29. *unpublished results provided to the research team*. Missouri Department of Transportation.
30. *unpublished result provided to the research team*. Nebraska Department of Transportation

31. Russell, E.R., M.J. Rys, and T.S. Brin, *US experience with centerline rumble strips on two-lane roads: Pattern research and North American usage.* ARRB Transport Research, Limited, 2003.
32. Persaud, B.N., R.A. Retting, and C.A. Lyon, *Crash reduction following installation of centerline rumble strips on rural two-lane roads.* Accident Analysis & Prevention, 2004. **36**(6): p. 1073-1079.
33. Porter, R., E. Donnell, and K. Mahoney, *Evaluation of Centerline Rumble Strips Effects on Lateral Placement and Speed.* Transportation Research Record, 2004(1862).
34. Miles, J.D., et al. (2005). *Traffic operational impacts of transverse, centerline, and edgeline rumble strips*. Retrieved from
35. Räsänen, M., *Effects of a rumble strip barrier line on lane keeping in a curve.* Accident Analysis & Prevention, 2005. **37**(3): p. 575-581.
36. Tuovinen, P. and A. Enberg. *Effects of Centerline Rumble Strips on Two-Lane Rural Highways in Finland*. in *5th International Symposium on Highway Capacity and Quality of ServiceTransportation Research Board*. 2006.
37. Harder, K.A., J.T. Carmody, and J. Bloomfield, *The Effect of Centerline Treatments on Driving Performance.* 2002.

38. Hirasawa, M., M. Asano, and K. Saito, *Study on development and practical use of rumble strips as a new measure for highway safety.* Journal of the Eastern Asia Society for Transportation Studies, 2005. **6**: p. 3697-3712.
39. Bahar, G. and M. Parkhill. *Synthesis of Practices for the Implementation of Centreline Rumble Strips*. in *2005 Annual Conference of the Transportation Association of CanadaTransportation Association of Canada*. 2005.
40. Gardner, L., M. Rys, and E. Russell, *Comparison of Football Shaped Rumble Strips versus Rectangular Rumble Strips, Final Report K-Tran: KSU 5-34050.* Kansas Department of Transportation, 2006.
41. Miller, K.W. (2008). *Effects of center-line rumble strips on non-conventional vehicles*. Retrieved from
42. Bucko, T. and A. Khorashadi, *EVALUATION OF MILLED-IN RUMBLE STRIPS, ROLLED-IN RUMBLE STRIPS AND AUDIBLE EDGE STRIPE.* 2001.
43. Noyce, D. and V. Elango, *Safety evaluation of centerline rumble strips: crash and driver behavior analysis.* Transportation Research Record: Journal of the Transportation Research Board, 2004(1862): p. 44-53.
44. Noyce, D.A. and D. Dulaski. *Development and Evaluation of Unique Centerline Rumble Strip Pattern to Improve Driver Comprehension*. in *Transportation Research Board 85th Annual Meeting*. 2006.
45. *Technical Advisory: Center Line Rumble Strips*. 2011, Federal Highway Administration: US.
46. Farmer, C.M., et al., *Fatal crashes of passenger vehicles before and after adding antilock braking systems.* Accident Analysis & Prevention, 1997. **29**(6): p. 745-757.
47. Scanlon, J.M., R. Sherony, and H.C. Gabler, *Injury mitigation estimates for an intersection driver assistance system in straight crossing path crashes in the US.* Traffic injury prevention, 2017(just-accepted): p. 00-00.
48. Scanlon, J.M., R. Sherony, and H.C. Gabler. *Preliminary potential crash prevention estimates for an Intersection Advanced Driver Assistance System in straight crossing path crashes*. in *Intelligent Vehicles Symposium (IV), 2016 IEEE*. 2016. IEEE.
49. Rizzi, M., A. Kullgren, and C. Tingvall. *The injury crash reduction of low-speed Autonomous Emergency Braking (AEB) on passenger cars*. in *Proc. of IRCOBI Conference on Biomechanics of Impacts*. 2014.
50. Gorman, T.I., K.D. Kusano, and H.C. Gabler. *Model of fleet-wide safety benefits of Lane Departure Warning systems*. in *16th International IEEE Conference on Intelligent Transportation Systems (ITSC 2013)*. 2013.
51. Holmes, D., H. Gabler, and R. Sherony, *Estimating Benefits of LDW Systems Applied to Cross-Centerline Crashes*. 2018, SAE International.
52. Kusano, K., et al., *Potential occupant injury reduction in the US vehicle fleet for lane departure warning–equipped vehicles in single-vehicle crashes.* Traffic injury prevention, 2014. **15**(sup1): p. S157-S164.
53. Riexinger, L.E., R. Sherony, and H.C. Gabler, *Methodology for Estimating the Benefits of Lane Departure Warnings using Event Data Recorders*. 2018, SAE International.
54. Scanlon, J.M., et al. *Potential Safety Benefits of Lane Departure Warning and Prevention Systems in the US Vehicle Fleet*. in *Proceedings of the Twenty-Fourth International Conference on Enhanced Safety of Vehicles, Paper*. 2015.
55. Samman, A.M., et al., *Vehicle blind spot monitoring system*. 2004, Google Patents.

56. Gordon, T., et al. (2010). *Advanced crash avoidance technologies (ACAT) program–Final report of the Volvo-Ford-UMTRI project: safety impact methodology for lane departure warning–Method development and estimation of benefits*. Retrieved from
57. Reagan, I.J. and A.T. McCartt, *Observed activation status of lane departure warning and forward collision warning of Honda vehicles at dealership service centers.* Traffic injury prevention, 2016. **17**(8): p. 827-832.
58. Chen, R., K.D. Kusano, and H.C. Gabler, *Driver Behavior During Overtaking Maneuvers from the 100-Car Naturalistic Driving Study.* Traffic Injury Prevention, 2015. **16**(sup2): p. S176-S181 DOI: 10.1080/15389588.2015.1057281.
59. Johnson, T., et al., *Investigation of Driver Lane Keeping Behavior in Normal Driving based on Naturalistic Driving Study Data.* SAE International Journal of Transportation Safety, 2016. **4**(2) DOI: 10.4271/2016-01-1449.
60. Johnson, T., R. Sherony, and H.C. Gabler, *Driver lane keeping behavior in normal driving using 100-car naturalistic driving study data*, in *2016 IEEE Intelligent Vehicles Symposium (IV)*. 2016, IEEE.
61. Scanlon, J.M., K.D. Kusano, and H.C. Gabler, *A Preliminary Model of Driver Acceleration Behavior Prior to Real-World Straight Crossing Path Intersection Crashes Using EDRs*, in *2015 IEEE 18th International Conference on Intelligent Transportation Systems*. 2015, IEEE.
62. Scanlon, J.M., R. Sherony, and H.C. Gabler, *Models of Driver Acceleration Behavior Prior to Real-World Intersection Crashes.* IEEE Transactions on Intelligent Transportation Systems, 2018. **19**(3): p. 774-786 DOI: 10.1109/tits.2017.2699079.
63. Schattler, K. and T. Datta, *Driver Behavior Characteristics at Urban Signalized Intersections.* Transportation Research Record: Journal of the Transportation Research Board, 2004. **1862**: p. 17-23 DOI: 10.3141/1862-03.
64. Scanlon, J.M., K.D. Kusano, and H.C. Gabler. *The influence of roadway characteristics on potential safety benefits of lane departure warning and prevention systems in the US vehicle fleet*. in *Proceedings of the 3rd International Symposium on Future Active Safety Technology Towards Zero Traffic Accidents. Gothenburg, Sweden*. 2015.
65. Jermakian, J.S., *Crash avoidance potential of four passenger vehicle technologies.* Accident Analysis & Prevention, 2011. **43**(3): p. 732-740 DOI: http://dx.doi.org/10.1016/j.aap.2010.10.020.
66. *Report to Congress: NHTSA NASS Data Needs*. 2011, National Highway Traffic Safety Administration: United States.
67. Zellner, J.W., et al., *Extension of the Honda-DRI "Safety Impact Methodology" (SIM) for the NHTSA Advanced Crash Avoidance Technology (ACAT) Program and Application to a Prototype Advanced Collision Mitigation Braking System.* SAE Int. J. Passeng. Cars – Mech. Syst., 2009. **2**(1): p. 875-894 DOI: 10.4271/2009-01-0781.
68. Van Auken, R., et al. *Progress Report on Evaluation of a Pre-Production Head-On Crash Avoidance Assist System Using an Extended "Safety Impact Methodology"(SIM)*. in *22nd International Technical Conference on the Enhanced Safety of Vehicles (ESV)*. 2011.
69. Zellner, J., et al., *Extension of the Honda-DRI "Safety Impact Methodology" (SIM) for the NHTSA Advanced Crash Avoidance Technology (ACAT) II Program and Application to the Evaluation of a Pre-Production Head-On Crash Avoidance Assist System - Progress Report.* 2012 DOI: 10.4271/2012-01-0291.

70. Zellner, J.W., et al. *Evaluation of a Pre-Production Head-on Crash Avoidance Assist System using an Extended "Safety Impact Methodology"(SIM)*. in *24th International Technical Conference on the Enhanced Safety of Vehicles (ESV)*. 2015.
71. *National motor vehicle crash causation survey: Report to congress*. 2008, National Highway Traffic Safety Administration.
72. *National automotive sampling system*. 1979, NHTSA.
73. Hampton, C.E. and H.C. Gabler. *Evaluation of the accuracy of NASS/CDS Delta-V estimates from the enhanced WinSmash algorithm*. in *Annals of Advances in Automotive Medicine/Annual Scientific Conference*. 2010. Association for the Advancement of Automotive Medicine.
74. Hampton, C.E. and H.C. Gabler. *NASS/CDS delta-V estimates: the influence of enhancements to the WinSmash crash reconstruction code*. in *Annals of Advances in Automotive Medicine/Annual Scientific Conference*. 2009. Association for the Advancement of Automotive Medicine.
75. Niehoff, P. and H.C. Gabler. *The accuracy of WinSmash delta-V estimates: the influence of vehicle type, stiffness, and impact mode*. in *Annual Proceedings/Association for the Advancement of Automotive Medicine*. 2006. Association for the Advancement of Automotive Medicine.
76. Sharma, D., et al. *An overview of NHTSA's crash reconstruction software WinSMASH*. in *Proceedings of the 20th International Technical Conference on Enhanced Safety of Vehicles*. 2007.
77. Gennarelli, T.A. and E. Wodzin, *AIS 2005: a contemporary injury scale.* Injury, 2006. **37**(12): p. 1083-1091.
78. Compton, C.P., *Injury Severity Codes: A Comparison of Police Injury Codes and Medical Outcomes as Determined by NASS CDS Investigators.* Journal of Safety Research, 2005. **36**(5).
79. Farmer, C.M., *Reliability of Police-Reported Information for Determining Crash and Injury Severity.* Traffic Injury Prevention, 2003. **4**(1): p. 38-44 DOI: 10.1080/15389580309855.
80. Bareiss, M., M. David, and H.C. Gabler, *Preliminary Estimates of Near Side Crash Injury Risk in Best Performing Passenger Vehicles*, in *SAE WCX World Congress Experience 2018*, N. Fought, Editor. 2018: Detroit, Michigan.
81. Tsoi, A.H., J. Hinch, and H. Gabler, *Analysis of Event Data Recorder Survivability in Crashes with Fire, Immersion, and High Delta-V*, in *SAE Technical Paper Series*. 2015, SAE International.
82. Tsoi, A.H., et al., *Survivability of Event Data Recorder Data in Exposure to High Temperature, Submersion, and Static Crush*, in *SAE Technical Paper Series*. 2015, SAE International.
83. Gabler, H.C., J.A. Hinch, and J. Steiner, *Event Data Recorder. A Decade of Innovation*. 2008.
84. Scanlon, J.M., K.D. Kusano, and H.C. Gabler, *Analysis of driver evasive maneuvering prior to intersection crashes using event data recorders.* Traffic injury prevention, 2015. **16**(sup2): p. S182-S189.
85. Datentechnik, S., *PC-CRASH–A Simulation Program for Vehicle Accidents: Technical Manual*. 2006, Version.

86. Cliff, W.E. and D.T. Montgomery. (1996). *Validation of PC-Crash-A momentum-based accident reconstruction program* (0148-7191). Retrieved from 960885
87. Cliff, W.E. and A. Moser. (2001). *Reconstruction of twenty staged collisions with PC-Crash's optimizer* (0148-7191). Retrieved from 2001-01-0507
88. *National Motor Vehicle Crash Causation Survey (NMVCCS): Field Coding Manual*. 2008, National Highway Traffic Safety Administration.
89. *Decode the VIN*. [cited 2018 February 26]; Available from: https://www.dmv.org/vehicle-history/vin-decoder.php.
90. *Chevrolet and GMC School Bus Chassis*, G. Motors, Editor. 2012: online.
91. Gabauer, D. and H.C. Gabler, *Correlating Delta-V to occupant injury using event data recorders.* Annual Proceeds/Association for the Advancement of Automotive, 2006: p. 57-1.
92. (2010). *NCHRP 17-43 [Active] Long-Term Roadside Crash Data Collection Program*. Retrieved from
93. Ivey, D.L. and K.S. Adamson. (2006). *Speed Losses During Vehicle Overturning, Influence of Body Shape And Tripping Mechanism*. Retrieved from
94. Rose, N.A. and G. Beauchamp. (2009). *Analysis of a Dolly Rollover with PC-Crash* (0148-7191). Retrieved from
95. Kusano, K.D., R. Sherony, and H.C. Gabler, *Methodology for using advanced event data recorders to reconstruct vehicle trajectories for use in Safety impact methodologies (SIM).* Traffic injury prevention, 2013. **14**(sup1): p. S77-S86.
96. Kudarauskas, N., *Analysis of emergency braking of a vehicle.* Transport, 2007. **22**(3): p. 154-159.
97. Dingus, T.A., et al. (2006). *The 100-car naturalistic driving study, Phase II-results of the 100-car field experiment*. Retrieved from DOT HS 810 593
98. Nygård, M., *A method for analysing traffic safety with help of speed profiles.* 1999.
99. Blau, P.J., *Friction science and technology: from concepts to applications*. 2008: CRC press.
100. Kozak, K., et al. *Evaluation of lane departure warnings for drowsy drivers*. in *Proceedings of the human factors and ergonomics society annual meeting*. 2006. Sage Publications Sage CA: Los Angeles, CA.
101. Rimini-Doering, M., et al. *Effects of lane departure warning on drowsy drivers' performance and state in a simulator*. in *Proceedings of the third international driving symposium on human factors in driver assessment, training, and vehicle design*. 2005.
102. Suzuki, K., *An analysis of driver's steering behaviour during auditory or haptic warnings for the designing of lane departure warning system.* JSAE review, 2003. **24**(1): p. 65-70 DOI: 10.1016/S0389-4304(02)00247-3.
103. Johnson, T., *Fleetwide Models of Lane Departure Warning and Prevention Systems in the United States*. 2017, Virginia Tech.
104. O'Neill, B., *Preventing passenger vehicle occupant injuries by vehicle design—a historical perspective from IIHS.* Traffic injury prevention, 2009. **10**(2): p. 113-126.
105. Gabler, H.C., et al., *Side Impact Injury Risk for Belted Far Side Passenger Vehicle Occupants*, in *SAE Technical Paper Series*. 2005, SAE International.
106. Newland, C., et al. (2008). *Occupant-to-occupant interaction and impact injury risk in side impact crashes*. Retrieved from

107. Gabauer, D. and H. Gabler, *Methodology to Evaluate the Flail Space Model by Using Event Data Recorder Technology.* Transportation Research Record: Journal of the Transportation Research Board, 2004. **1890**: p. 49-57 DOI: 10.3141/1890-06.
108. Gabauer, D.J. and H.C. Gabler, *Comparison of roadside and vehicle crash test injury criteria in frontal crash tests.* International Journal of Vehicle Safety, 2008. **3**(1): p. 1 DOI: 10.1504/ijvs.2008.020075.
109. Gabauer, D.J. and H.C. Gabler, *Comparison of roadside crash injury metrics using event data recorders.* Accident Analysis & Prevention, 2008. **40**(2): p. 548-558 DOI: 10.1016/j.aap.2007.08.011.
110. Gabler, H.C., A.A. Weaver, and J.D. Stitzel, *Automotive Field Data in Injury Biomechanics*, in *Accidental Injury*. 2014, Springer New York. p. 33-49.
111. Kusano, K. and H.C. Gabler, *Comparison and Validation of Injury Risk Classifiers for Advanced Automated Crash Notification Systems.* Traffic Injury Prevention, 2014. **15**(sup1): p. S126-S133 DOI: 10.1080/15389588.2014.927577.
112. Tsoi, A.H. and H.C. Gabler, *Evaluation of Vehicle-Based Crash Severity Metrics.* Traffic Injury Prevention, 2015. **16**(sup2): p. S132-S139 DOI: 10.1080/15389588.2015.1067693.
113. Gaewsky, J.P., et al., *Driver injury risk variability in finite element reconstructions of Crash Injury Research and Engineering Network (CIREN) frontal motor vehicle crashes.* Traffic injury prevention, 2015. **16**(sup2): p. S124-S131.
114. Hershman, L.L. *The US new car assessment program (NCAP): Past, present and future*. in *International Technical Conference on the Enhanced Safety of Vehicles*. 2001.

Appendix

A.1 Cross-Centerline Measurements Reconstruction Protocol

The aim of this document is to lay out a protocol for taking scene diagram measurements on cross-centerline crashes. These measurements will be used to reconstruct these crashes in order to simulate the effects and potential benefits of a LDW system.

Download Scene Diagrams

1. Download Easy Street Draw File from NVMCCS
2. As shown below, use the measuring tape tool to draw a ruler on drawing to at least 10 meters.

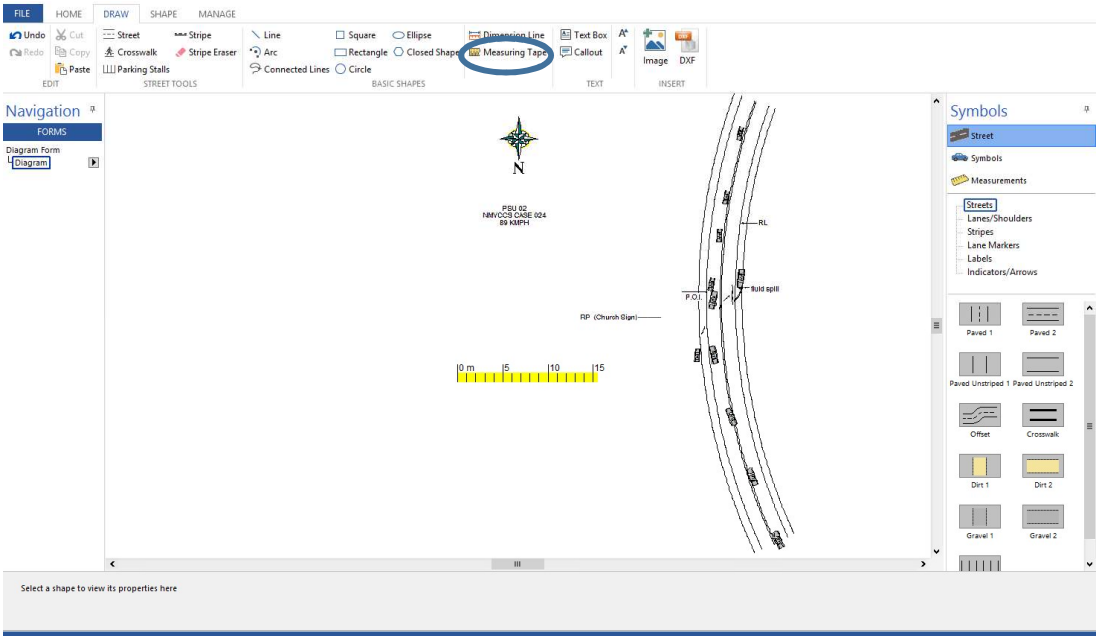

3. Click on the measuring tape and check the box that says Include Measuring Tape in Printed Drawing.

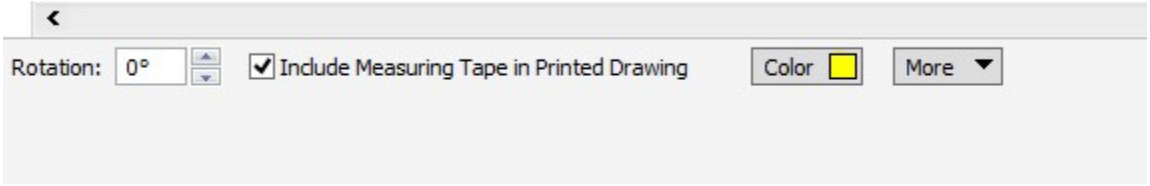

4. Go to the Manage Tab and click on Save as Image. Or you can use the shortcut Control-E to export as a TIFF and save as the case id.
5. If the drawing is in Visio – simply click File – Export – AutoCad Drawing. You will not need to scale the drawing. This means that you can skip to step #10.

Taking Measurements in AutoCAD

6. Open AutoCAD
7. Go to Insert – Reference Panel – Attach

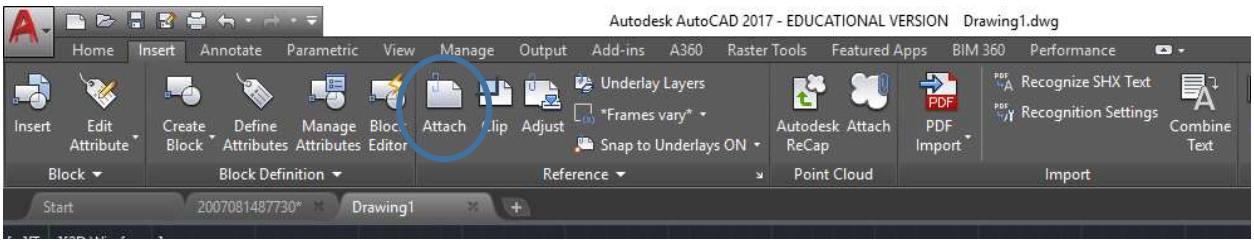

8. Navigate to the file location where the exported scene diagram is
9. **Unclick** Specify on Screen and Scale Factor On Screen then press Ok.

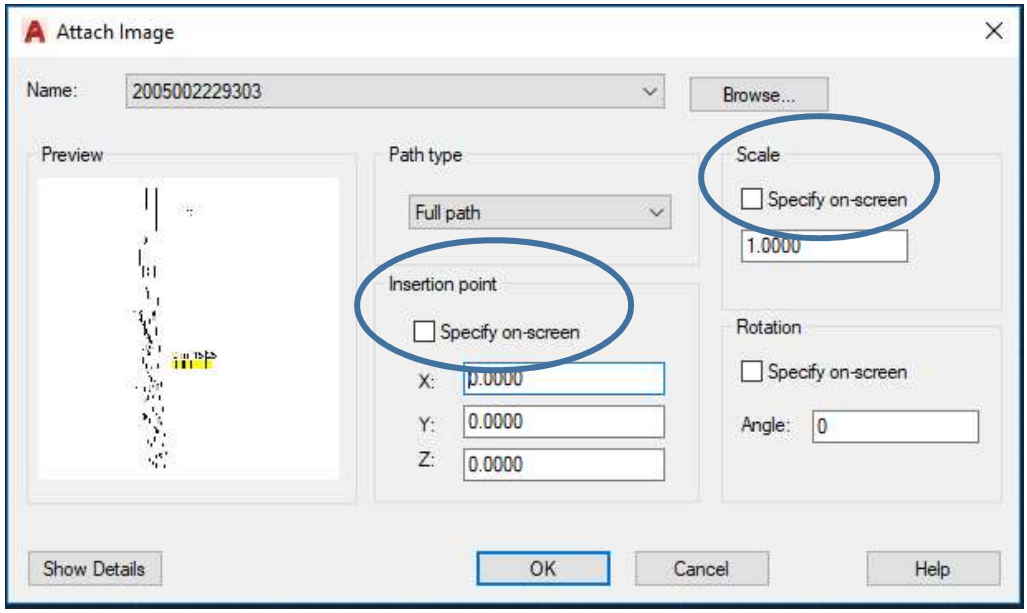

10. Type Scale into the command line at the bottom of the screen and press enter.
    a. Select the entire image and press enter again.
    b. Choose the Base point as the start of the measuring tape
    c. Type R and press enter
    d. Drag the line out to the 10
    e. Type 10 and press enter. The image should be properly scaled now.
    f. You can test this by going to the Annotate Tab and choosing the Dimension tool. Measure the Ruler to ensure that it shows the correct length(optional)
11. Go to the Home Panel and in the Properties Tab Change the color for Red. Go to the Utilities Tab click on the arrow down, and click on Point Style.

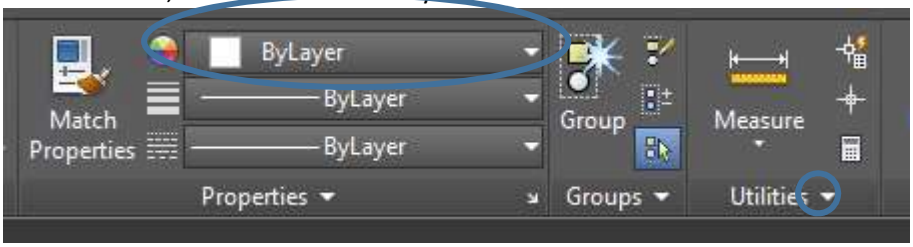

12. Choose the point style 3 to the right and 1 down. Change the size of the point to 3 units. Make sure it is absolute units.

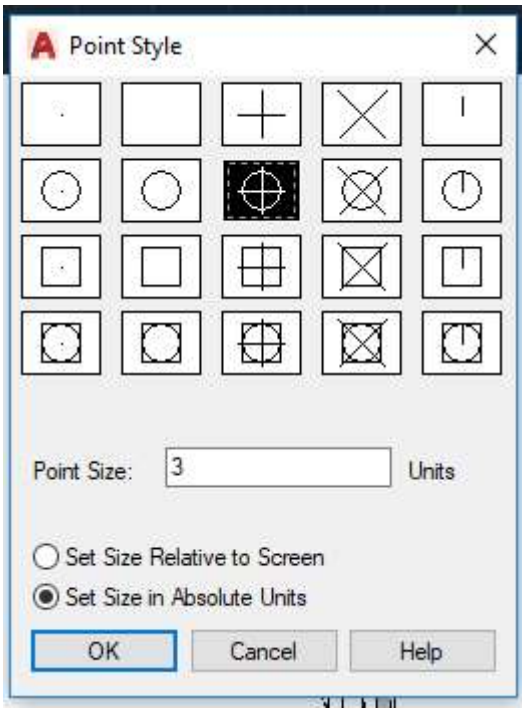

13. Type " _style" in the command box at the bottom of the page to open up the style dialog box. Change the Text Height to 2 to make it readable without zooming in.

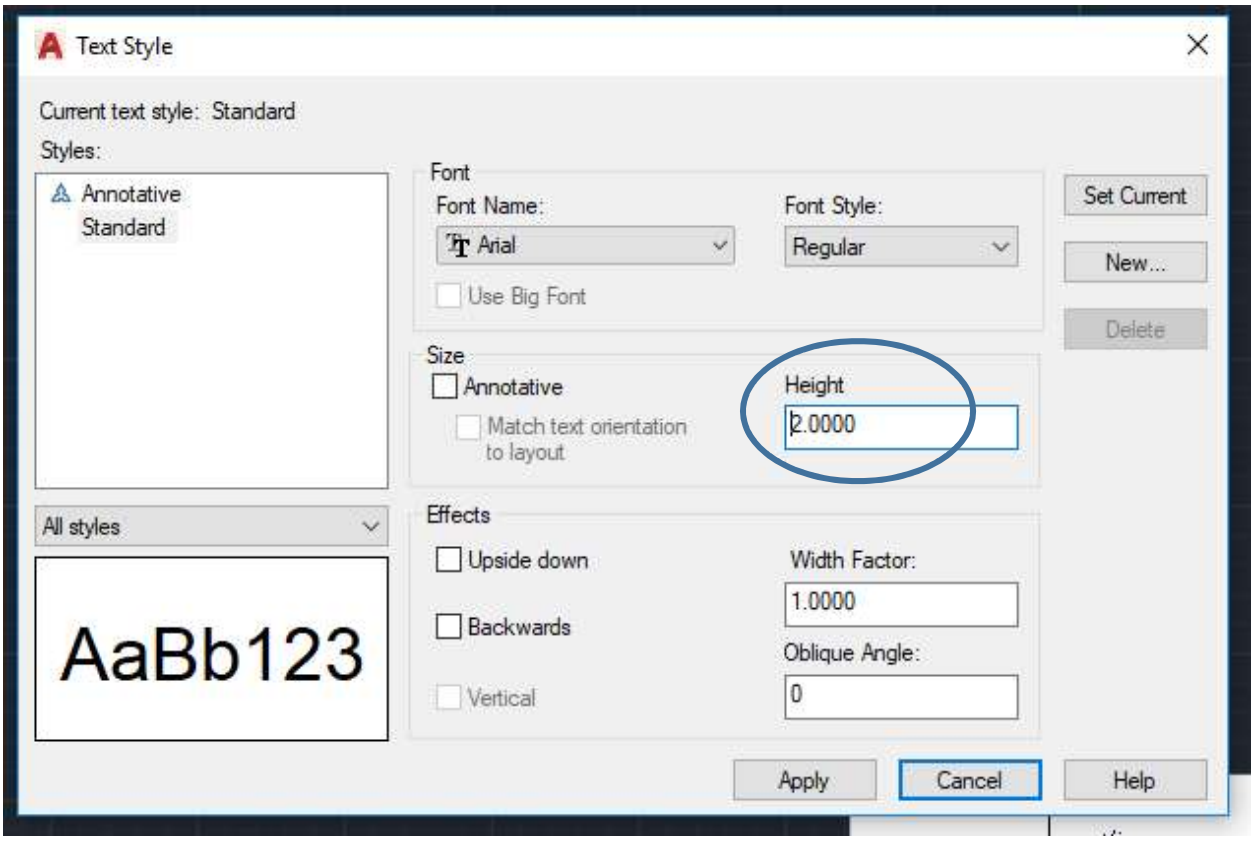

14. Take all of the points for V1 up to and including the impact position. You don't need to take points for any vehicle positions that occurred after impact. Use Red for V1, Blue for V2, and Green for the Lane Markings.
    a. Place the Points at the front center of each of the vehicle positions up to and including the impact position.
    b. For lane markings place a point at each of the end points of the lane. If it is curved please also include the curve direction and radius of curvature taken from Easy Street Draw.
    c. If the lane is straight, place points at the endpoints of the lane.
    d. For every part of the lane markings, there should be two points: one at the start and one at the end. For example if there was a curve initially and then it turns straight, place points at the start and end of the curve and measure the radius of curvature and direction. Use the point at the end of the curve as the start point for the next section(just copy and paste it in a new row).
    e. The final result should look similar to this:

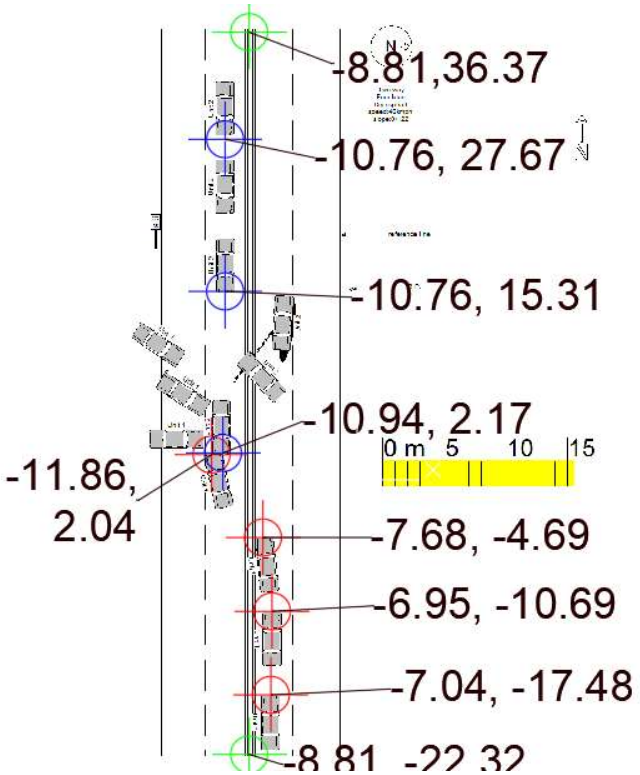

    f. Radius of Curvature should be taken from Easy Street Draw. If the diagram is in Visio, draw an arc using AutoCad. The first point of the lane markings should always be the bottom one.
        i. To draw an arc, look at the ribbon for the Draw Panel in the upper left. Click on the arrow underneath Arc, and choose "Start, End, Direction" . Click on the start and end points of the curve and drag the arc until it is in the center of the lane line.

ii. To find the radius of curvature of this arc, click on Annotate at the very top of the window. Next, click on the arrow underneath Dimension. Click the Radius dimension button and click on the arc. Click again to place the dimension label where you can read it.

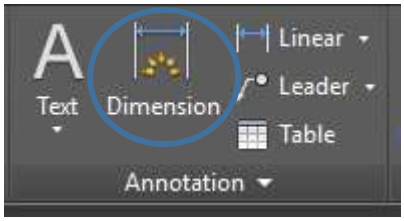

g. To see the point coordinates, type LB in the command line. Click once at the point center and then again to place the text. Repeat for all of the points.

h. Place all of the points into Excel.

i. When inputting the points, start at the POI and work backwards for both vehicles.

15. Determine the Path between Points for each vehicle

a. Classify the transition from point to point as either straight or curved under the Path2Pt1 variable. An example diagram to assist you is shown below. In the below image, the vehicle is most likely to follow the path of the curve(green line) instead of immediately shifting direction and going straight(the black line illustrates this scenario).

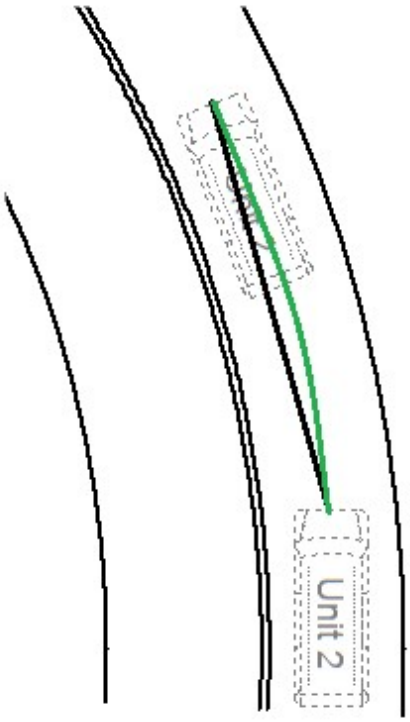

Figure 44-The black line depicts a straight line transition between the points and the green line depicts a curved transition. As can be seen the green line most closely approximates the likely vehicle path.

b. Work backwards from the point of impact. If you having difficulty classifying it, put yourself in the driver's seat. What is the most likely path that you would take?
c. Note that this is a classification of the segments between the points. So if you have 3 points you will only have 2 paths to point.

A.2 PC-Crash Reconstruction Protocol

PC-Crash Data Collection Protocol
Developed by John Scanlon

Overview
Objective: To determine the impact velocities of vehicles involved in SCP intersection crashes within the NMVCCS
Required Tools:

1) Data Input Spreadsheet (Results.xlsx): Reconstruction results will be put into this spreadsheet.
2) Vehicle Information Spreadsheet (Vehicle_Info.xls): Two sheets are contained in this spreadsheet.
    a. *Generation Table* contains vehicle make, model, year, generation years, and alternative model. This table will be useful for determining if the vehicle chosen from the vehicle database will be sufficient.
    b. *Vehicle Table* contains the make, model, and year of vehicles included in the vehicle database, as well as dimensional measurements for running PC-Crash Simulations.
3) Case Viewer Program (NASS_PIC.exe): Will contain two important components for completing reconstructions. An annotated image of the case viewer program interface can be seen in the appendix.
    a. *Scene narrative* is included on the right side of the case viewer. This summary contains a detailed account of the crash and crash conditions. The involved vehicle makes and models, road conditions, and road gradient can all be found in this account.
    b. *Easy Street Draw File Link* is shown by the button "Open Scene Diagram in Easy Street Draw". This scene diagram will be used for reconstructions.
4) Easy Street Draw software: An annotated screen shot of the program interface can be seen in the appendix.
5) PC-Crash Reconstruction Software: This software will be the platform for performing all crash reconstructions.

Methods

Step 1: Setup

Prior to beginning the reconstruction protocol, five files/applications/folders should be open.

1) The case viewer program should be opened within a remote desktop connection to Abyss.
2) The "Results.xlsx" spreadsheet should be opened for data input

3) The “Vehicle_Info.xlsx” spreadsheet should be opened for finding vehicle parameters.
4) PC-Crash should be opened on the local device.
5) The “Case Folders” directory should be opened on the Abyss share-drive. A folder has been generated for each case and should be used to store the completed case reconstructions.

Step 2: Importing a Scaled Scene Diagram into PC-Crash

The scene diagram acts a tool for overlaying the crash scene for accurate reconstructions. Step 2 describes the process for importing a scaled diagram into the PC-Crash program.

1) Within the search tool in the case viewer program, use the case “key” to select the crash of interest.
2) Click “Open Scene Diagram in Easy Street Draw” to open the scene diagram in easy street draw.
3) Use the measuring tape tool to draw a 10-meter long scale.
4) Left click the measuring tape and check the “include Measuring Tape in Printed Drawing” check box in the bottom panel of the window.
5) Select the “Save as Image” option on the top left corner of the interface.
    a. Save the image as a .tif and place it into its appropriate folder.
6) Load the scene diagram into PC-Crash by selecting file→ Import→Bitmap and browsing for the case file
7) Scale the scene diagram using the  tool. This tool works by selecting the 0 and 10 m location on the sale, then imputing the “actual distance” as 10 m.

Step 3: Adding Vehicles to PC-Crash

Every SCP intersection crash that will be reconstructed will involve at least two vehicles. Occasionally, additional vehicle(s) may be involved. It is important to add all involved vehicles for accurate reconstructions.

The following protocol should be repeated for all involved vehicles.

1) Load the vehicle by selecting the  icon.
2) Make sure the database “DSD 2011” is selected.
3) Use the case viewer scene narrative to correspond the vehicle number in the scene diagram to a make, model, and year
4) Search for the make an model within the DSD 2011 database
    a. If the vehicle cannot be found, use the generation sheet in the Vehicle Info spreadsheet to search for a suitable alternative model.
    b. Compare the track width and vehicle length in the vehicle info table to verify the selected vehicle in the DSD database is appropriate

c. Input the selected vehicle into the results spreadsheet.

5) Modify vehicle specifications by right clicking in the window and selecting “vehicle settings”
    a. Select “occupants and cargo” tab
    b. Add the weights in the results spreadsheet into the appropriate front occupants, rear occupants, and trunk cargo columns
6) Use the  tool to move the vehicle to its respective impact location
    a. The impact location represents the location where that that vehicle was first contacted.
    b. Cars should be overlapping at this position.
    c. Note: The car can be moved and rotated by clicking and dragging the center and edge of the vehicle, respectively.
    d. Note: all positions prior to impact are irrelevant for this analysis and should be ignored.

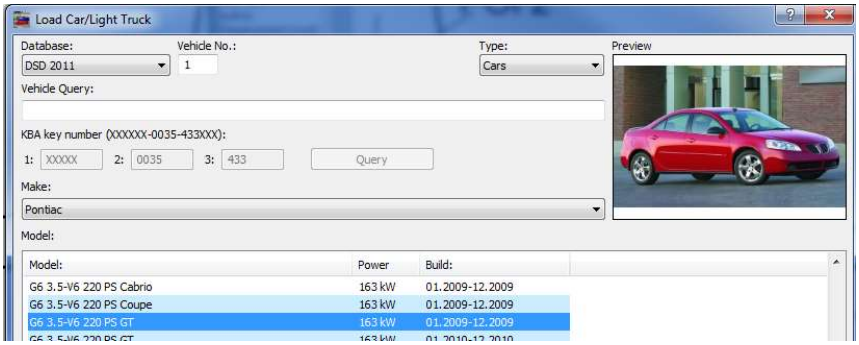

Step 4: Adding Roadside Objects to the Scene

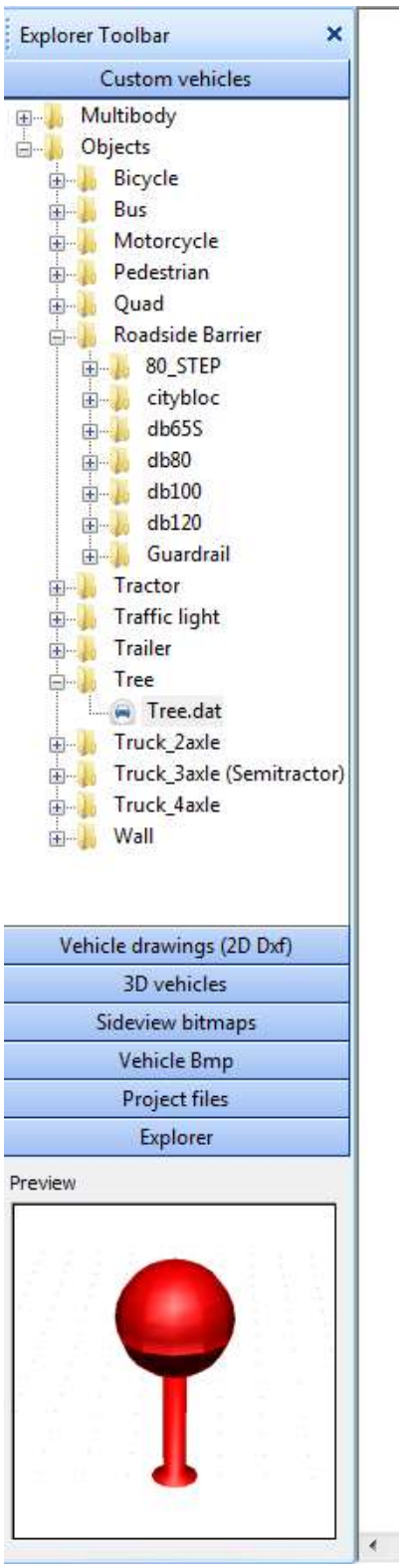

Roadside objects should only be added if they are impacted. If you are unsure whether an object was impacted, refer to the scene narrative and scene pictures in the case viewer. As a rule of thumb, when in doubt, include the object.

Roadside objects can be added using the following protocol:

1. On the right side of the page in the explorer tool bar, select custom vehicles → objects to find a list of roadside objects.
2. Three potential objects that can be added are trees (assign poles as trees), walls, and road side barriers.
3. Modify the object geometry by right clicking in blank space → selecting vehicle settings → selecting the object of interest in the drop down → modifying the height and width of the object.
   a. Note: Height and width of the object can be determined by taking measurements using the  on the scene diagram.

Step 5: Adding Intermediate/rest Vehicle Positions and tire marks

Adding vehicle positions and tire marks post impact give the collision optimizer a means an objective trajectory.

Intermediate and rest vehicle positions can be input using the following protocol:

1. Select Impact→Intermediate→ Intermediate Position # OR Select Impact→Rest
   a. Note: Intermediate Position 1 corresponds to the first depicted position post impact.
2. A tow truck will appear and can be used to drag the impact vehicle to the intermediate vehicle positions.
   a. Note: this will not move the impact vehicle, but will create a new vehicle that can be moved.

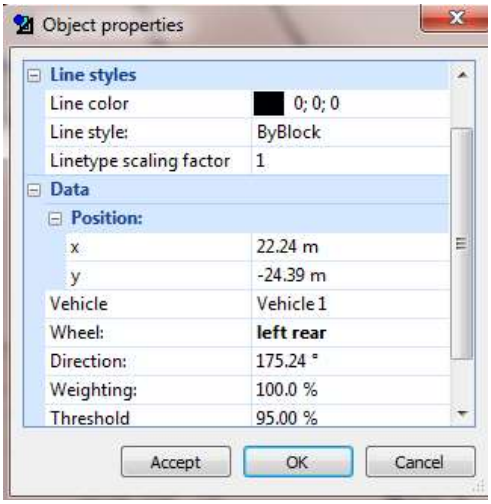

If present, tiremarks should be added at their appropriate locations. These tiremarks are important for the collision optimizer. The tiremark can be moved and rotated, and do not have a length component. The tiremark should be added to the beginning of the tiremark at the angle depicted.

1. Select  to add a tiremark.
2. Use  to select, move, and rotate the tiremark.
    a. Note: a tiremark can be removed by selecting a tiremark, then deleting it using the  tool.
    b. Note: The tiremark cross should be moved to the beginning tiremark, then rotated to follow the depicted markings.
3. After placing the tiremark in its location and direction double click on the tiremark cross using the  .
4. The tiremark now must be assigned to the vehicle and tire of interest.
    a. Under Data, Position change the vehicle and wheel to their appropriate setting.

Step 6: Modify Road Friction

Road friction should be modified within for the entire depicted trajectories of both vehicles. Surface conditions can be determined. There are five possible selections for road friction: (1) dry, (2) wet, (3) very wet, (4) snow, and (5) ice. These are already given for you in the Results.xlsx spreadsheet.

Road friction should be modified using the following protocol:

1) Locate the following toolbar:  .
2) Select the  button in the tool bar.
3) Left click to draw a polygon around the entire depicted trajectories.
4) After the polygon is completed, right click to finish drawing.
5) A coefficient of friction window will automatically open.
    a. Use the drop down to change the surface conditions to their appropriate value

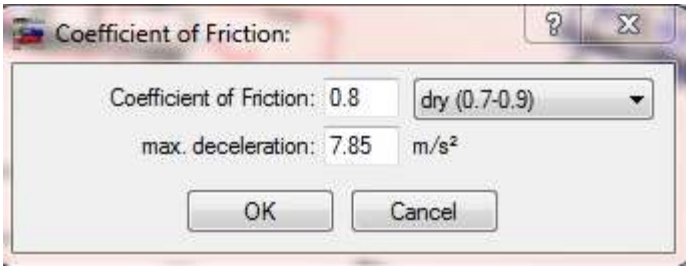

Step 7: Collision Optimization

Collision optimization is the final step in determining impact velocities. It is important to note that each crash is unique. Although the following protocol

attempts to reconstruct crashes in a systematic way, there is still some "finesse" involved in properly reconstructing crashes. The following steps should be implemented for collision optimization:

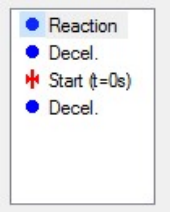

The "sequence" of events for each vehicle needs to be initialized

1) Select Dynamics → Sequences to open the sequences window
    a. By default the window to the sequence depicted to the right will appear in the window for each vehicle involved.
2) Double click on the second decal. and a window will open for changing the decal. step in the sequence (shown to the right)
3) change the sequence duration to a reasonable duration.
    a. This decel sequence duration affects the run time post impact.
    b. A safe decel sequence duration is 15 s.
    c. Alter the decel sequence duration for all vehicles
4) The presence of wheel lockup should also be added
    a. Examine scene crash photos and the scene narrative to determine whether wheel lockup occurred. The vehicle should look bent/out-of-line
    b. If wheel lockup occurred, change the brake factor for that wheel to 100. This indicates 100% braking on that wheel. Note that the braking can go up to 500%.
    c. If wheel lockup occurred, add it to the results spreadsheet.

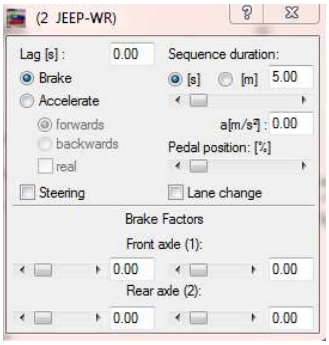

The first pass at collision optimization should be implemented. If this first pass through the optimization is "sufficient", the results will be saved. A "sufficient" result will be one where the vehicle approximately stops at the depicted rest position.

1) Select Impact → collision optimizer
    a. Two windows will open:
        i. The collision optimizer window
        ii. The crash simulation window
2) In the crash simulation window:
    a. Select point of impact
    b. Click a location within the two vehicles overlapping area
    c. Unselect point of impact
3) Within the optimize tab in the collision optimizer window, verify that impact velocities, point of impact, and contact plane are selected, and the genetic algorithm routine has been selected. See the exemplary screen shot to the right for what this should look like.
4) In the crash simulation window, change the pre-impact velocities to be 30 kph each. These will serve as initial guesses.

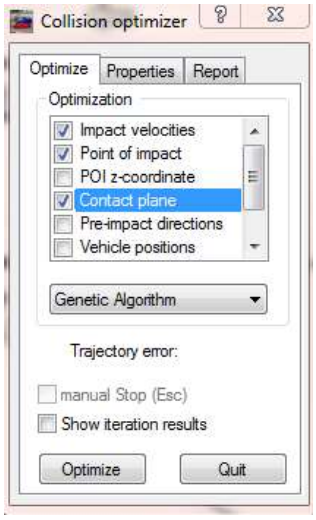

5) Click Optimize in the collision optimizer window.

The results of the collision optimizer can be found by first selecting options → Values to open the values window, then within the Values window, selecting Settings→ Report. The impact values should be listed under START VALUES.

If the results of the collision optimizer seem reasonable after watching the animation, the impact velocities can be input into the results table. A reasonable result is one where the vehicles stop at their approximate rest location and rest heading.

If the results seem unreasonable, three things can be done to make the results more reasonable. **First**, if the vehicle does not come to a stop, which happens frequently for the vehicle that do not strike a roadside object(s), braking should be added. **Second**, if the trajectory indicates some turning, steering can be added using the path following tool or manually. If lockup occurred, use the manual steering input.

If braking is required, perform the following steps:

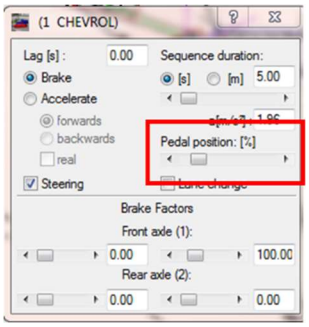

1) Open the sequences window by selecting Dynamics → Sequences
2) Under the vehicle of interest, double click the post-start decel.
3) Add braking using the pedal position scroll.
    a. As a rule of thumb, it is best to add braking in 10 % intervals

If steering is required, perform one of the following set of steps:

<u>For manual steering input,</u> (Note: should be used if lockup occurred)

1) Open the sequences window by selecting Dynamics → Sequences
2) Under the vehicle of interest, double click the post-start decel.
3) Check the steering check box to open up a steering options window (shown to right)
4) Change the Time to 0 s.
5) Steering should be added to the red boxed area
    a. Positive steering rotates the vehicle counter-clockwise
    b. As a rule of thumb, add steering in 15 degree increments.

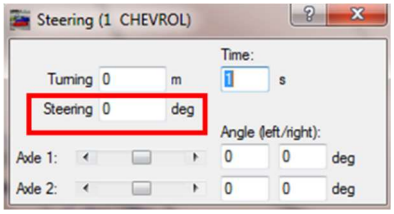

<u>For path following steering input,</u>

1) Locate the following toolbar: 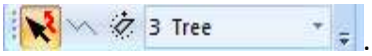

.
2) Select the button in the tool bar.
3) Left click to draw the vehicle path in segments
4) After the path has been drawn, right click to finish drawing.
5) The path can be deleted by clicking the trajectory line using the  then clicking delete.

A.3 Heavy Vehicle Specification Sheet Example

	3500 G33503	3500 G33803	4500 G33803
			
Powertrain/Mechanical			
Engine	Vortec 4.8L	Vortec 6.0L	Vortec 6.0L
Optional engine	Vortec 6.0L /Duramax 6.6L diesel	Duramax 6.6L diesel	Duramax 6.6L diesel/LPG
Base transmission	HD 6-spd. auto. (MYD)	HD 6-spd. auto. (MYD)	HD 6-spd. auto. (MYD)
Horsepower @ rpm	280 @ 5,200	324 @ 4,700	324 @ 4,700
Torque ft.-lbs. @ rpm	295 @ 4,600	373 @ 4,400	373 @ 4,400
Standard axle ratio	3.42	3.73	4.1
Available axle ratio	3.42/3.73/3.54	3.73	4.1/3.73
Fuel system	SFI	SFI	SFI
Battery	HD 600 CCA	HD 600 CCA	HD 600 CCA
Alternator	145-amp	145-amp	145-amp
50-state emissions[1]	FE9/YF5/NE1	FE9/YF5/NE1	FE9/YF5/NE1
Frame, yield strength (psi)	33,000	33,000	33,000
GVWR standard (lbs.)[2]	9,900	12,300	14,200
GVWR options (lbs.)[2]	10,100[3]/12,300	—	—
GAWR (lbs.) front spring/axle[1]	4,100–4,600	4,300–4,600	4,600
GAWR (lbs.) rear axle[1]	6,084–8,600	8,600	9,600
Curb weight (lbs.)[1]	4,496–5,657	4,967–5,566	5,022–6,043
Payload options (lbs.)[1,4]	4,557–7,307	6,714–7,310	8,135–9,156
Fuel tank capacity (gal.)[5]	33	33	33/35 LPG
Wheels	SRW/DRW	DRW	DRW
Exterior Dimensions			
Wheelbase (in.)	139	159	159
Overall length (in.)	246.7	266.7	266.7
Overall height (in.)	82.9	82.9	82.9
Body width (in.)	79.1	79.1	79.1
Cab to axle (in.)	80	100	100
Cab to end of frame (in.)	148.5	168.5	168.5
Ground clearance front/rear (in.)	7.6/6.8	7.6/7.0	7.6/7.0
Turning diameter (ft.)	43.4	54.5	54.5

[1] See Order Guide for complete details.
[2] Gross Vehicle Weight Rating (GVWR). When properly equipped, includes vehicle, passengers, cargo and equipment.
[3] Available in 2013.
[4] Maximum payload capacity includes weight of driver, passengers, optional equipment, upfitter installed body and equipment and cargo. Cargo and load capacity is limited by gross front and rear axle weight ratings and GVWR.
[5] Fuel capacity is approximate.

A.4 Special Vehicle PC-Crash Rollover Reconstruction Protocol

Overview

Objective: To determine the impact velocities of vehicles involved in rollover crashes within NMVCCS

Process: Initial reconstructions will be performed using PC-Crash to get an impact speed and trip velocity. Then NCHRP 17-43 Rollover reconstruction methodology will be used to reconstruct backwards from the final rest of the vehicle experiencing rollover and obtain a trip speed using the Kildare curves. These trip speeds will be compared and used to modify the PC-Crash simulation.

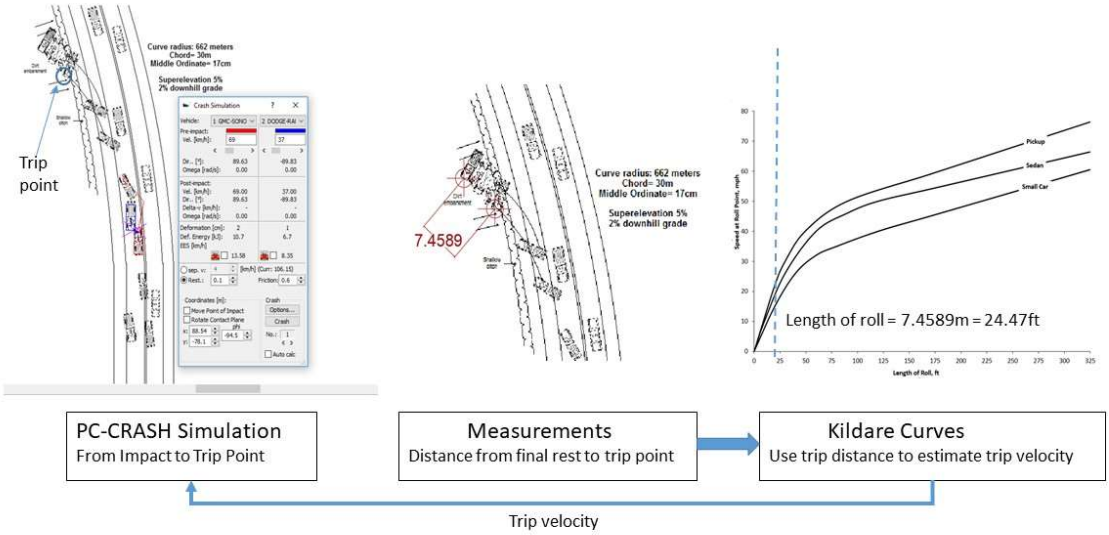

Required Tools:

6) Data Input Spreadsheet (Results.xlsx): Reconstruction results will be put into this spreadsheet.
7) Vehicle Information Spreadsheet (Vehicle_Info.xls): Two sheets are contained in this spreadsheet.
    a. *Generation Table* contains vehicle make, model, year, generation years, and alternative model. This table will be useful for determining if the vehicle chosen from the vehicle database will be sufficient.
    b. *Vehicle Table* contains the make, model, and year of vehicles included in the vehicle database, as well as dimensional measurements for running PC-Crash Simulations.
8) Easy Street Draw software: An annotated screen shot of the program interface can be seen in the appendix.
9) PC-Crash Reconstruction Software: This software will be the platform for performing all crash reconstructions.

Methods

Step 1: Setup

Prior to beginning the reconstruction protocol, three files/applications/folders should be open.

6) The "Results.xlsx" spreadsheet should be opened for data input
7) PC-Crash should be opened on the local device.
8) Easy Street Draw software should be opened through a remote desktop connection with Abyss.

Step 2: Opening and Importing Scene Diagram Into PC-Crash

The scene diagram acts a tool for overlaying the crash scene for accurate reconstructions. Step 2 describes the process for importing a scaled diagram into the PC-Crash program.

1) In the remote desktop connection to Abyss, navigate to the folder where all of the cases are stored. This may differ for different projects.
    a. For this project, navigate to David's folder (davidh94) on Abyss. The relevant cases will be under Special Vehicle Reconstruction Methodology\Rollovers. Open up the relevant case folder and click on the scene diagram. Easy Street Draw should open.
2) Use the measuring tape tool to draw a 10-meter long scale.

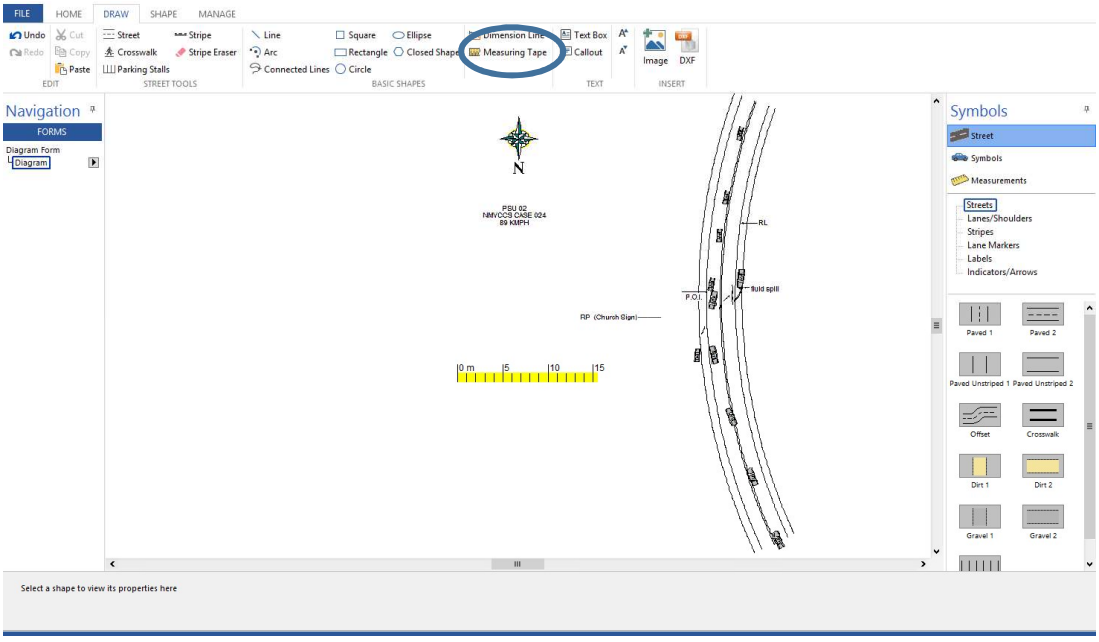

3) Left click the measuring tape and check the "include Measuring Tape in Printed Drawing" check box in the bottom panel of the window.

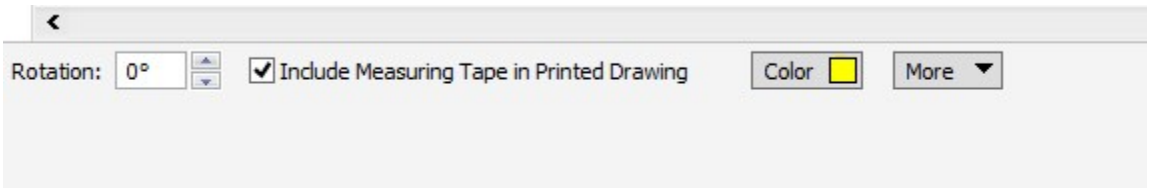

4) Go to the Manage Tab and click on Save as Image. Or you can use the shortcut Control-E to export as a TIFF and save as the case id.
    a. Save the image as a .tif
5) Load the scene diagram into PC-Crash by selecting file→ Import→Bitmap and browsing for the case file
6) Scale the scene diagram using the 1:n tool. This tool works by selecting the 0 and 10 m location on the sale, then imputing the "actual distance" as 10 m.

Step 3: Adding Vehicles to PC-Crash

Most crashes reconstructed using this methodology will involve at least two vehicles. Note that if there is a heavy or unusual vehicle (such as big trucks, school buses, tractor-trailers or motorhomes), please refer to the document titled Heavy Vehicle Crashes In PC-Crash.

1) Open up the vehicle database by selecting the icon.

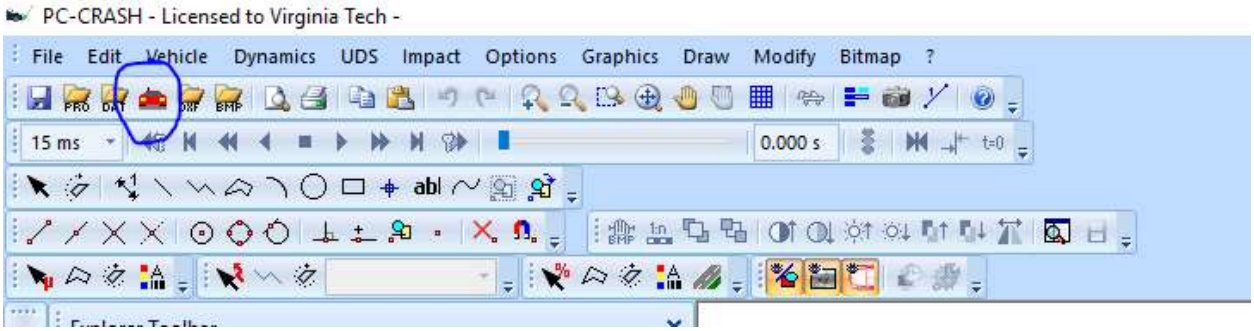

2) Check the vehicle make, model, and year from the information on the NMVCCS online case viewer. You can also use the vehicle photos to narrow down the car make and model more.
    a. If the vehicle cannot be found, open up the Vehicle_Info.xlsx sheet. Find the missing vehicle model and year and look at the alternate models for that model and year. Use this alternate model for PC-Crash Simulation.
    b. Input the selected vehicle make and model into the Results spreadsheet.

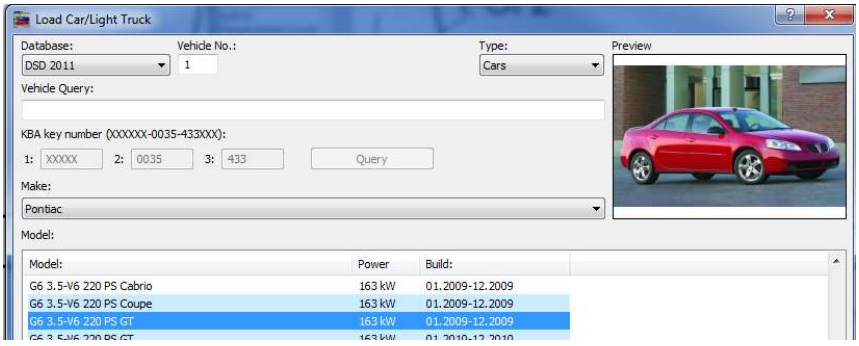

3) Modify vehicle specifications by right clicking in the window and selecting "vehicle settings"
    a. Select "occupants and cargo" tab

b. Add the weights in the results spreadsheet into the appropriate front occupants, rear occupants, and trunk cargo columns

4) Use the  tool to move the vehicle to its respective impact location
    a. The impact location represents the location where that that vehicle was first contacted.
    b. Cars should be overlapping at this position.
    c. Note: The car can be moved and rotated by clicking and dragging the center and edge of the vehicle, respectively.
    d. Note: all positions prior to impact are irrelevant for this analysis and should be ignored.

Step 4: Adding Intermediate/rest Vehicle Positions and tire marks

Adding vehicle positions and tire marks post impact give the collision optimizer a means an objective trajectory.

Intermediate and rest vehicle positions can be input using the following protocol:

3. Select Impact→Intermediate→ Intermediate Position # OR
   Select Impact→Rest
    a. Note: Intermediate Position 1 corresponds to the first depicted position post impact.
4. A tow truck will appear and can be used to drag the impact vehicle to the intermediate vehicle positions.
    a. Note: this will not move the impact vehicle, but will create a new vehicle that can be moved.
5. Place intermediate positions for every vehicle drawn that is still on 4 wheels.
6. For the vehicle that did not experience rollover, place all intermediate and rest positions.

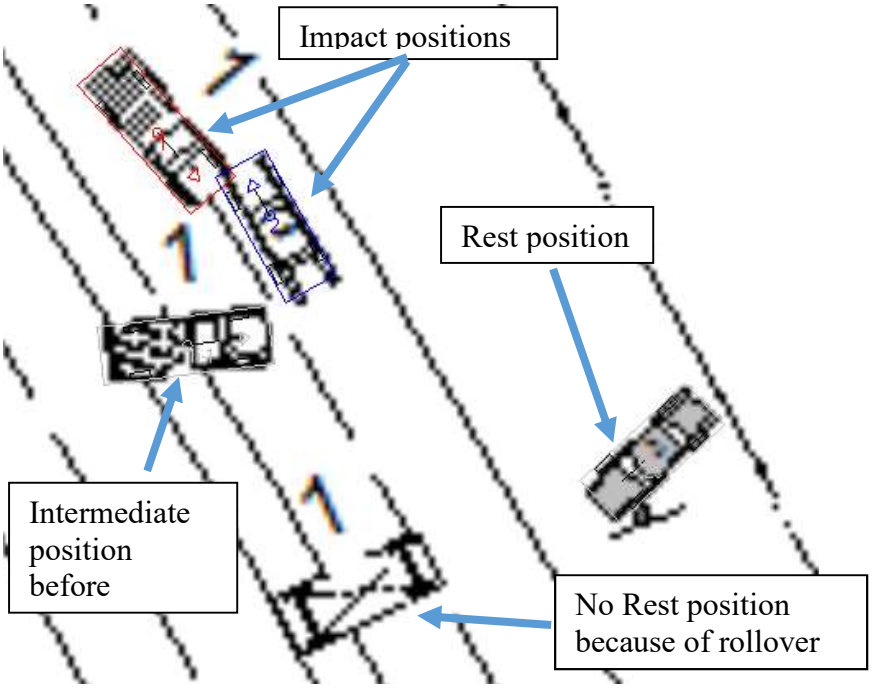

Step 6: Modify Road Friction

Road friction should be modified within for the entire depicted trajectories of both vehicles. Surface conditions can be determined. There are five possible selections for road friction: (1) dry, (2) wet, (3) very wet, (4) snow, and (5) ice. These are already given for you in the Results.xlsx spreadsheet.

Road friction should be modified using the following protocol:

6) Locate the following toolbar:  .
7) Select the  button in the tool bar.
8) Left click to draw a polygon around the entire depicted trajectories.
9) After the polygon is completed, right click to finish drawing.
10) A coefficient of friction window will automatically open.
    a. Use the drop down to change the surface conditions to their appropriate value

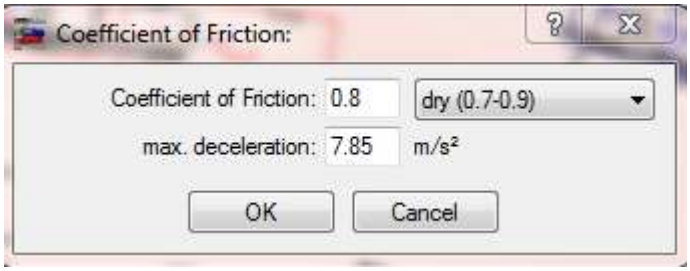

Step 7: Collision Optimization

Collision optimization is the final step in determining impact velocities in PC-Crash. It is important to note that each crash is unique. Although the following protocol attempts to

reconstruct crashes in a systematic way, there is still some "finesse" involved in properly reconstructing crashes.

Note that this protocol covers rollover crash reconstruction using a 2D method. **The aim of collision optimization in PC-Crash will be to get a speed at trip** which can then be compared to traditional NCHRP 17-43 rollover reconstructions later in the process.

First, the "sequence" of events for each vehicle needs to be initialized.

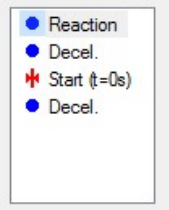

5) Select Dynamics → Sequences to open the sequences window
    a. By default the window to the sequence depicted to the right will appear in the window for each vehicle involved.
6) Double click on the second Decel. and a window will open for changing the decel. step in the sequence (shown to the right)
7) Change the sequence duration to 15s.
    a. This decel sequence duration affects the run time post impact.
    b. A safe decel sequence duration is 15 s.
    c. Alter the decel sequence duration for all vehicles

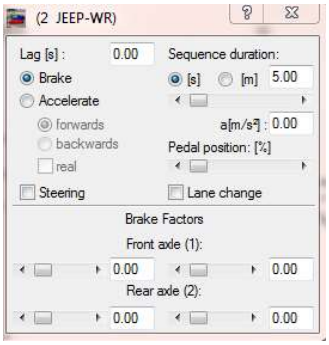

8) The presence of wheel lockup should also be added
    a. Examine scene crash photos and the scene narrative to determine whether wheel lockup occurred. The vehicle wheel should look bent/out-of-line. An example is shown below. Note how the wheel is bent off-axis from the rest of the vehicle.

    b. If wheel lockup occurred, change the brake factor for that wheel to 100. This indicates 100% braking on that wheel. Note that the braking can go up to 500%.
    c. If wheel lockup occurred, add it to the results spreadsheet.

The first pass at collision optimization should be implemented. If this first pass through the optimization is "sufficient", the results will be saved. A "sufficient" result will be one where the

vehicle approximately stops at the depicted rest position. The goal with this reconstruction methodology will be to minimize trajectory error.

6) Select Impact → collision optimizer
    a. Two windows will open:
        i. The collision optimizer window
        ii. The crash simulation window
7) In the crash simulation window:
    a. Select point of impact
    b. Click a location within the two vehicles overlapping area
    c. Unselect point of impact

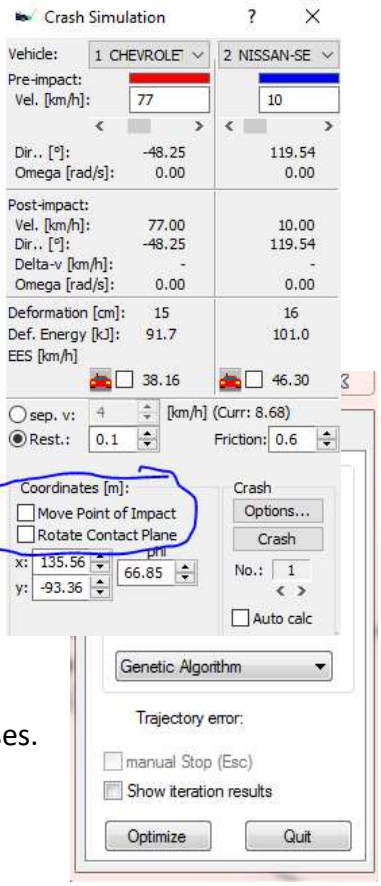

8) Within the optimize tab in the collision optimizer window, verify that impact velocities, point of impact, and contact plane are selected, and the genetic algorithm routine has been selected. See the exemplary screen shot to the right for what this should look like.
9) In the crash simulation window, change the pre-impact velocities to be 30 kph each. These will serve as initial guesses.
10) Click Optimize in the collision optimizer window.

The results can be found in the Crash Simulation window. They can also be seen by selecting options → Values to open the values window, then within the Values window, selecting Settings→ Report. The impact values should be listed under START VALUES.

Step 8: Ways to Reduce Trajectory Error

If the results seem unreasonable, three things can be done to make the results more reasonable. **First**, if the vehicle does not come to a stop, which happens frequently for the vehicle that do not strike a roadside object(s), braking should be added. **Second**, if the trajectory indicates some turning, steering can be added using the path following tool or manually. If lockup occurred, use the manual steering input.

If braking is required, perform the following steps:

4) Open the sequences window by selecting Dynamics → Sequences
5) Under the vehicle of interest, double click the post-start decel.
6) Add braking using the pedal position scroll.
    a. As a rule of thumb, it is best to add braking in 10 % intervals

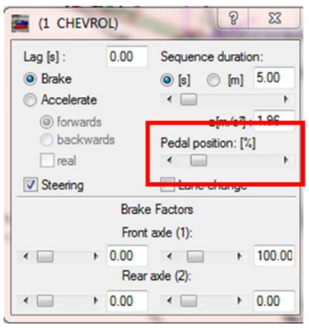

If steering is required, perform one of the following set of steps:

<u>For manual steering input,</u> (Note: should be used if lockup occurred)

6) Open the sequences window by selecting Dynamics → Sequences
7) Under the vehicle of interest, double click the post-start decel.
8) Check the steering check box to open up a steering options window (shown to right)
9) Change the Time to 0 s.
10) Steering should be added to the red boxed area
    a. Positive steering rotates the vehicle counter-clockwise
    b. As a rule of thumb, add steering in 15 degree increments.

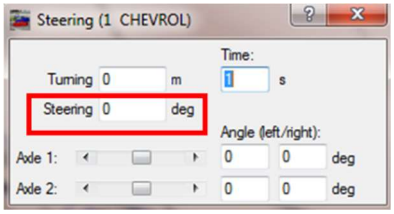

<u>For path following steering input,</u>

6) Locate the following toolbar: 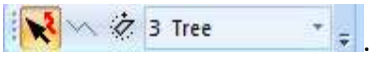

.
7) Select the button in the tool bar.
8) Left click to draw the vehicle path in segments
9) After the path has been drawn, right click to finish drawing.
10) The path can be deleted by clicking the trajectory line using the  then clicking delete.

Step 9: Measuring the Trip Speed in PC-Crash

For rollover reconstructions, we are interested in determining the trip speed and comparing it to the results of the NCHRP 17-43 reconstruction methodology.

1) Using the crash simulation toolbar slowly step through the time steps post-impact using the fast forward button until the vehicle is roughly at the intermediate position.
2) Using the post-impact velocity in the Crash Simulation window, record the velocity at this time.

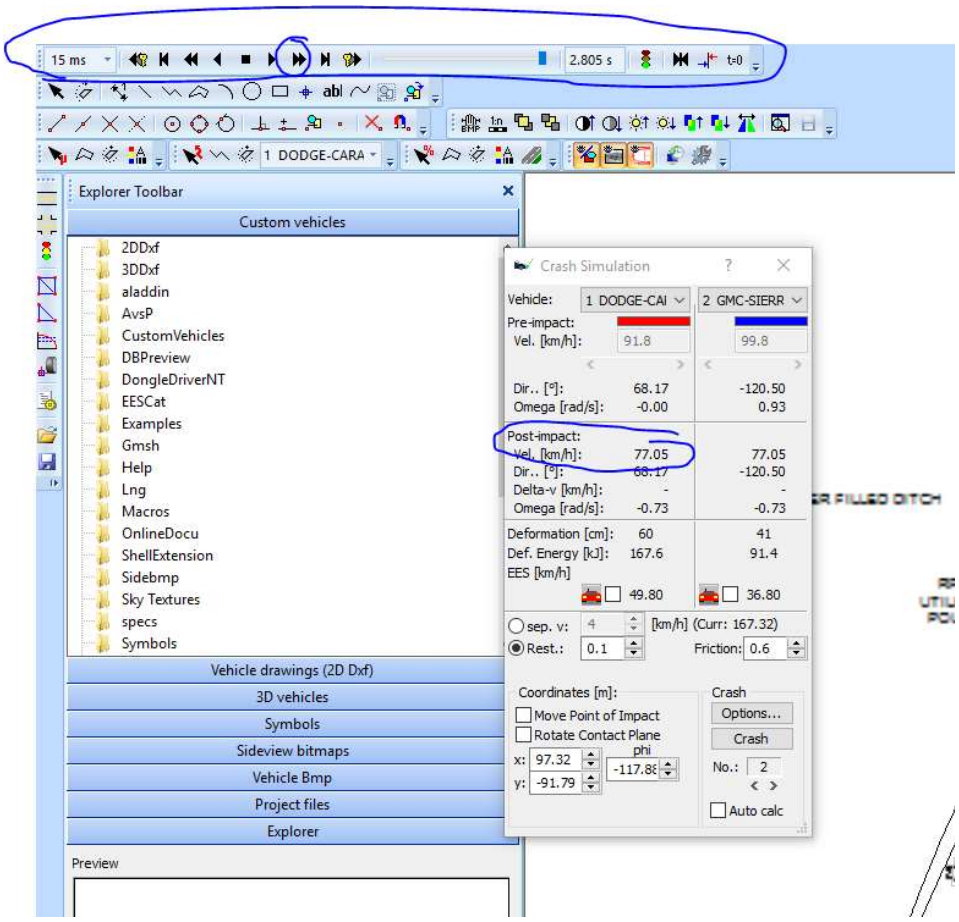

Step 10: Reconstructing a Rollover Crash using NCHRP 17-43 Methodology

This methodology relies on reconstructing a crash using an energy basis. The vehicle is assumed to have no kinetic energy or velocity at the final rest position of the vehicle. Then the vehicle's speed is constructed using conservation of energy. In rollovers, this is accomplished by stepping back through each vehicle center of gravity (CG) trajectory segment, each point of impact (POI), and estimating the speed/energy dissipated through vehicle tire-ground interaction (think friction), the rollover event, and vehicle crush.

Previous studies developed the so-called Kildare Curves, shown below, to correlate vehicle body type and roll distance to rollover trip speed. Based on testing vehicles with various inertial properties, these curves were generated to estimate the speed dissipated throughout the rollover event. These curves are the basis of our speed reconstruction protocol for cases involving a rollover event.

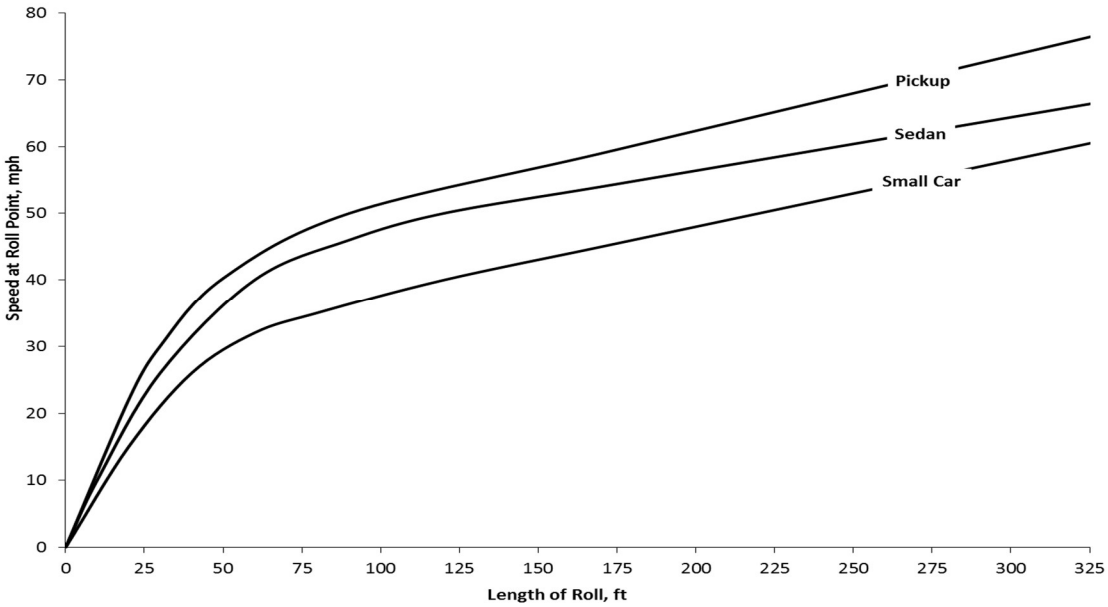

1) Take measurements of the roll distance using Easy Street Draw
    a. Remember that measurements of roll distance should start from the last position shown where the vehicle is on all four wheels and continue until the final rest position of the vehicle.
    b. If a vehicle experiences a quarter turn, the estimated trip point should be right beside the vehicle. An example is shown below. Vehicle 1's motion is shown in black and the yellow point is the initial point where the rollover should be measured from.

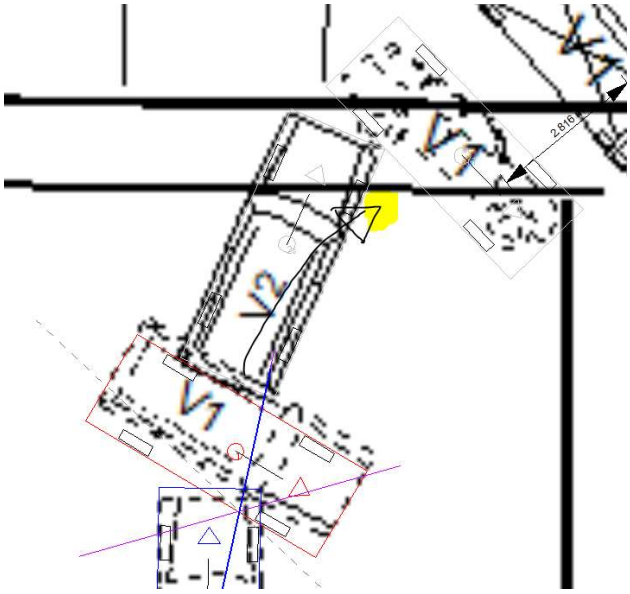

    c. Each distance measurement should be done from the CG of each vehicle. The CG of each vehicle is approximately located in the middle between the driver and

the passenger seats.

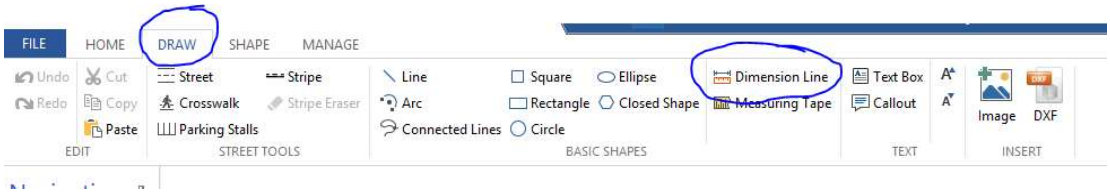

d. To take measurements, go to the Draw tab at the top of the screen and use the Dimension Line.
e. An example measurement is shown below.

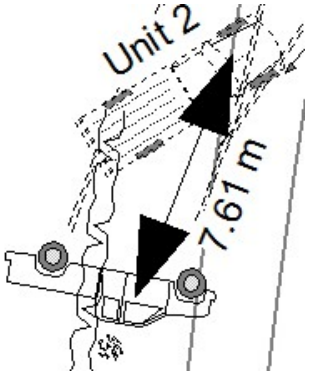

1) Open the file named SpeedReconTemplate_Rollover.xlsx . This is where you will enter the data to calculate speed. Data should only be entered in the yellow sections. The white sections contain programmed equations and autofill data. The impact and departure speed will appear in the green boxes once the form is filled out.
2) Determine if the vehicle is a small car, sedan, or pickup and select it from the dropdown menu next to Vehicle type. If the vehicle that experienced rollover is none of those, the case cannot be reconstructed and you should note that in the Reconstruction excel file as “Heavy Vehicle Rollover”.
3) To find the vehicle mass, go to PC-Crash, right click and choose vehicle settings. The vehicle mass is shown on the right side of the dialog box.
4) Enter in the distance under the Segment length section of the spreadsheet.
5) In the first template column Rollover Locations, select from the dropdown menu where the trip point was (Begin Roll), and where the vehicle stopped rolling (End Roll).
6) Between the cells selected for Begin Roll and End Roll, select Rolling to indicate the vehicle was in rotation during these trajectory segments. As these boxes are filled in, two things will happen: 1) the Min/Max Segment Friction boxes for the corresponding rows will turn red, and 2) a 1 (true) value will populate in the Point of Trip column to mark where the event started.

Step 11: Accounting for Elevation Change

Elevation change is included in terms of potential energy. If the vehicle departed up a steep hill, for example, more energy/higher speeds would have been required for the vehicle to travel up the hill compared to the vehicle traversing a level plane. Elevation change is not typically readily available in the databases and must be estimated based on scene photos or scene diagrams.

1) Determine the elevation change using scene diagram photos or information on the scene diagram
2) Input it in the Energy Change due to Elevation Change box in the spreadsheet.
3)

Notes:

- Slope/Grade: In some cases, the investigator will denote the roadway grade or slope (e.g., 5% or 41/209) for the roadside. If this is available, use the equation $\frac{(vehicle\ mass * 9.81 * \Delta height_{\ segment})}{1000}$ in the corresponding rows to manually compute energy. In this case, the height change for each segment can be computed as $m * \Delta X$ or $m * \Delta Y$, where *m* is the grade/100 or slope and $\Delta X/\Delta Y$ is the change in lateral/longitudinal distance for that segment depending on which orientation the slope is defined. Always check the computed Energy Added sign and compare with whether the vehicle was traveling up/downhill.
- Photograph: If no slope is measured/provided, and a significant change in elevation is seen in photographs, make an educated guess. Think about typical heights of people (5' is about 1.5m; 6' is about 1.8m), cars (), etc. If this height change is for a single segment, you can enter it in the Energy Change due to Elevation Change box in the Excel worksheet. If not, you will need to split up the changeover segments and manually input the equation $\frac{(vehicle\ mass * 9.81 * \Delta height_{segment})}{1000}$ in the corresponding rows.
- Negligible/Level: If no evidence of an elevation change is present, enter 0 in the box.

Step 12: Compare Trip Velocity from NCHRP 17-43 Methodology with PC-Crash

1) The trip velocity from PC-Crash and NCHRP 17-43 should be compared. If there are significant differences, return to the PC-Crash simulation and modify it to get to the approximate trip speed that the NCHRP 17-43 methodology came up with.
2) Use your discretion when comparing the trip speeds. They should be relatively similar but they do not have to be exact.